

FILE COPY

NO 2



RESTRICTED

Copy No.

167

RM No. L8H19

CLASSIFICATION CANCELLED



NACA

RESEARCH MEMORANDUM

CASE FILE COPY

WIND-TUNNEL TESTS OF A SWEEPED-BLADE PROPELLER AND RELATED STRAIGHT BLADES HAVING THICKNESS RATIOS OF 5 AND 6 PERCENT

By

W. H. Gray

Langley Aeronautical Laboratory
Langley Field, Va.

NASA FILE COPY
Loan expires on last date stamped on back cover.
PLEASE RETURN TO:
REPORT DISTRIBUTION SECTION
LANGLEY RESEARCH CENTER
NATIONAL AERONAUTICS AND SPACE ADMINISTRATION
Langley Field, Virginia

NASA FILE COPY
THIS DOCUMENT ON LOAN FROM THE NATIONAL ADVISORY COMMITTEE FOR AERONAUTICS
Langley Field, Hampton, Virginia
RETURN TO THE ABOVE NATIONAL AERONAUTICS AND SPACE ADMINISTRATION
Langley Field, Virginia

NATIONAL ADVISORY COMMITTEE FOR AERONAUTICS
1512 H STREET, N. W.
WASHINGTON 25, D. C.

CLASSIFIED DOCUMENT
This document contains classified information affecting the National Defense of the United States within the meaning of the Espionage Act, USC 50:31 and 32. Its transmission or the revelation of its contents in any manner to an unauthorized person is prohibited by law. Information so classified may be imparted only to persons in the military and naval services of the United States, appropriate civilian officers and employees of the Federal Government who have a legitimate interest therein, and to United States citizens of known loyalty and discretion who of necessity must be informed thereof.

CLASSIFICATION CANCELLED
BY AUTHORITY J. W. CROWLEY
CHANGE #1703 DATE 12-10-53 T.C.F.

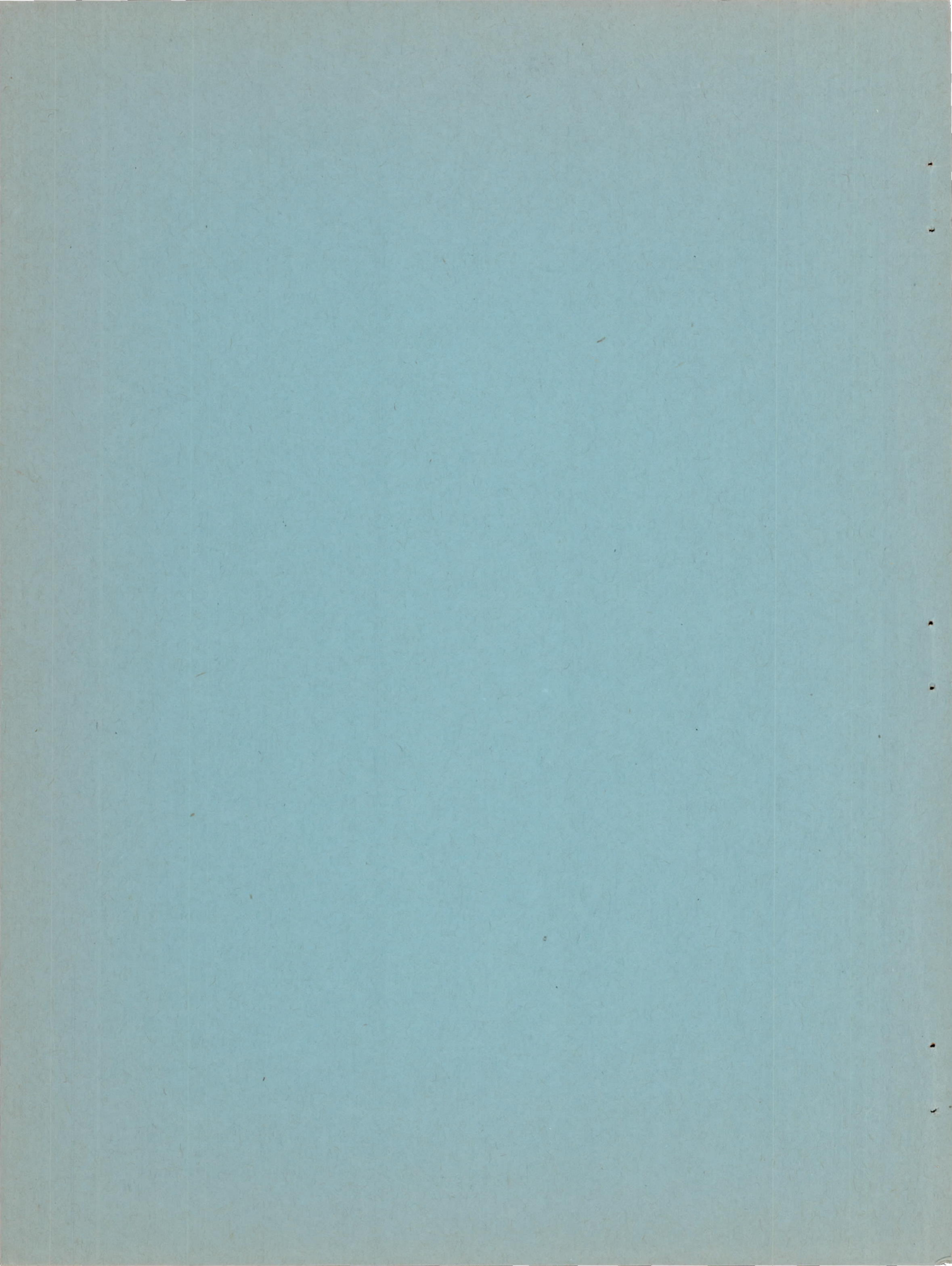
NATIONAL ADVISORY COMMITTEE FOR AERONAUTICS

WASHINGTON

November 10, 1948

RESTRICTED

NACA RM No. L8H19



NATIONAL ADVISORY COMMITTEE FOR AERONAUTICS

RESEARCH MEMORANDUM

WIND-TUNNEL TESTS OF A SWEEP-BLADE PROPELLER AND
RELATED STRAIGHT BLADES HAVING THICKNESS
RATIOS OF 5 and 6 PERCENT

By W. H. Gray

SUMMARY

The aerodynamic characteristics of three sets of blades were investigated over as wide a range of operating conditions as possible. One set of blades, conventional in design, was compared with a second set, which differed principally in that the blades embodied sweep, and with a nonswept set having thinner blade sections. The test conditions did not duplicate the blade design conditions although the actual thrust loadings were very nearly those for the design condition of the conventional straight blades but not for the sweptback blades.

The sweptback blades were in general inferior to the straight blades; however, the test Mach numbers were insufficiently high to encompass the speeds for which sweepback is believed to be beneficial. The envelope efficiency of the straight thin blades was as much as 2.5 percent higher than for the other sets of blades and the effect of rotational speed on the thin blades was negligible.

INTRODUCTION

The design of propeller blades for high-speed, especially transonic-speed, operation is hampered by a lack of adequate airfoil-section data. Likewise, the testing of such blades, including those with sweepback, is hampered by lack of suitable facilities for testing at the necessarily high speeds which duplication of design conditions requires. Wind-tunnel tests reported previously have indicated varying amounts of benefit from sweep, but none of these tests approached actual full-scale flight conditions. References 1 and 2, for instance, employed blades of small scale, approximately $3\frac{1}{2}$ feet and 1 foot in diameter, respectively. The tests of reference 3 employed a 10-foot-diameter propeller, but only the immediate tip sections of the blades were swept back.

Flight tests of several full-scale three-blade propellers embodying both sweptback and related conventional blades of Curtiss design have been conducted by Curtiss Propeller Division, Curtiss-Wright Corporation.

No conclusive evidence was obtained in these flight tests to establish any definite proof of superiority for the sweptback blades.

The flight tests were followed by a wind-tunnel program at the Langley 16-foot high-speed tunnel employing the identical blades in a two-blade version. Two propellers, approximately 13 feet in diameter, whose blades differed in that one pair employed sweep, were compared with a third pair of the same diameter also with straight blades but differing in section thickness and section design lift coefficients from the first straight-blade propeller. Neither the design conditions nor the flight-test conditions could be duplicated in the wind tunnel. It was hoped, however, that for the possible test conditions definite aerodynamic trends could be established. In addition, the actual blade loading was to be measured by means of a propeller-wake survey rake.

APPARATUS

Dynamometer.— The tests described in the present paper were conducted in the Langley 16-foot high-speed tunnel using the 2000-horsepower-propeller dynamometer in a modified configuration. No spinner was used to cover the hub and blade shanks for these tests. The resulting arrangement, therefore, was similar to that used in reference 3. Figure 1 shows a general view of the test setup with the sweptback blades installed.

Propeller blades.— Three sets of blades, each embodying 16-series sections, were tested in two-blade configurations. The geometric characteristics of these three Curtiss Propeller Company designs are shown in figure 2. Throughout this report each set of blades will be identified by Roman numerals. The sweptback blades, Curtiss design 109494, designated set I, which are fully described in reference 4, have essentially the same section thickness ratios, width ratios, and design lift coefficients perpendicular to the blade center line as the straight-blade Curtiss design 109390, hereinafter referred to as set II. The blades of set II were designed for a high-speed flight condition of the XP-47M airplane, whereas those of set I were designed for a high-speed dive condition of the P47D-30 airplane. This airplane was equipped with an R-2800-59 engine having a 0.5 gear ratio. The itemized dive conditions are 600 miles per hour at 2100 brake horsepower, 2550 engine rpm, and 23,000-foot altitude. The amount of sweep incorporated in this blade is shown in figure 3. A certain amount of sweepforward is incorporated on the inner blade sections to balance the bending moments incurred by the sweepback of the outer blade sections. Sweep angles exceed 30° only outboard of the 90-percent-radius station and are only 45° at the tip. As mentioned in reference 4 the sweepback distribution was purely arbitrary and was a compromise required by the considerations of the effect of sweepback on aerodynamic improvements, blade stress, twisting moment, and bending moments. Somewhat less twist has been incorporated in the blades of set I for sections less than 50 percent radius and somewhat more twist at greater radii than has been incorporated in the

blades of set II. This twist differs because not only were the design conditions of the two blades slightly different, but also the pitch distribution of the sweptback blades is affected by the incorporation of sweep and the necessary allowances for the differences in sectional velocities from those of unswept blades.

The thin straight blades, Curtiss design 109498, designated as set III, have considerably thinner blade sections throughout. The sections are 5 percent thick or less from the 50-percent-radius station outboard as compared with about 7 percent for the blades of sets I and II. The design lift coefficient for this set has been reduced as well. The maximum design lift coefficient is 0.41 compared with 0.51 for the other two sets of blades.

SYMBOLS

The symbols and definitions used in the present paper are as follows:

b	blade chord, feet
c_{l_d}	design section lift coefficient
C_P	power coefficient $\left(P/\rho n^3 D^5 \right)$
C_T	thrust coefficient $\left(T/\rho n^2 D^4 \text{ or } \int C_{T'} dx \right)$
$C_{T'}$	blade-section thrust coefficient
D	propeller diameter (approx. 13 ft)
h	blade-section maximum thickness, feet
J	advance ratio (V/nD)
M	free-stream Mach number
M_t	helical-tip Mach number $\left(M \sqrt{1 + \left(\frac{\pi}{J} \right)^2} \right)$
n	propeller rotational speed, rps
P	power absorbed by propeller, foot-pounds per second
T	propeller thrust, pounds
V	free-stream airspeed, feet per second
x	fraction of propeller-tip radius

β	blade angle, degrees
β_{42}	blade angle at the 42-inch radius, degrees
η	efficiency
ρ	mass density of air, slugs per cubic foot

TESTS AND METHODS

Scope.— The three sets of blades were tested over as great a range as possible within the power and speed limitations of the dynamometer and the wind tunnel. All tests were made at constant propeller speed for three rotational speeds: 960, 1350, and 1500 rpm. All blade angles were set at the 42-inch radius and the tests at each rotational speed were made in 5° increments through as wide a range of blade angles as possible. A summary of the tests is made in table I.

Effects of diameter.— The sweptback blades, set I, changed diameter with blade angle — decreasing blade angle resulted in increasing diameter. The change in diameter for the blade-angle range of these tests was only 0.07 feet, or 0.5 percent. This characteristic was accounted for in the evaluation of the data throughout the tests by the use of the actual diameter at each blade angle.

Correction for tunnel interference.— All velocity data are for equivalent free-stream airspeed. The large ratio of propeller-disk area to tunnel-throat area necessitated relatively large correction to the velocity, but it was assumed that Glauert's method of correction from tunnel datum to equivalent free-stream velocity was still valid. The blade tips were operating well outside the boundary layer which has been found to be 8 inches thick at the propeller plane.

Evaluation of tares.— As mentioned previously, no spinner was used to cover the hub and blade shanks for these tests and, therefore, careful evaluation of the tare drag was necessitated. Figure 4 shows a close-up of the hub tare setup. For the blade angles and rotational speeds employed it was evident that the bracelets used to clamp the blade shanks in the hub adapters acted sufficiently like small though inefficient airfoils to cause appreciable changes in the tare thrust or drag. Separate tares were required for each blade angle. The changes in torque caused by the action of these bracelets was inconsistent and negligible.

By proper evaluation of the tares, "propeller" efficiency rather than "propulsive" efficiency was derived from the data. Reduction of the force data to this form was necessary in order to compare the force data with survey-rake data which naturally are "propeller" data. Actually the results will differ from propeller results, because the drag of hub barrels

containing stub blade ends (fig. 4) has been assumed to be the same as for hub barrels containing blades. This assumption is not strictly true, but it was believed to be sufficiently accurate for the present tests.

Survey rake.— The propeller-wake survey rake used in these tests was installed in a vertical position with the tube orifices 16 inches downstream of the propeller-hub center line. There were 12 total tubes and 4 static tubes located within the propeller slipstream and 1 total tube and 1 static tube were outside the propeller slipstream. The total heads also incorporated yaw tubes which were intended for determination of torque data. It was found that the characteristics of these yaw heads in the oscillating flow behind the propeller were not sufficiently good to give satisfactory results, especially at the higher test Mach numbers. Therefore, only results of the thrust distribution as obtained from the total heads are presented in this paper. The values of propeller thrust coefficient are obtained in the usual manner by integration of the plots of section thrust coefficient against radial tube location.

RESULTS

General aerodynamic characteristics - force data.— Thrust coefficient, power coefficient, and efficiency comprise the aerodynamic-characteristic curves presented in figures 5 to 13. (Any figures desired may readily be selected by reference to table I.)

The envelopes of the efficiency curves are compared in figure 14 for each propeller at the three rotational speeds. Figure 14 shows that the sweptback propeller, set I, was most affected by increased rotational speed and the thin-blade propeller, set III, was least affected. The equivalent tip Mach number for each rotational speed and advance ratio may be determined from figure 15. An average diameter for the blades of set I was used in the preparation of this figure but the error thus introduced is well within the accuracy for determination of wind-tunnel Mach number. The maximum tip Mach number for which envelope comparisons may be made is exactly 1.0. Figure 16 repeats the curves for figure 14 by directly comparing the three sets of blades at each of the three rotational speeds. In general, the sweptback blades, set I, have the poorest efficiencies and the thinner blades, set III, the best efficiencies. The maximum difference between any of the three envelope efficiencies is about $2\frac{1}{2}$ percent. This latter difference occurs even at 1500 rpm at a value of J corresponding to the tip Mach number of 1.0.

These results are as inconclusive in regards to the benefits of sweepback as were the Curtiss flight tests, reference 5. In general, the trends indicated in the flight tests have been repeated in the wind-tunnel tests although the actual flight-test conditions could not be duplicated. The general conclusions that may be drawn from these results are that the test Mach numbers were insufficiently high to include the speed range for which sweepback is believed to be of benefit, and that other factors, such as

propeller operation away from the design conditions and too large blade thickness, may have affected the results. There is no question, however, that the effect of thin sections, as has been demonstrated many times previously, is beneficial.

General aerodynamic characteristics - survey data.- The integrated values of thrust coefficient obtained from the rake total-head tubes are compared with faired force data in figures 6(b), 9(b), and 12(b). The agreement may be considered very good. As mentioned above, the agreement for the integrated torque data was not as good and, because of discrepancies at higher Mach numbers, the data have not been presented.

Plots of section thrust coefficient obtained from the survey rake and force-data power coefficient are presented in figures 17 to 19 for 1350 rpm only. From these plots comparisons of thrust loading curves may be plotted for identical conditions for all three propellers within the limited range of the tests. This has been done for two particular cases in figure 20. Figure 20(a) compares the three propellers for a "climb" condition, $J = 0.9$ and $C_p = 0.06$, which represents the lowest values of J and C_p for which comparisons may be made from these test data, and figure 20(b) compares the propellers for a "cruising" condition, $J = 1.2$ and $C_p = 0.07$, which represents the largest values of J and C_p for which comparisons may be made from these data. The tip Mach numbers for the two conditions were 0.85 and 0.87, respectively. There is little difference in thrust distribution between the blades of sets II and III, but the sweptback blades, set I, appear to be more lightly loaded from $x = 0.55$ to 0.95 and more highly loaded towards the tip. The latter condition should have benefited the sweptback blades had the test conditions been at a sufficiently high Mach number. The actual design conditions of the sweptback blades result in a value of tip Mach number of 1.203, $J = 3.19$, and $C_p = 0.285$.

The integrated values of the section thrust distribution shown in figure 20(b) should bear the same qualitative relation to each other as was shown by the envelope curves of figure 16 at the same value of J . Figure 16 indicates that at $J = 1.2$ the blades of set III have the highest efficiency and the blades of set I the lowest. In figure 20(b) the blades of set I have the lowest integrated value of C_T , or efficiency, the other two blades have essentially the same values of C_T . The discrepancy may be ascribed to the necessary fairing of both the elemental thrust coefficients and force power coefficients in figures 17 to 19, from which the thrust distributions of figure 20 were derived.

The test conditions were so far from actual flight and design conditions that the results have been compared with the design condition for the blades of sets I and II in figure 21. The calculated design thrust loadings are obtained from reference 4. All curves have been adjusted so that the maximum section thrusts are equal. Inspection of the curves affords a qualitative comparison of the radial section thrust distribution. The straight blades,

set II, were apparently operating close to the design thrust loading (fig. 21(a)). The sweptback blades, set I, were operating far from the design thrust loading condition (fig. 21(b)). Although the curves have not been adjusted to have the same integrated value of thrust, it is obvious that in the test condition the inner blade sections were more heavily loaded and the tip sections were less heavily loaded than was the case for the design condition. Because the design loading was derived from a Betz loading condition and because the immediate tip sections ($x = 0.9$ to tip) incorporated the main portion of the blade sweep, it is not surprising that the sweptback blade had inferior characteristics when compared with blades which were operating nearer to their design conditions.

CONCLUSIONS

The following conclusions may be drawn for the particular blades tested within the limited range of speed and power of these tests which did not include the flight-test or design conditions:

1. The sweptback blades were in general inferior to the straight blades; however, the test Mach numbers were insufficiently high to encompass the speeds for which sweepback is believed to be beneficial.
2. The envelope efficiency of the straight thin blades was as much as 2.5 percent higher than for the other sets of blades and the effect of rotational speed on the thin blades was negligible.

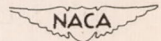
Langley Aeronautical Laboratory
National Advisory Committee for Aeronautics
Langley Field, Va.

REFERENCES

1. Quick, A.: Tests on Airscrews with Swept Curved Blade Axes. Repts. and Translations No. 48, British M.A.P. Völkenrode, Jan. 1946.
2. Seiferth, R.: Investigation on an Airscrew with Swept Back Blade Tips at High Tip Speed. Repts. and Translations No. 102, British M.A.P. Völkenrode, April 1, 1946.
3. Evans, Albert J., and Klunker, E. Bernard: Preliminary Investigation of Two Full-Scale Propellers to Determine the Effect of Sweptback Blade Tips on Propeller Aerodynamic Characteristics. NACA RM No. L6J21, 1946.
4. Warsett, P.: Aerodynamic Analysis of Sweep-back as Incorporated in High-Speed Propeller Blades and the Design of the 109494 Blades. Rep. No. C-1679, Curtiss Propeller Div., Curtiss-Wright Corp., Feb. 21, 1946.
5. Holford, Fred R., and Kasley, J. H.: Flight Test Comparisons of Propeller with 836-14C2-18R1, 109390, 109494, and 109498 Blades in Level Flight Conditions. Rep. No. C-1795, Curtiss Propeller Div., Curtiss-Wright Corp., March 6, 1947.

TABLE I
SUMMARY OF TESTS

Figure	Blades	Propeller speed (rpm)	Blade angle, β , at 42-inch radius (deg)								
			20	25	30	35	40	45	50	55	60
5	Set I	960	20	25	30	35	40	45	50	55	60
6	Set I	1350		25	30	35	40	45	50	55	
7	Set I	1500	20	25	30	35	40	45	50		
8	Set II	960	20	25	30	35	40	45	50	55	60
9	Set II	1350	20	25	30	35	40	45	50		
10	Set II	1500	20	25	30	35	40	45			
11	Set III	960	20	25	30	35	40	45	50	55	60
12	Set III	1350	20	25	30	35	40	45	50		
13	Set III	1500	20	25	30	35	40	45			



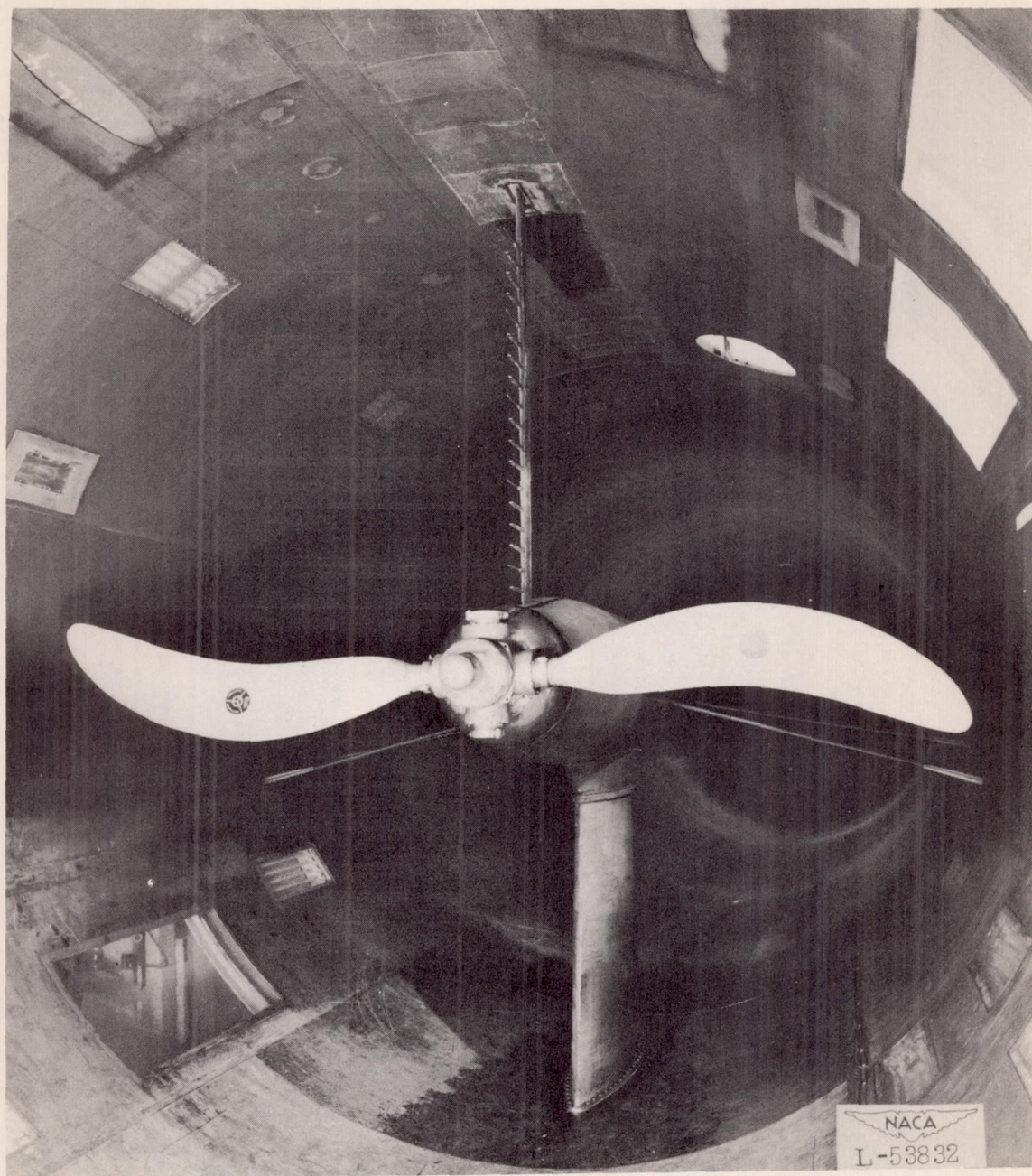
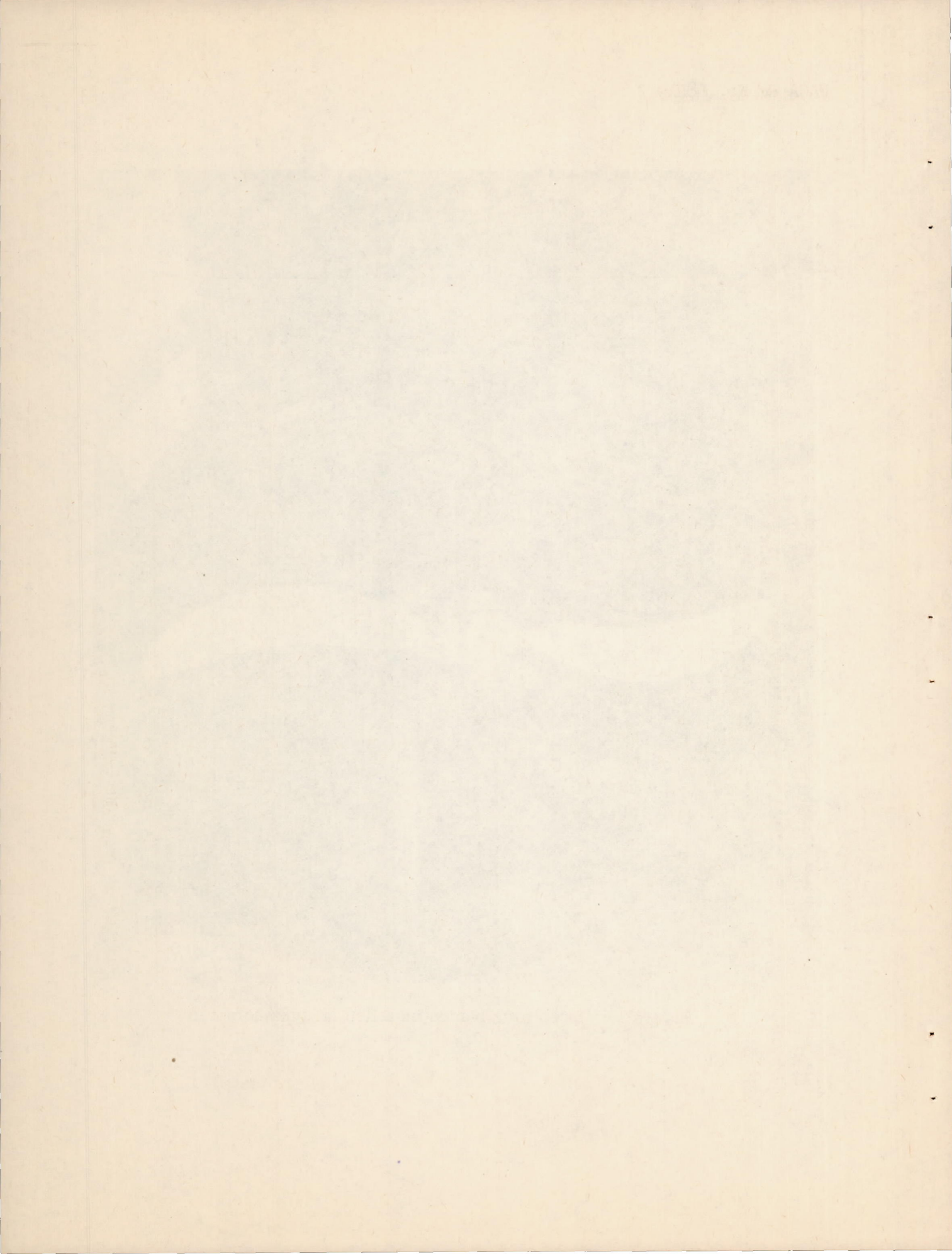


Figure 1.- Sweptback blades installed on dynamometer.



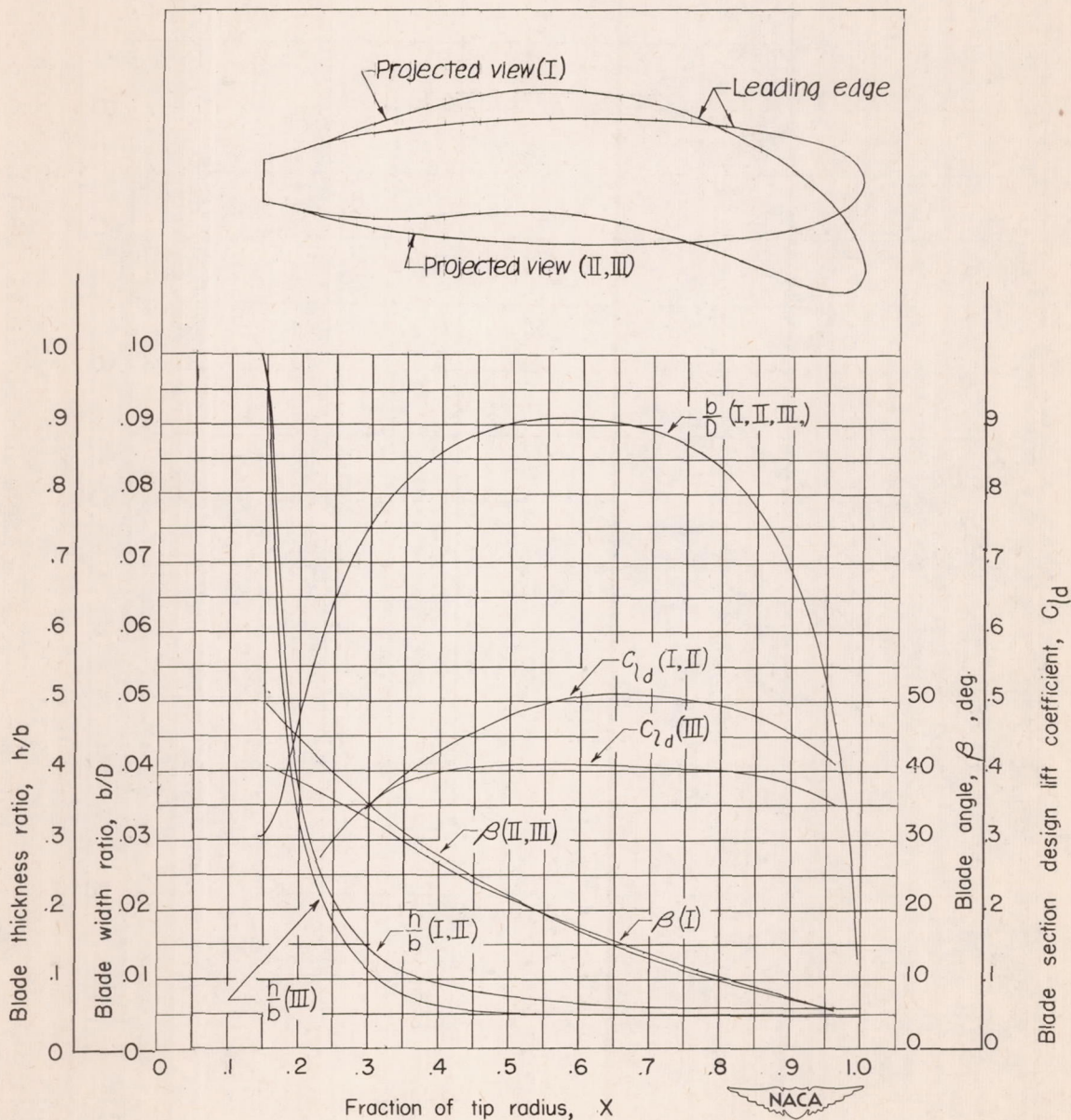


Figure 2.- Blade-form curves for the propellers tested.

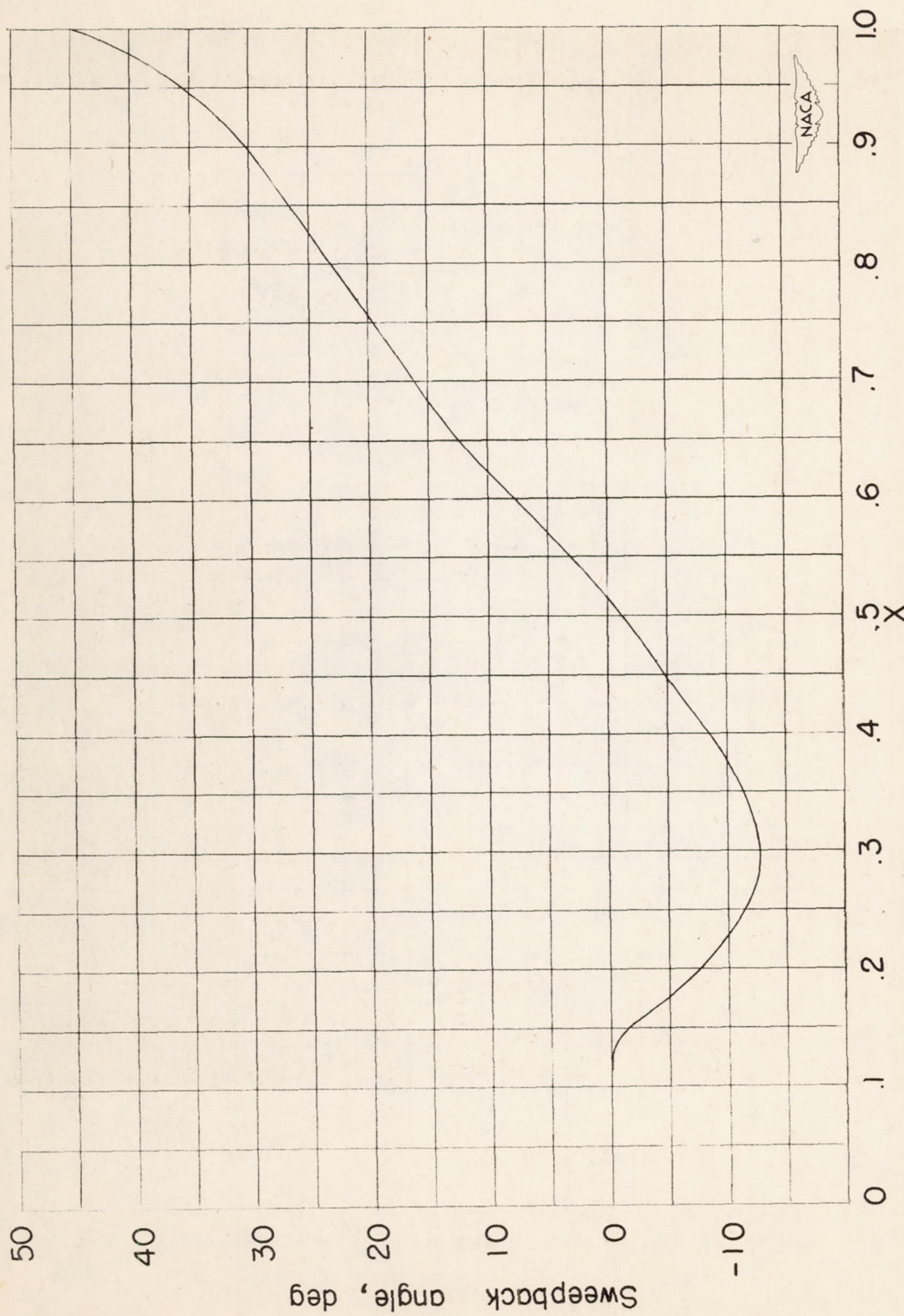


Figure 3.- Sweepback angle used on blades of set I.

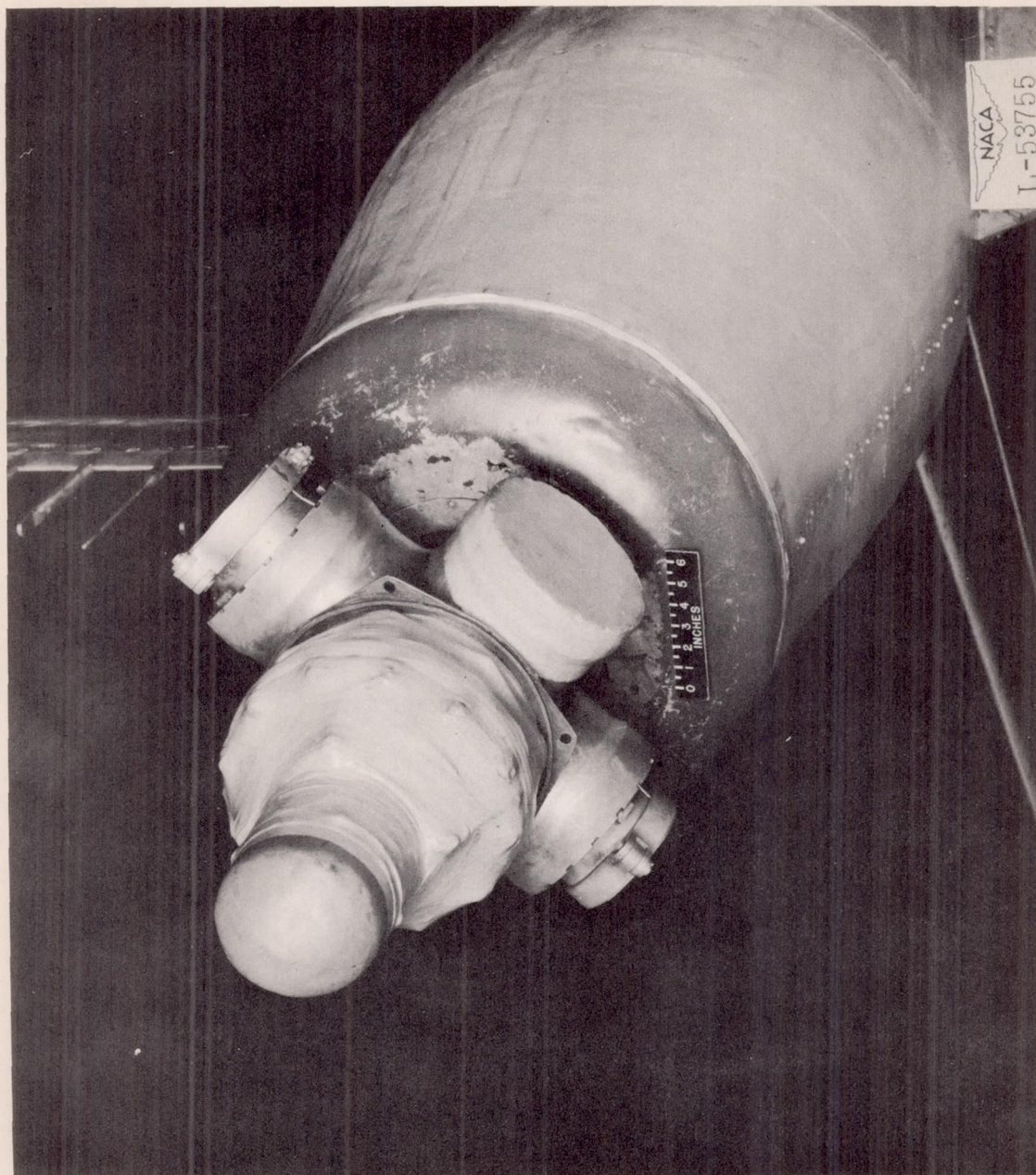
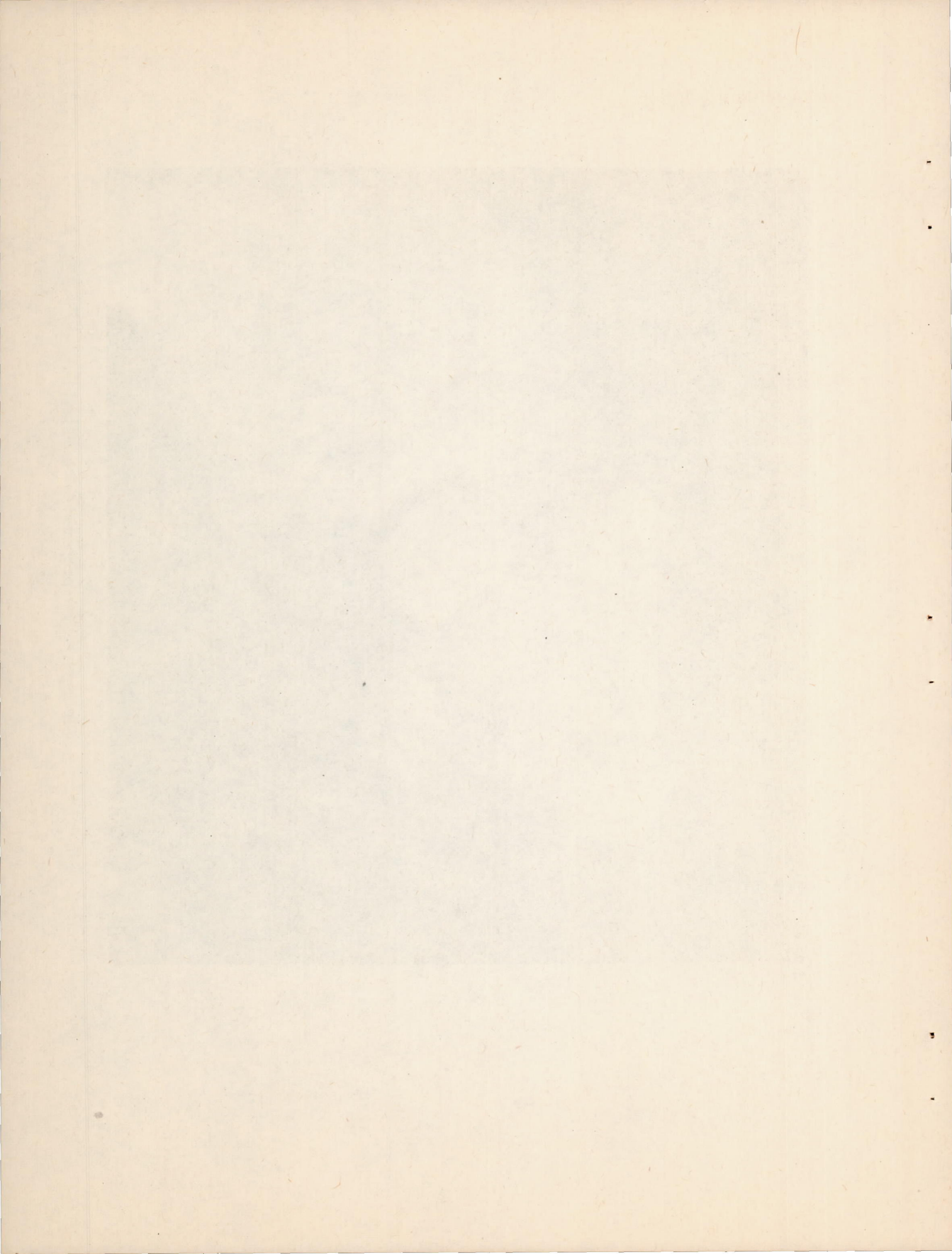
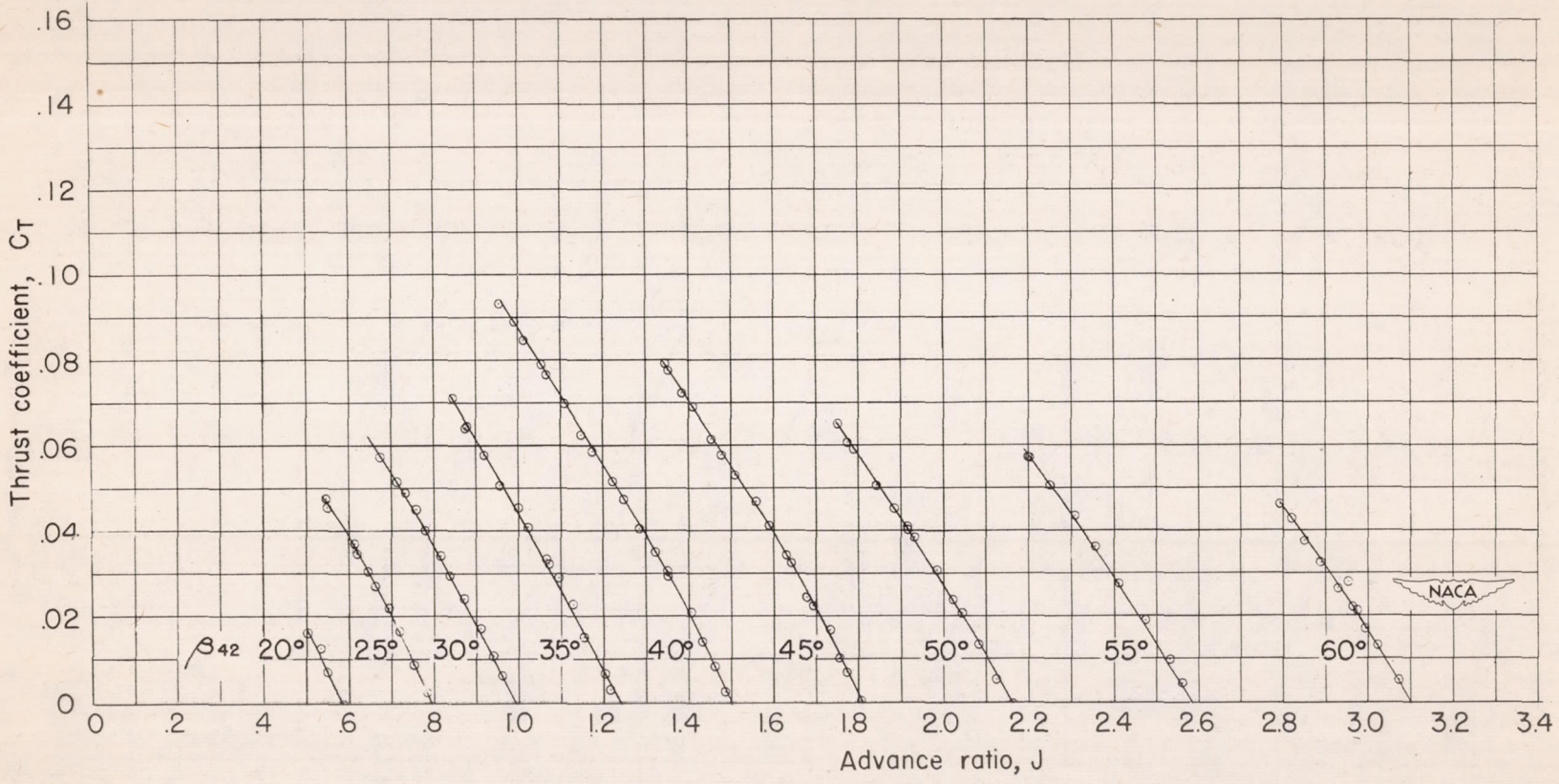


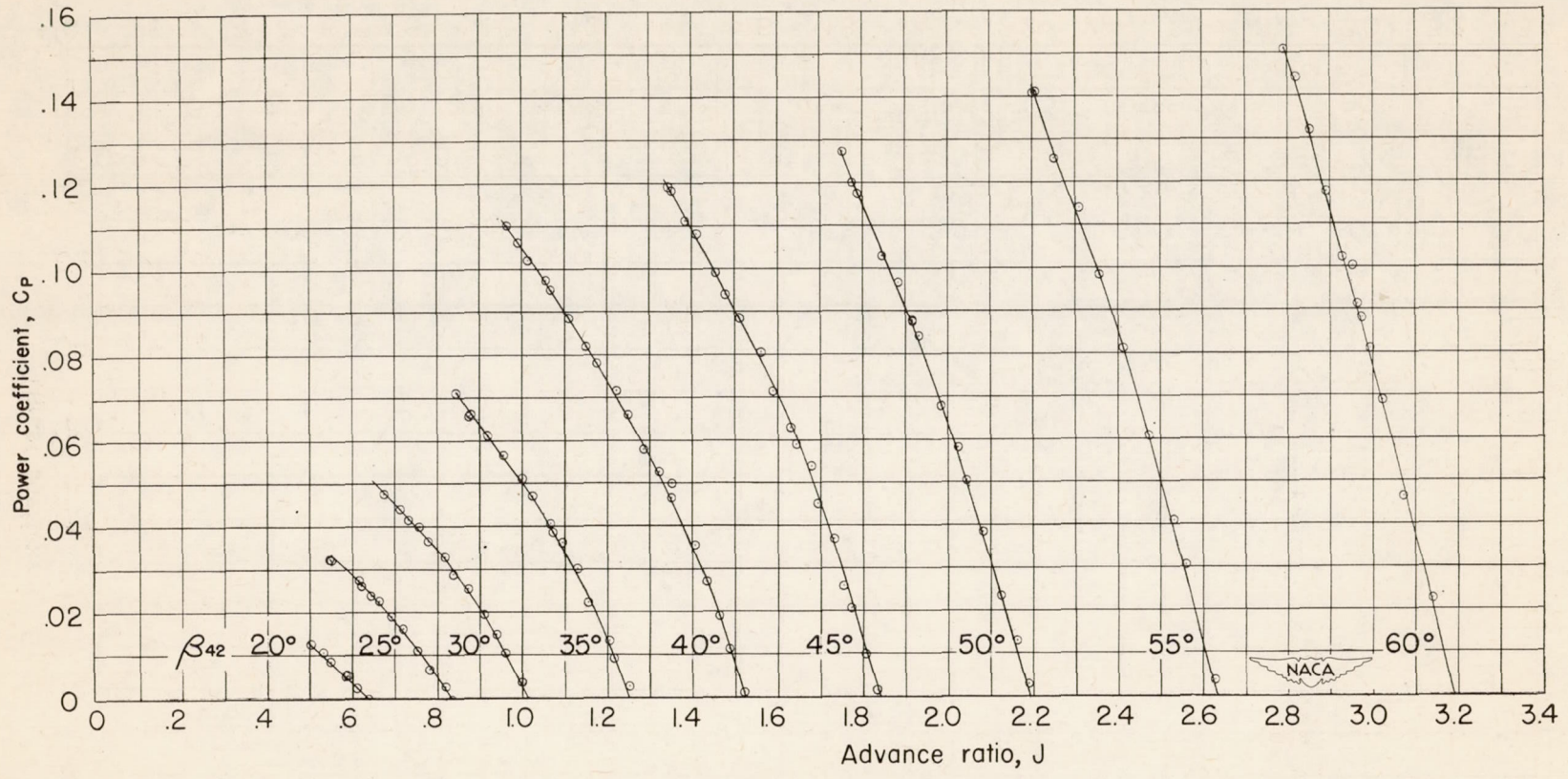
Figure 4.- Hub prepared for tare tests.





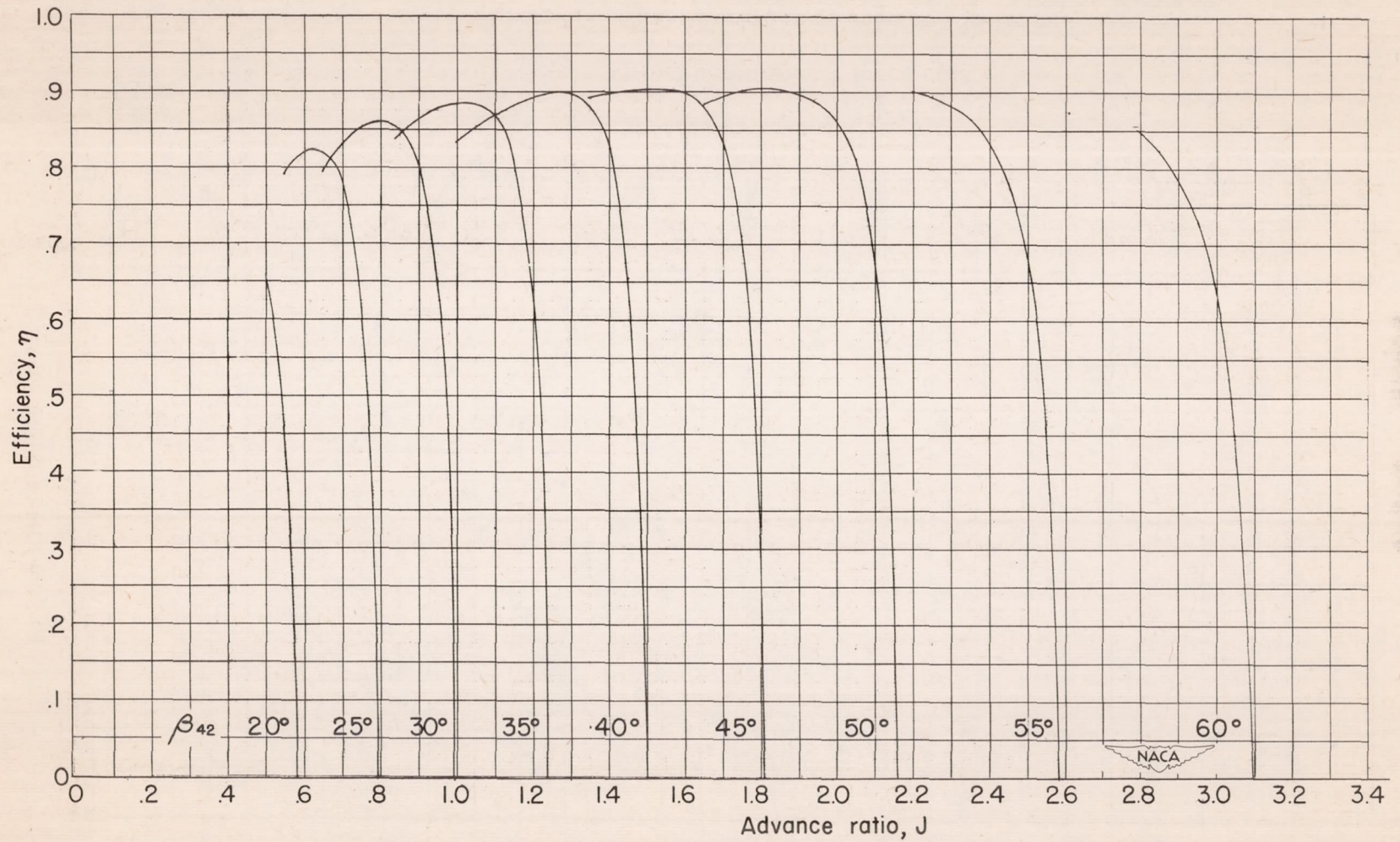
(a) Thrust coefficient.

Figure 5.- Characteristics of set I at 960 rpm.



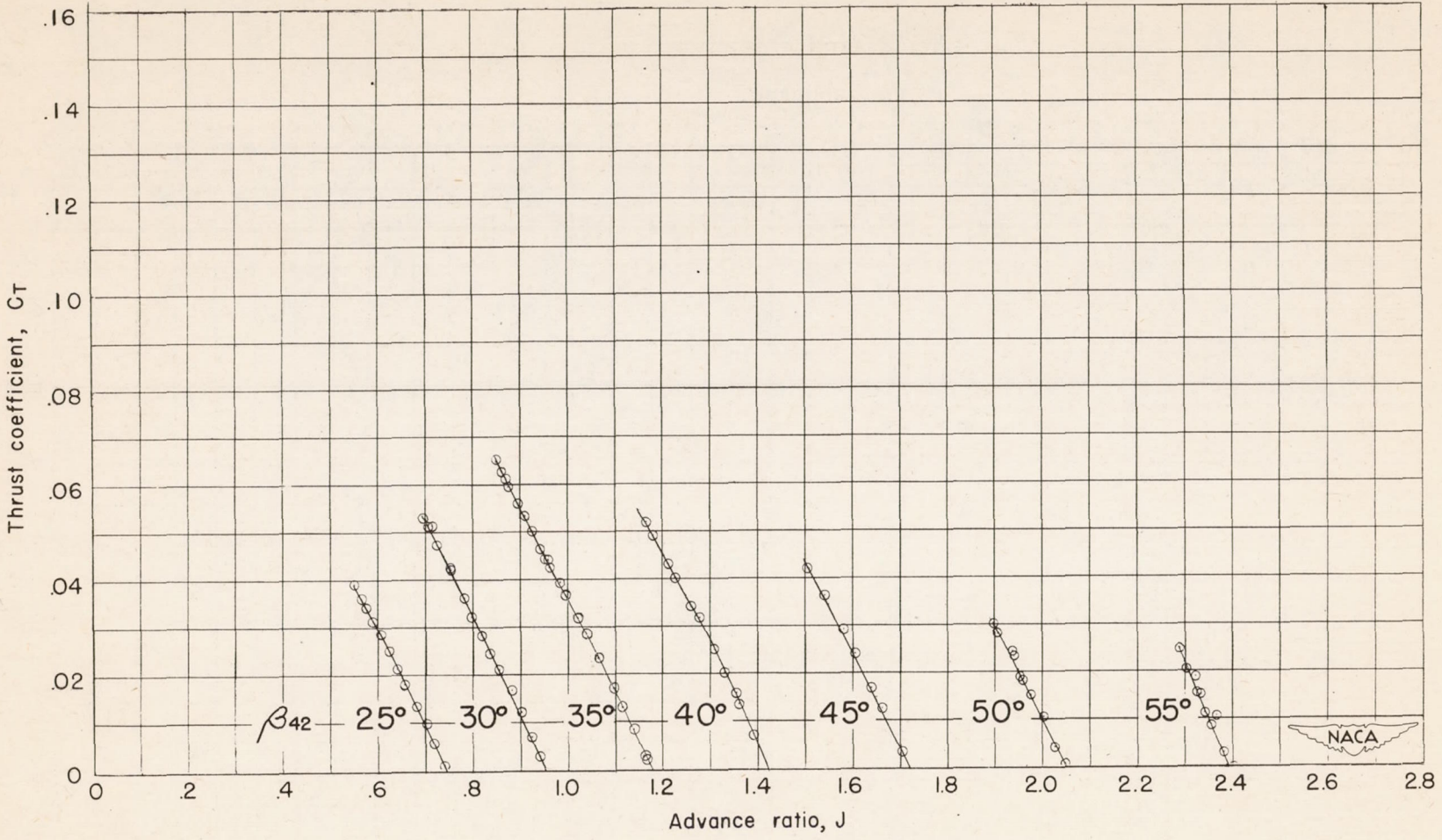
(b) Power coefficient.

Figure 5.- Continued.



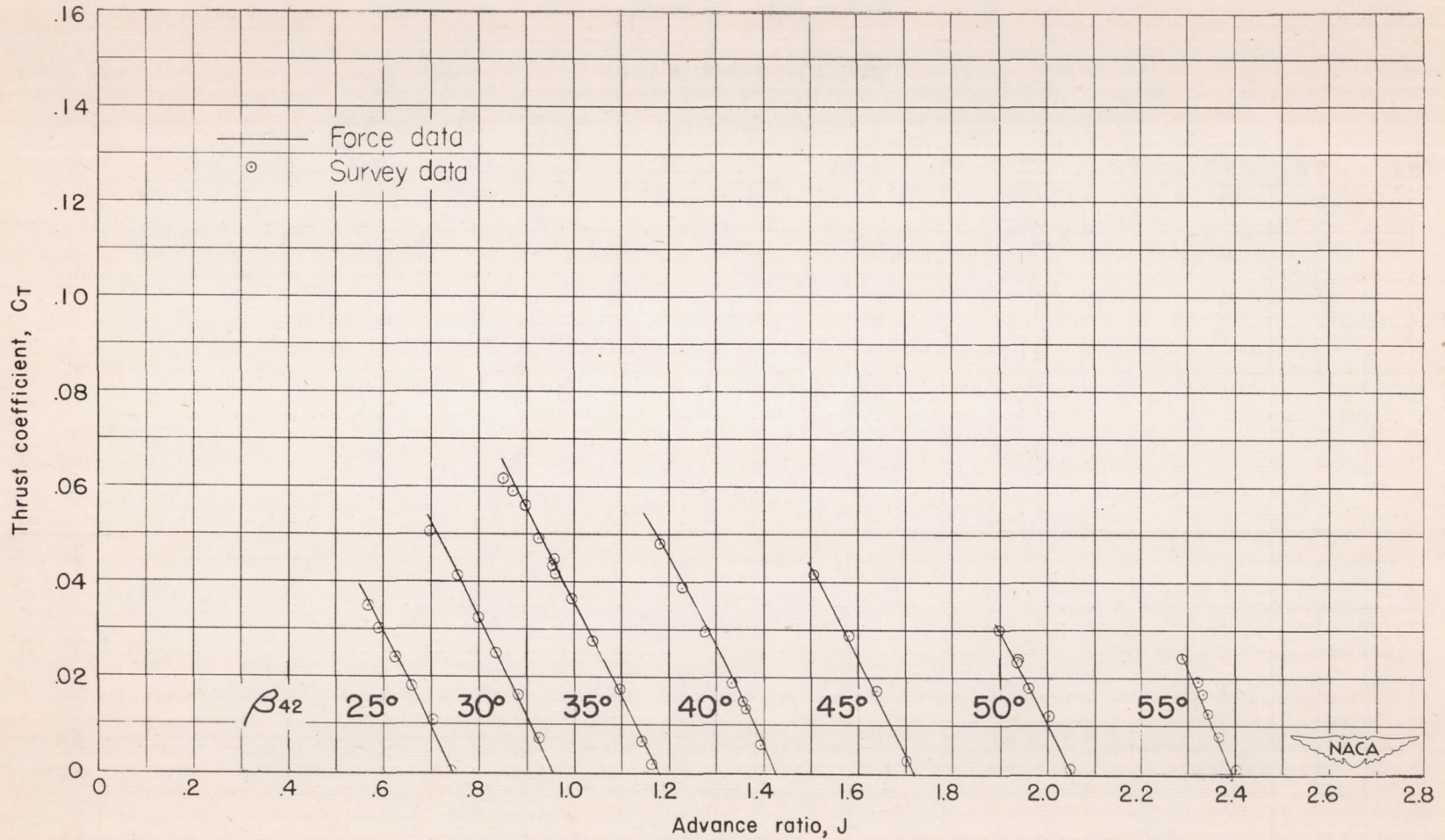
(c) Efficiency.

Figure 5.- Concluded.



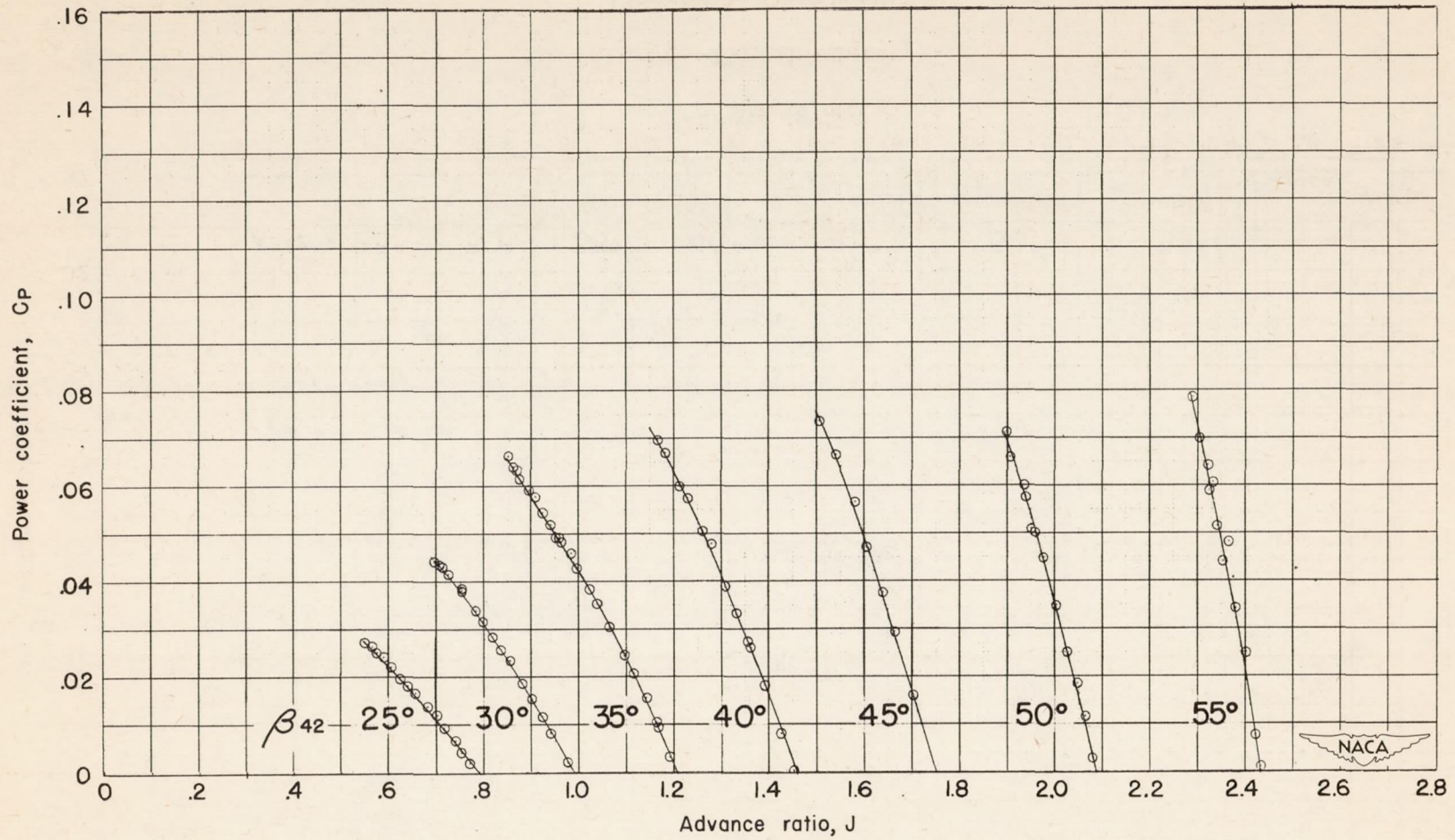
(a) Thrust coefficient - force data.

Figure 6.- Characteristics of set I at 1350 rpm.



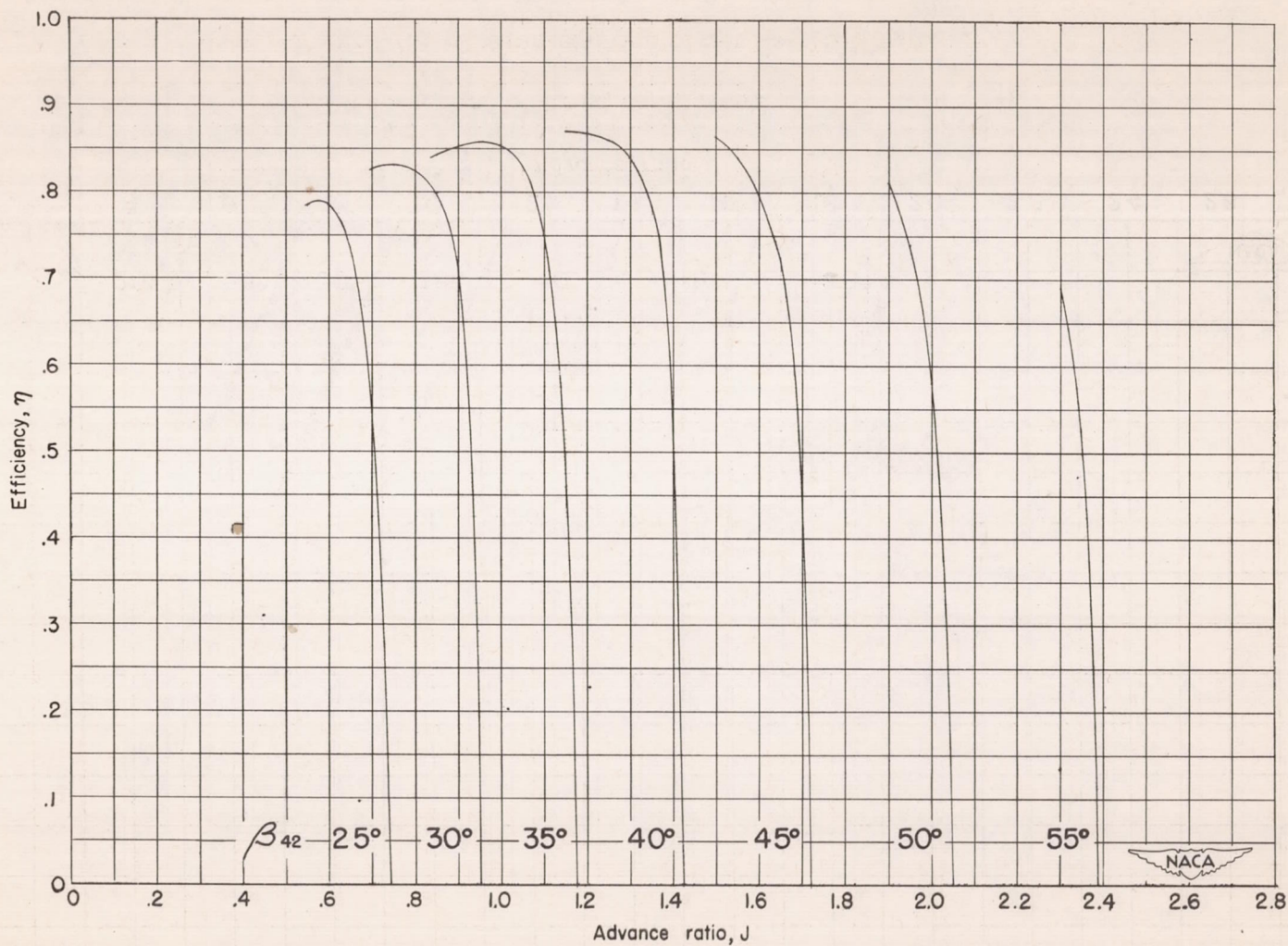
(b) Thrust coefficient - survey data.

Figure 6.- Continued.



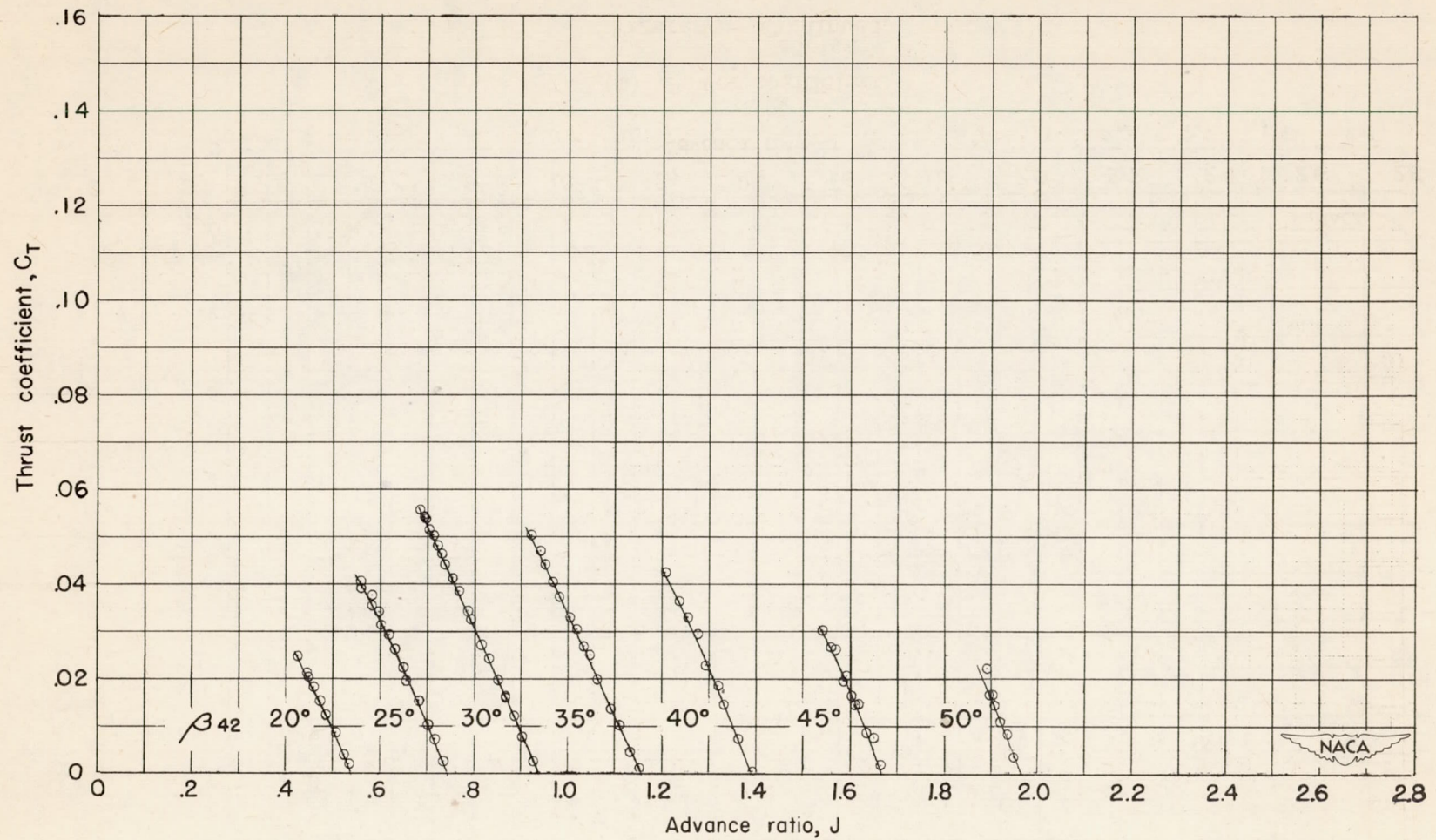
(c) Power coefficient.

Figure 6.- Continued.



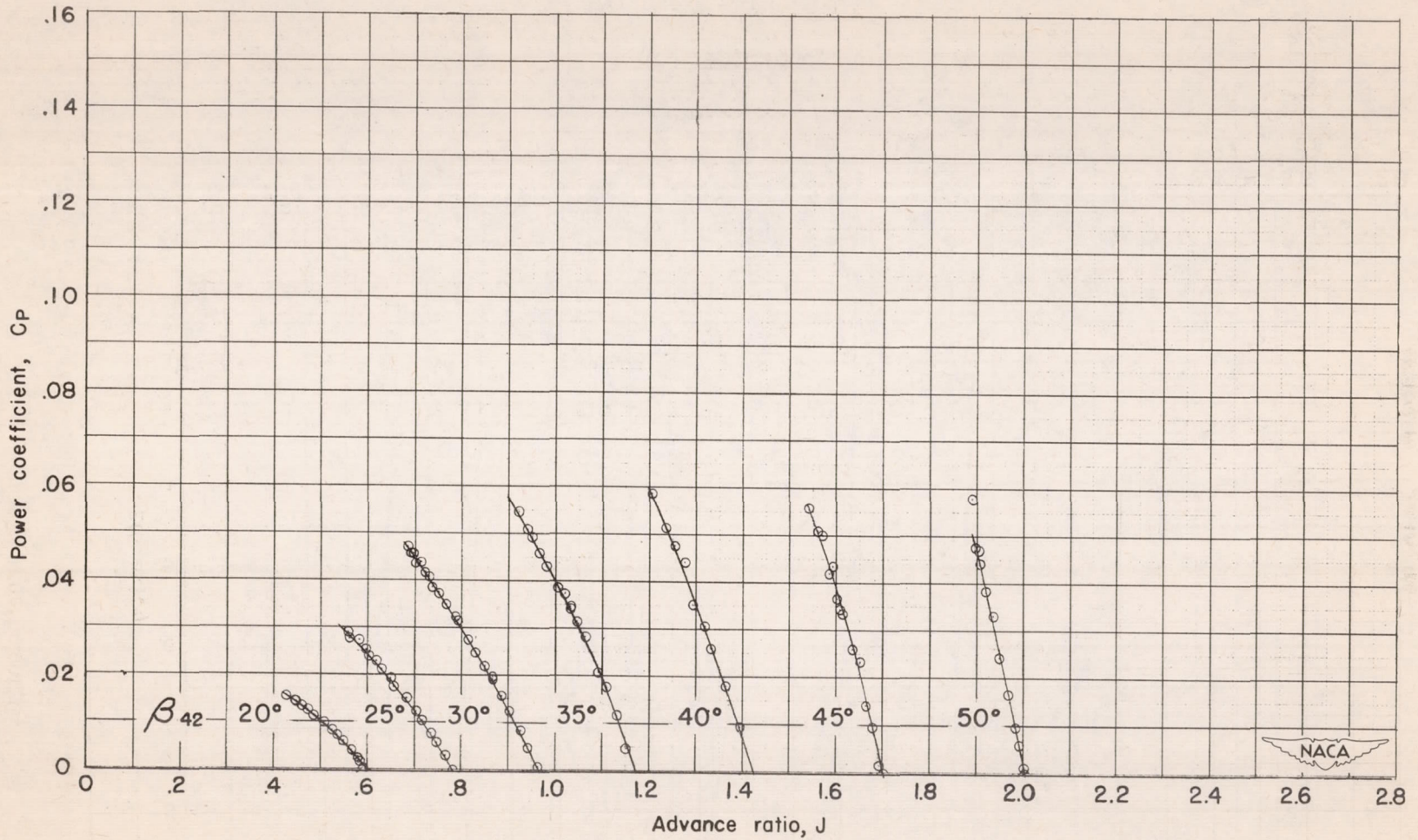
(d) Efficiency.

Figure 6.- Concluded.



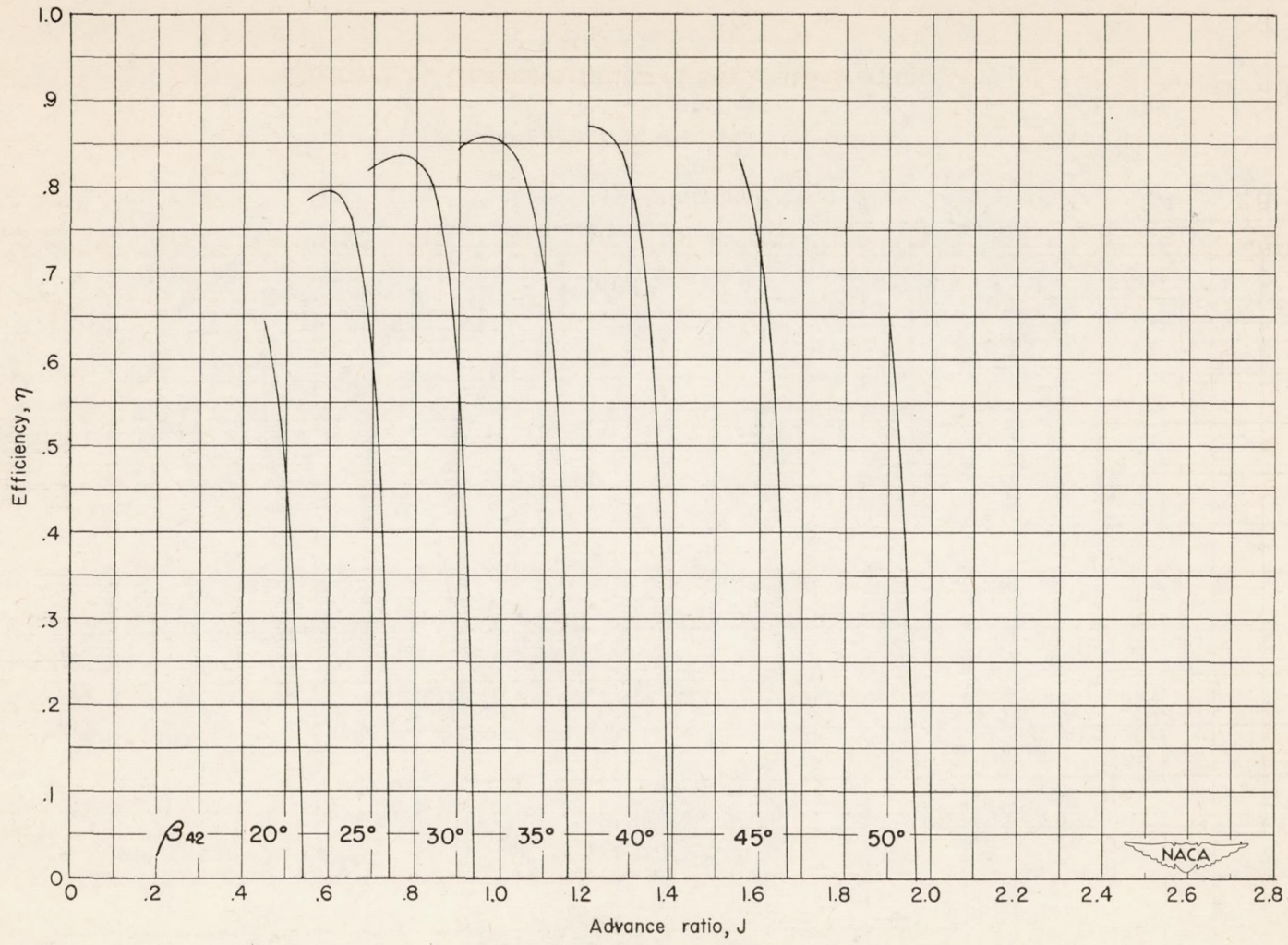
(a) Thrust coefficient.

Figure 7.- Characteristics of set I at 1500 rpm.



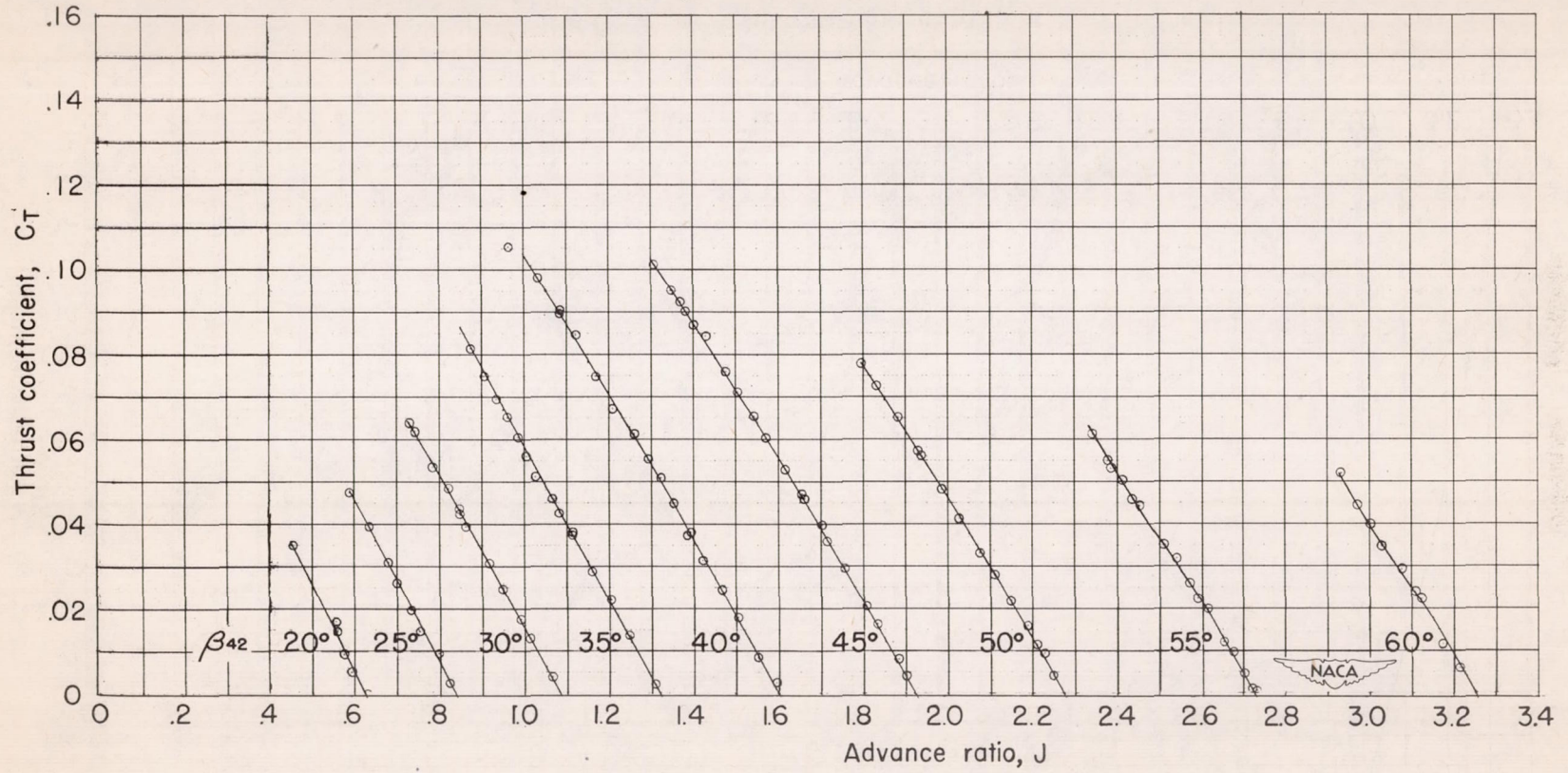
(b) Power coefficient.

Figure 7.- Continued.



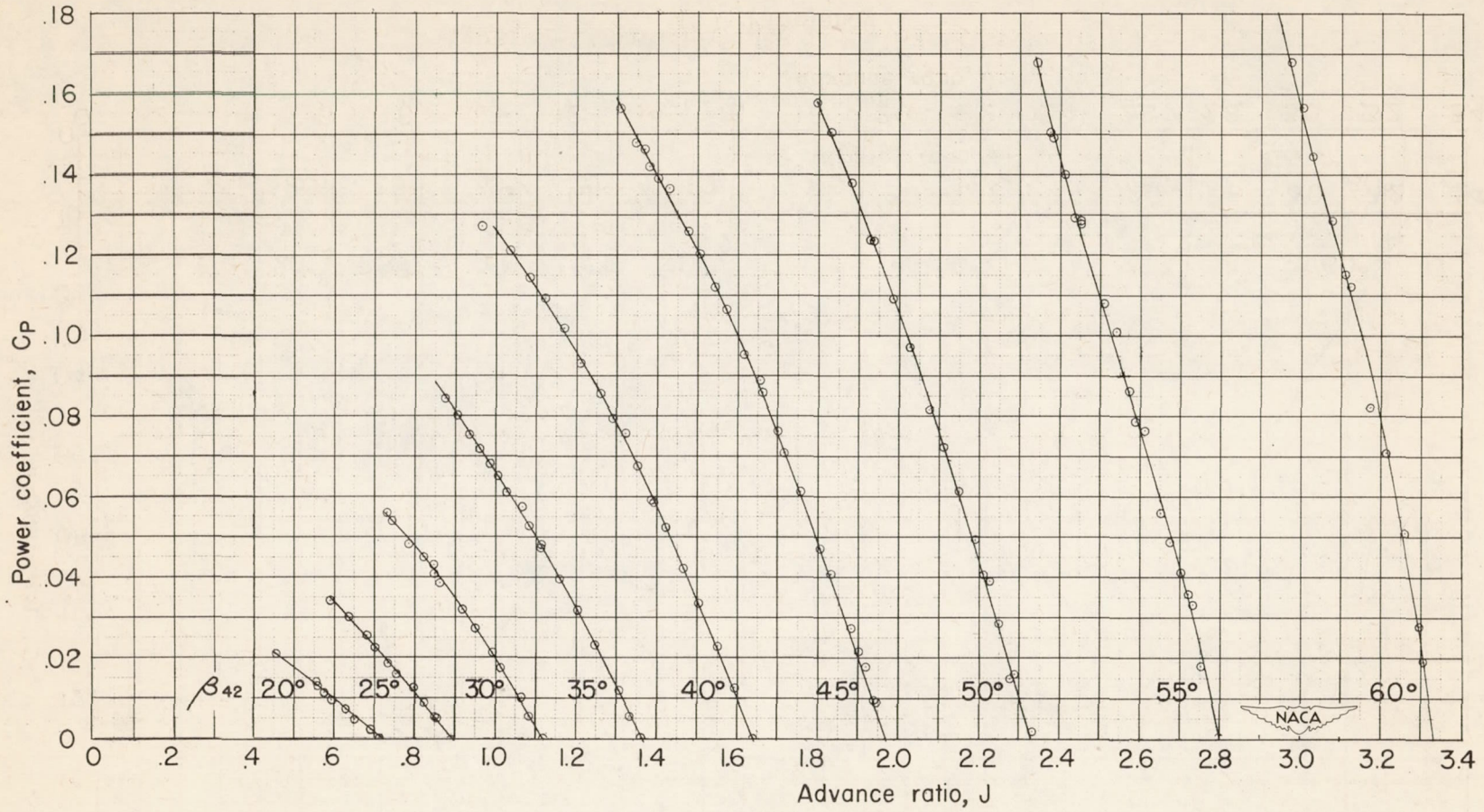
(c) Efficiency.

Figure 7.- Concluded.



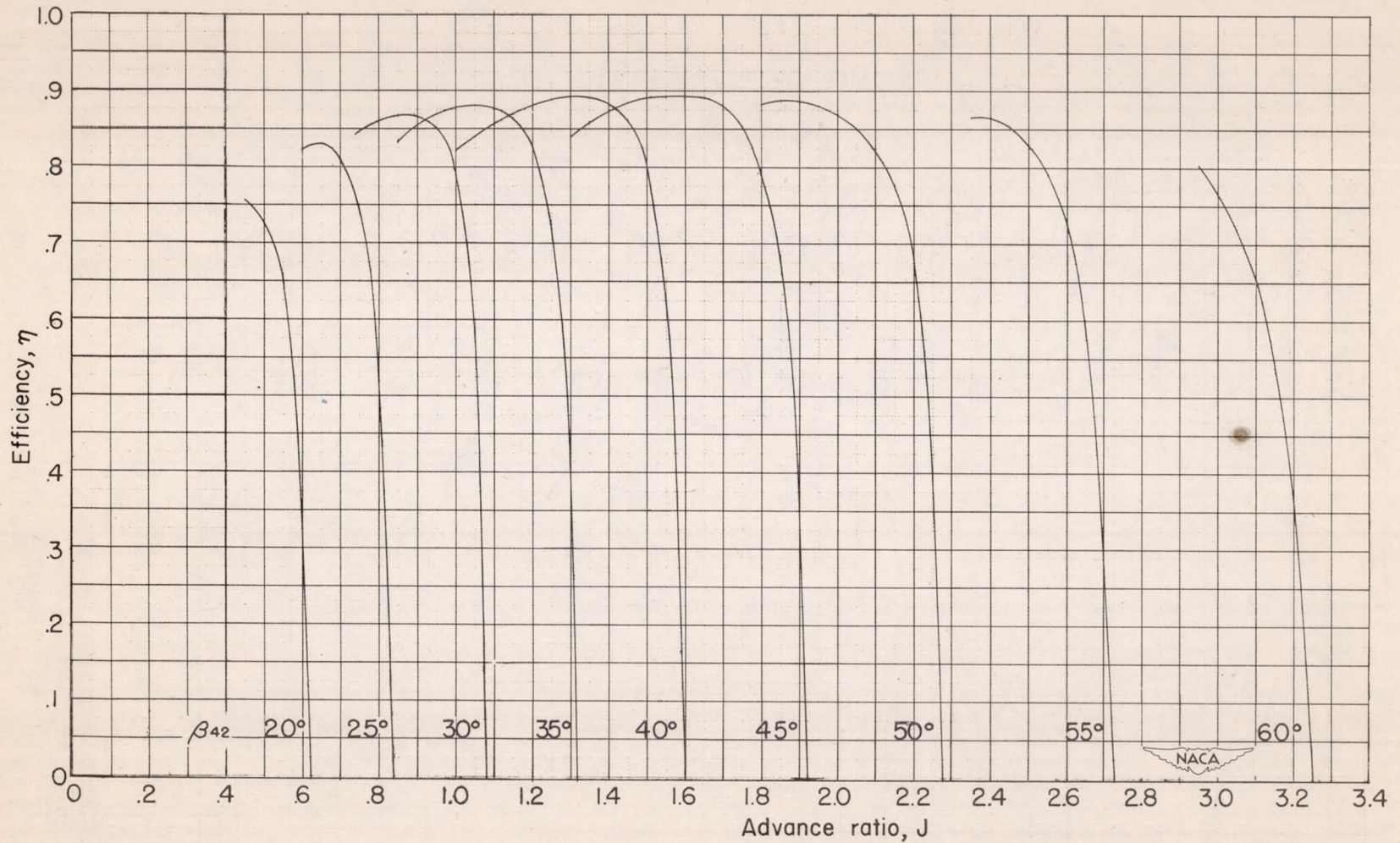
(a) Thrust coefficient.

Figure 8.- Characteristics of set II at 960 rpm.



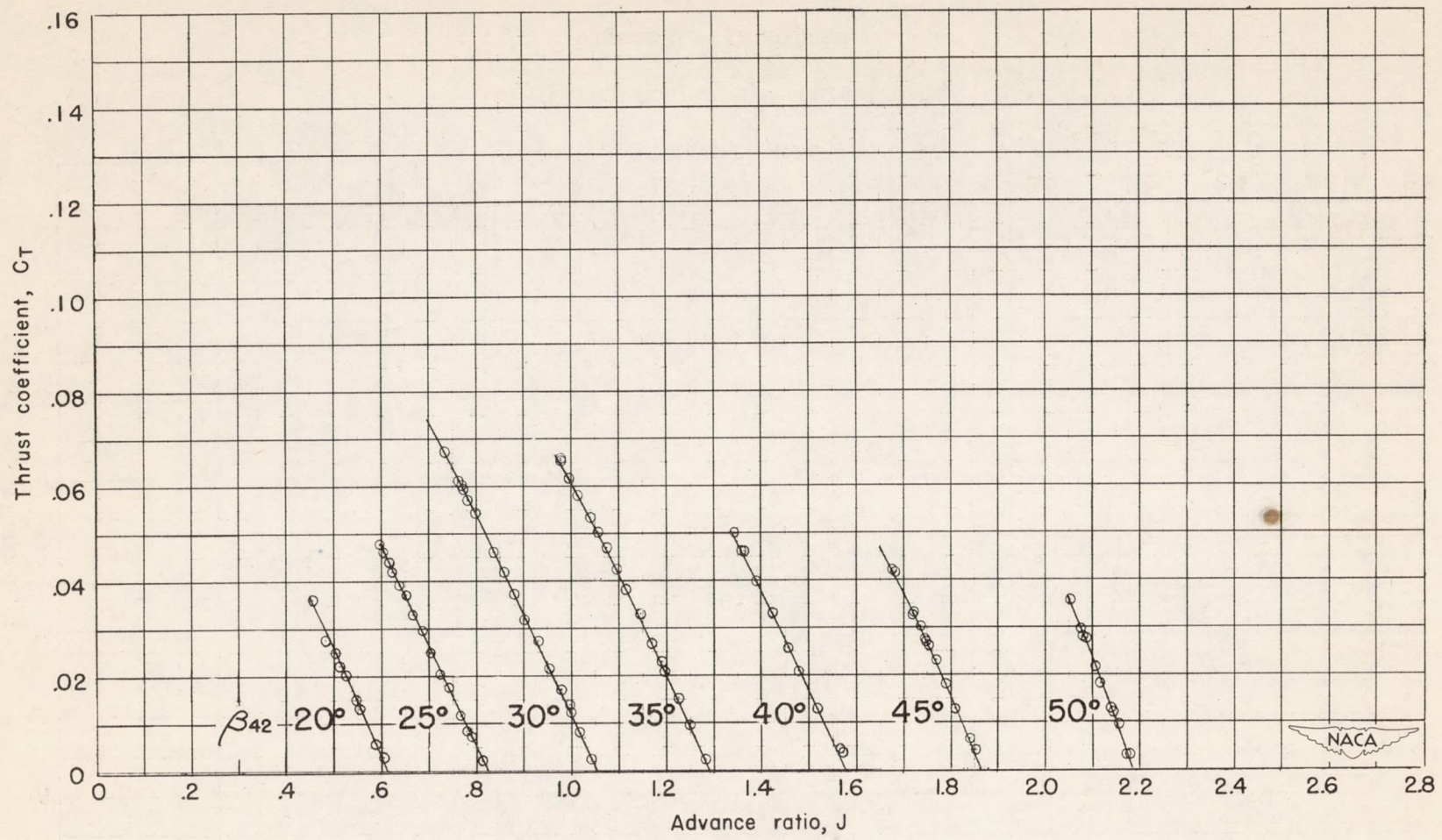
(b) Power coefficient.

Figure 8.- Continued.



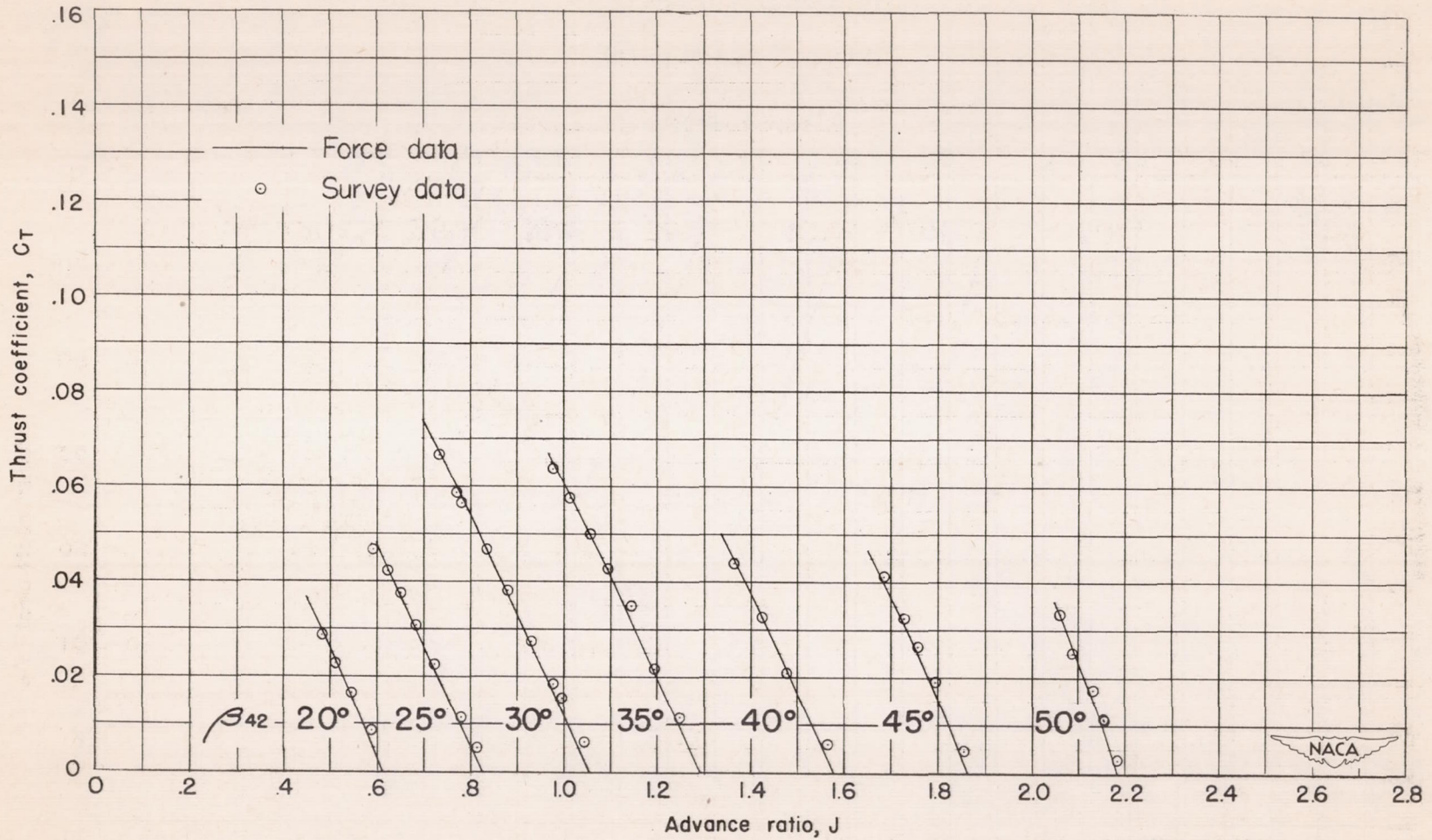
(c) Efficiency.

Figure 8.- Concluded.



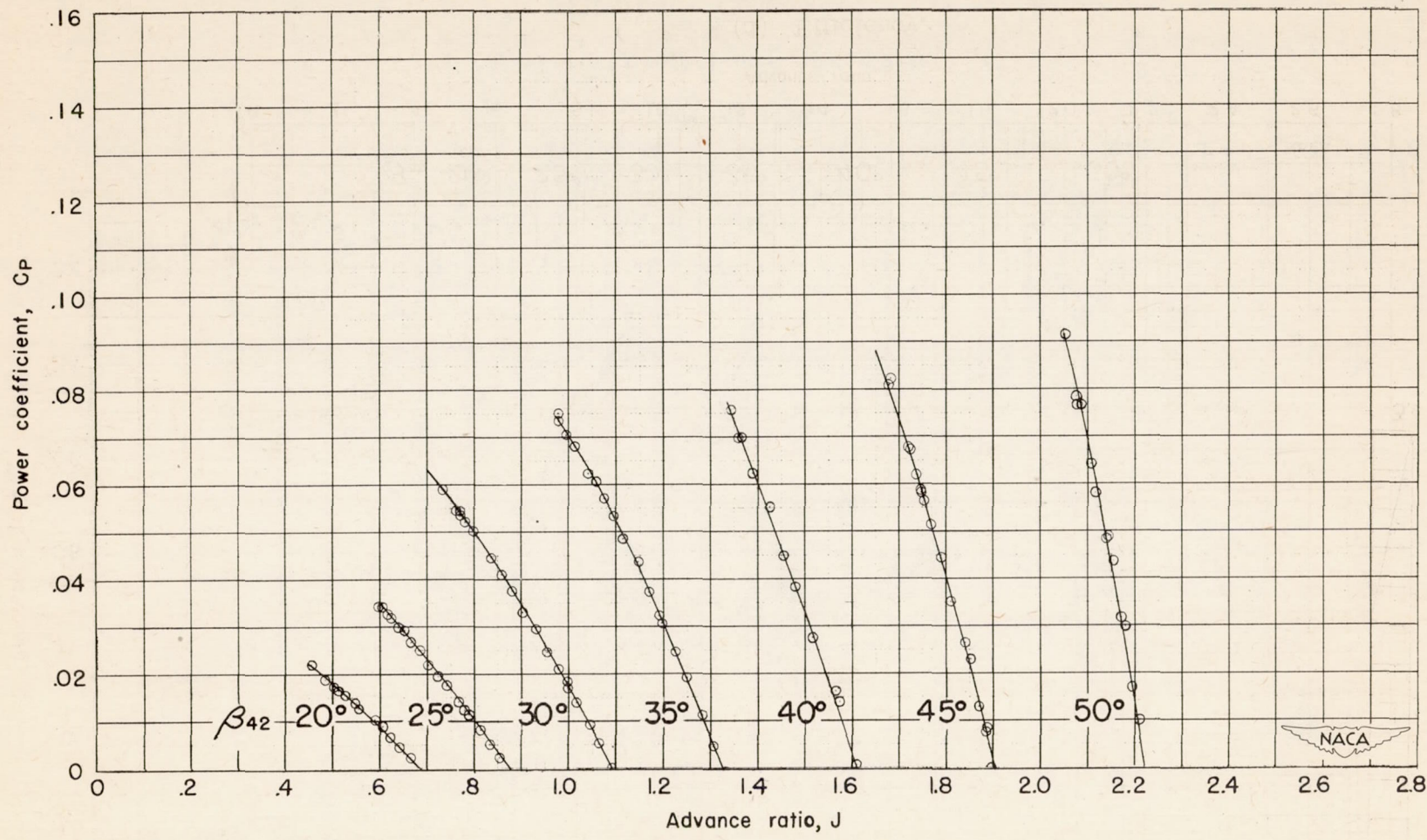
(a) Thrust coefficient - force data.

Figure 9.- Characteristics of set II at 1350 rpm.



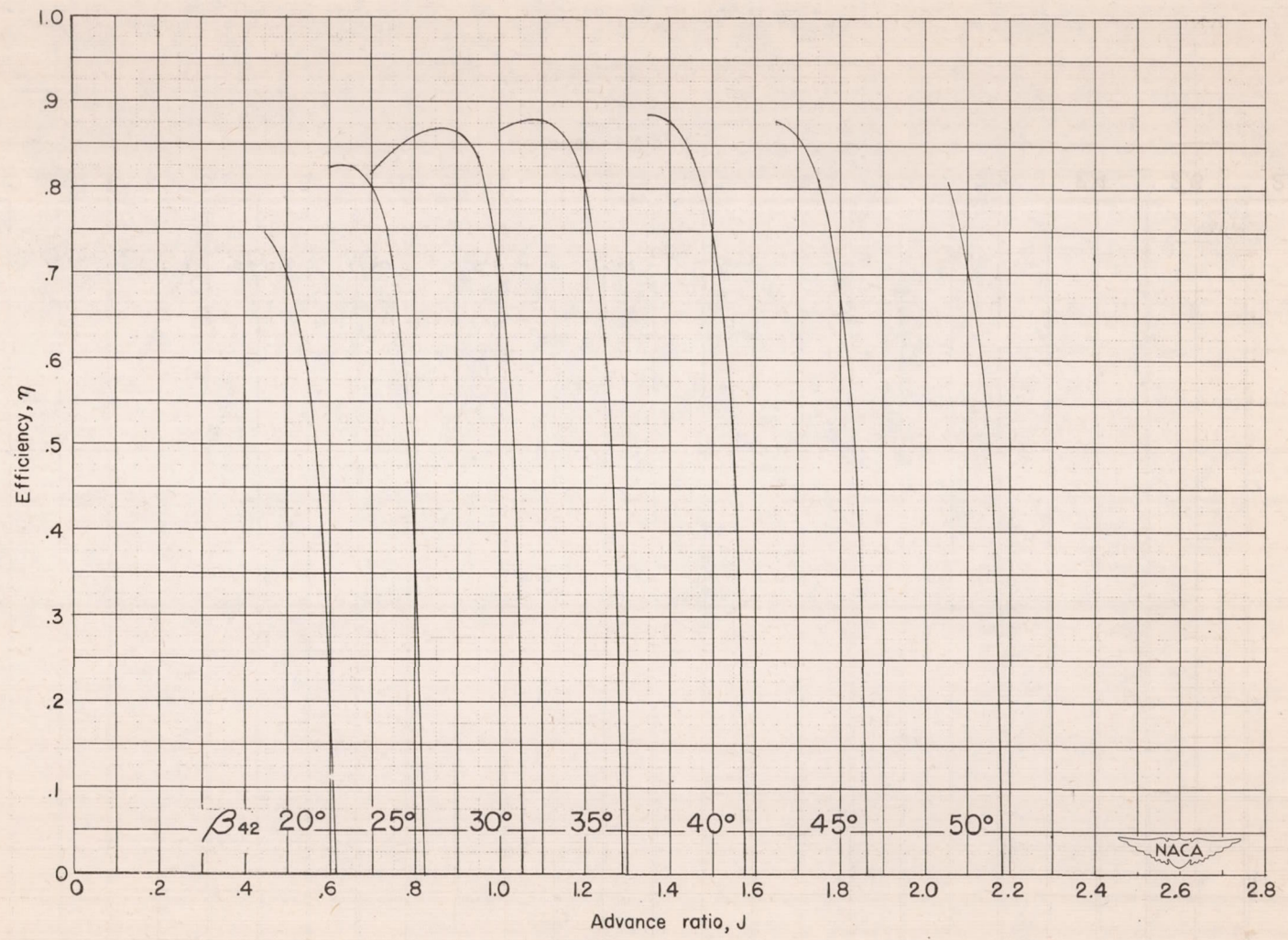
(b) Thrust coefficient - survey data.

Figure 9.- Continued.



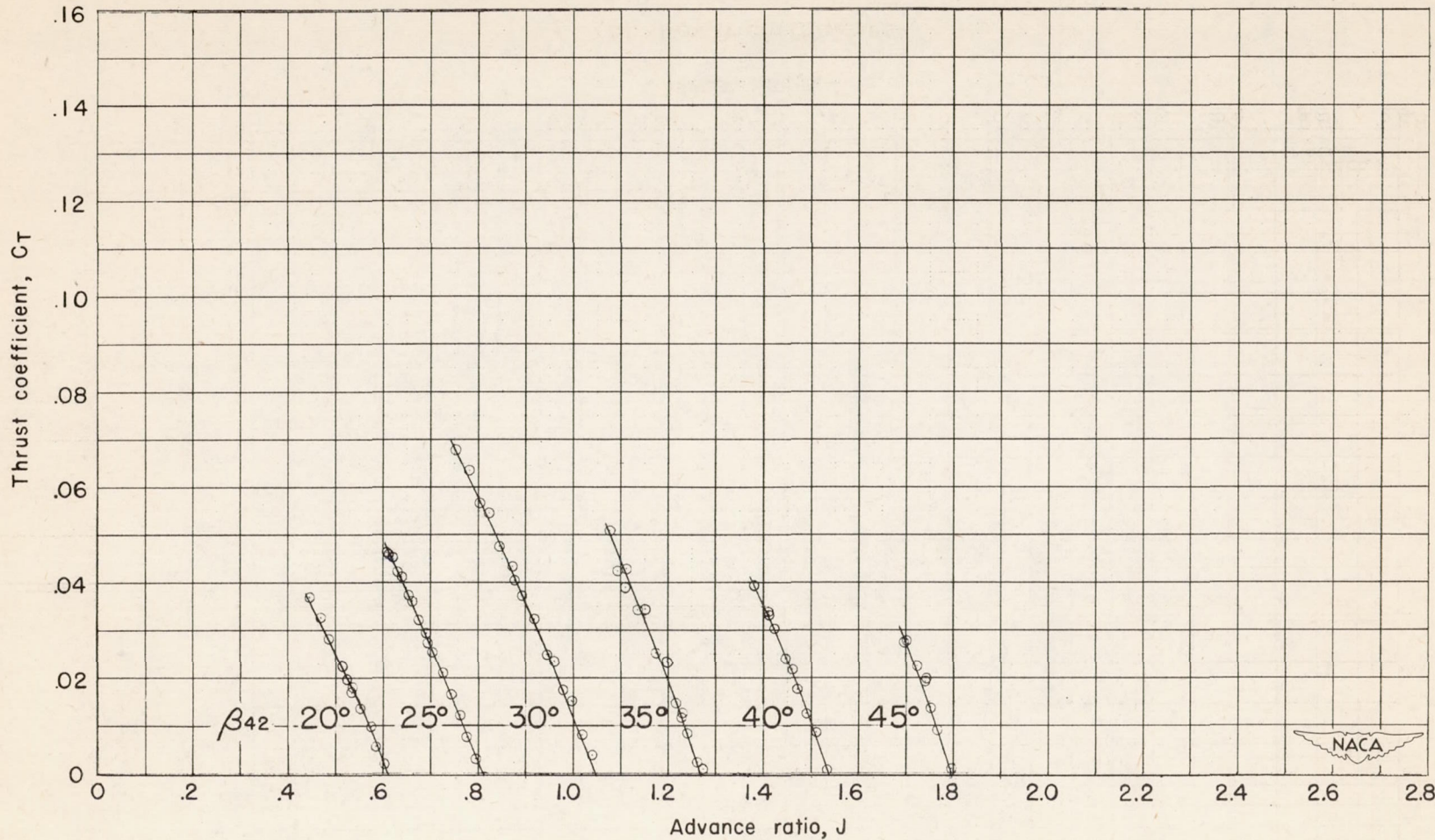
(c) Power coefficient.

Figure 9.- Continued.



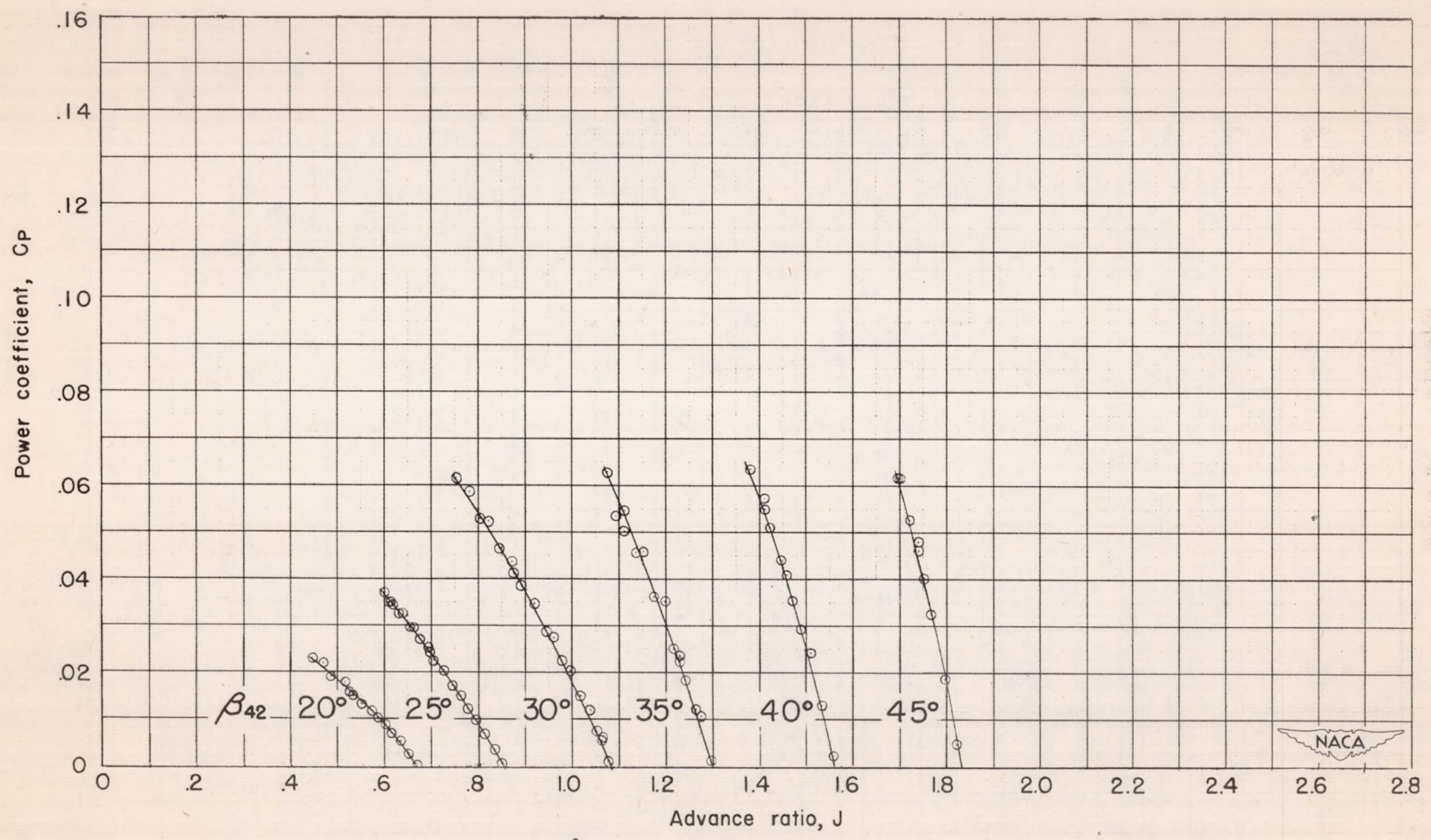
(d) Efficiency.

Figure 9.- Concluded.



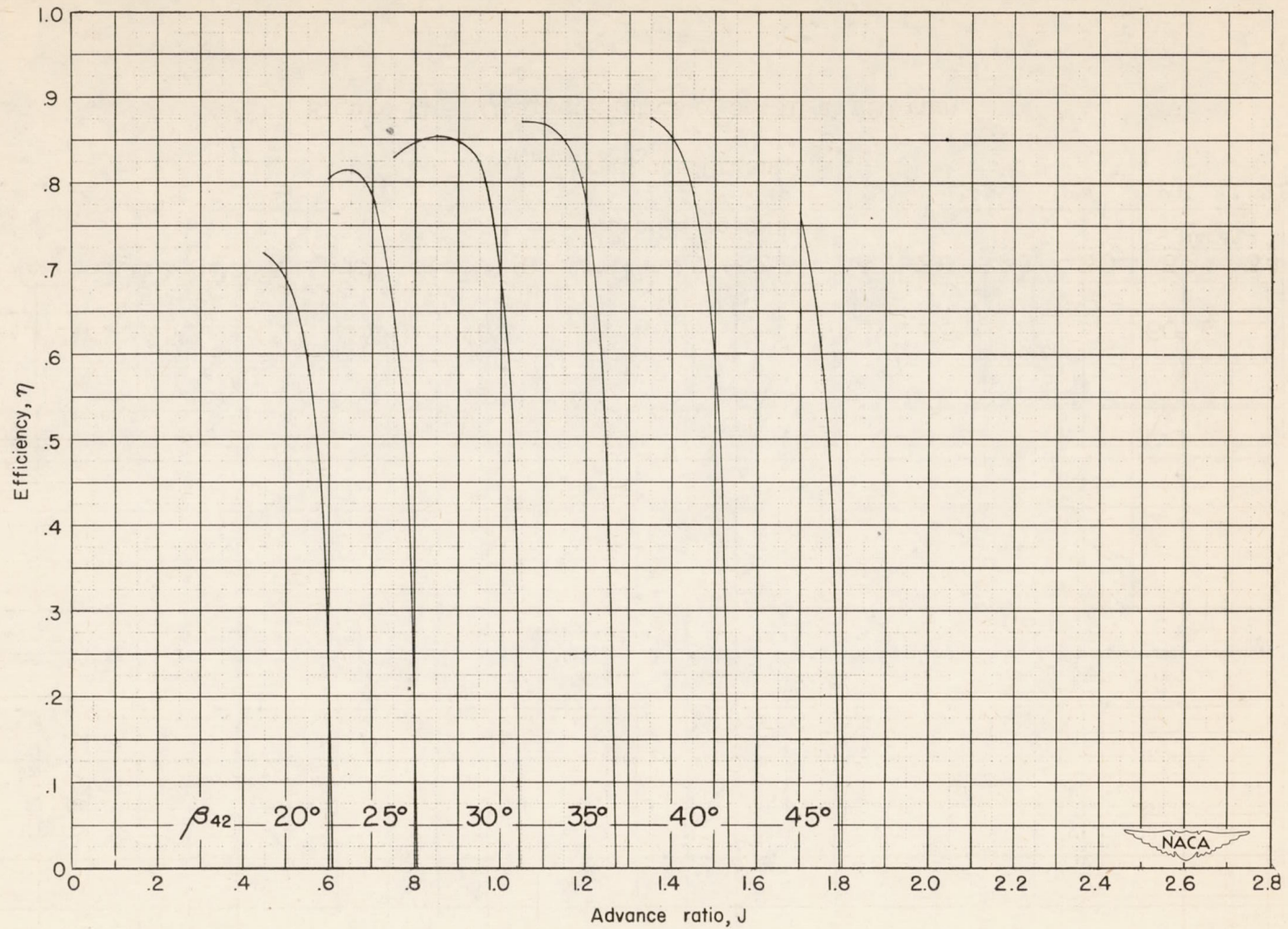
(a) Thrust coefficient.

Figure 10.- Characteristics of set II at 1500 rpm.



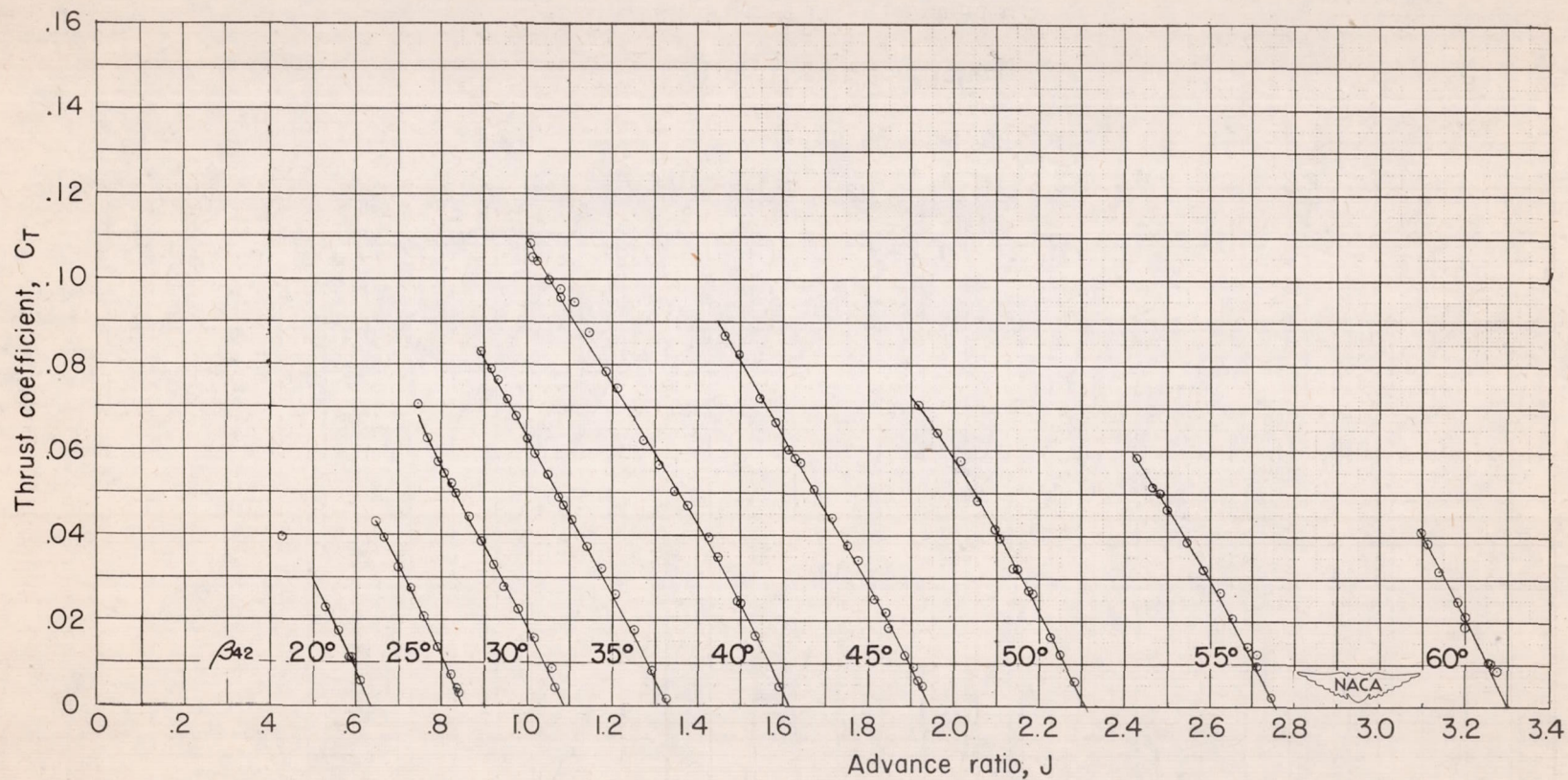
(b) Power coefficient.

Figure 10.- Continued.



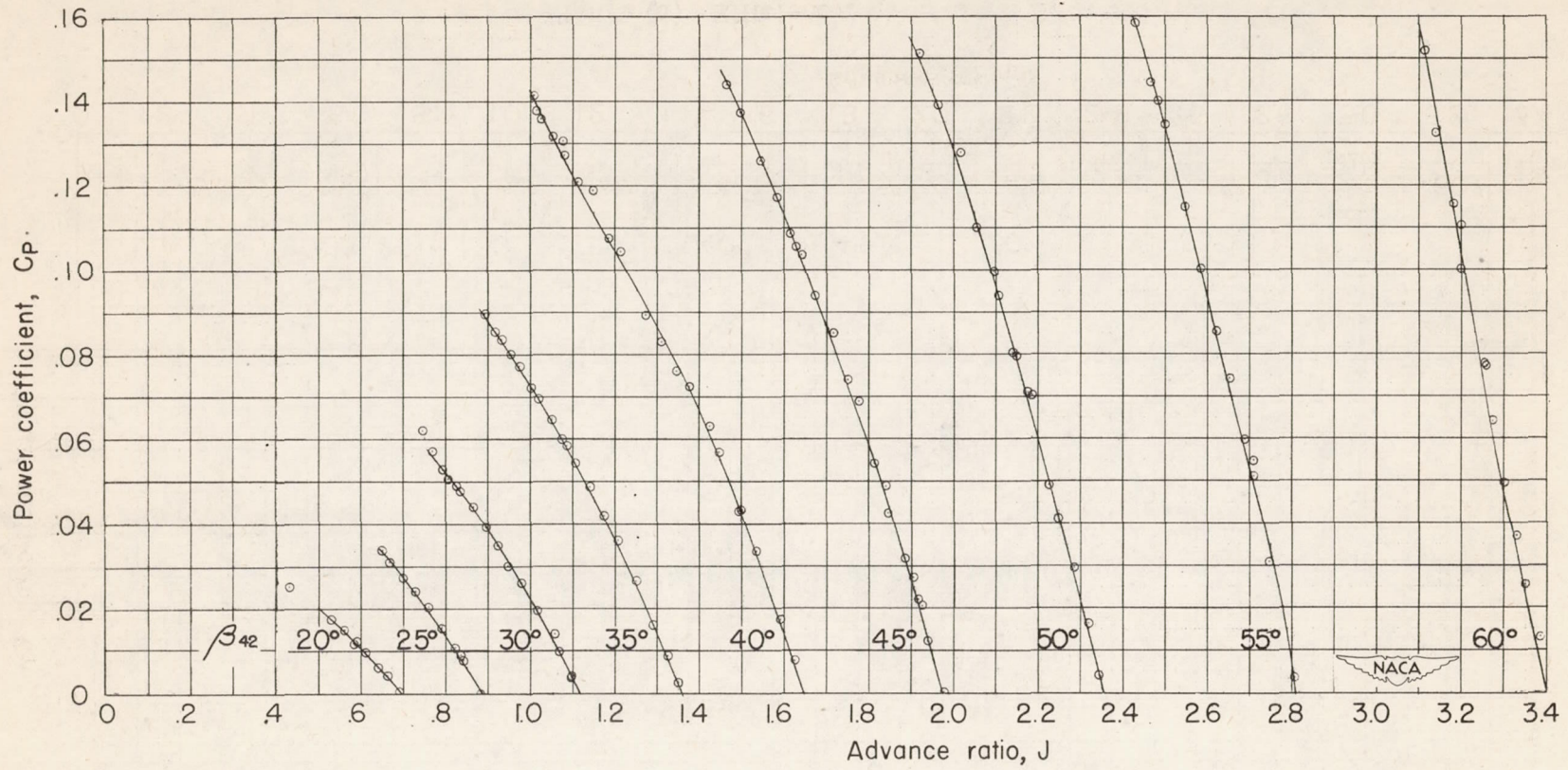
(c) Efficiency.

Figure 10.- Concluded.



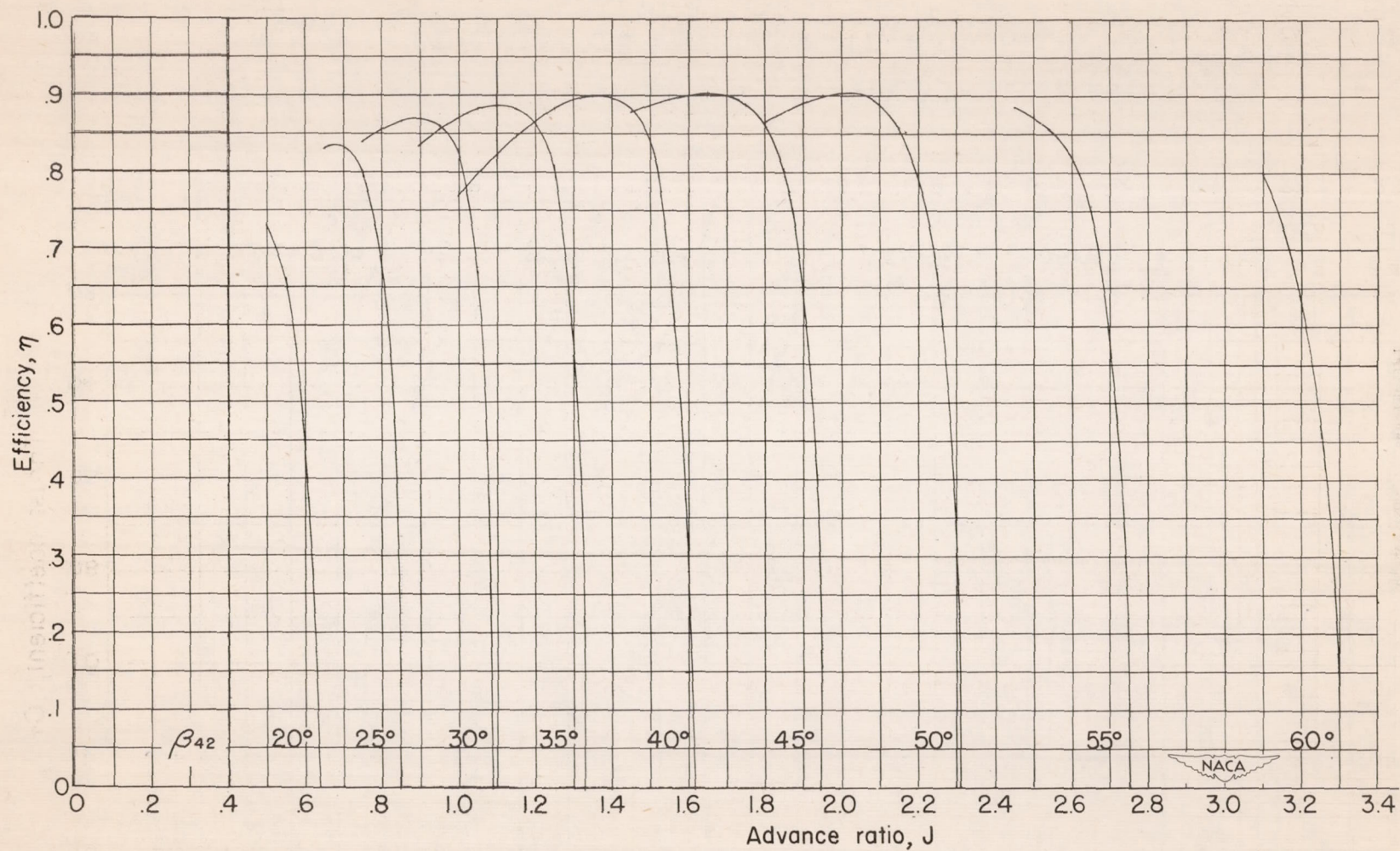
(a) Thrust coefficient.

Figure 11.- Characteristics of set III at 960 rpm.



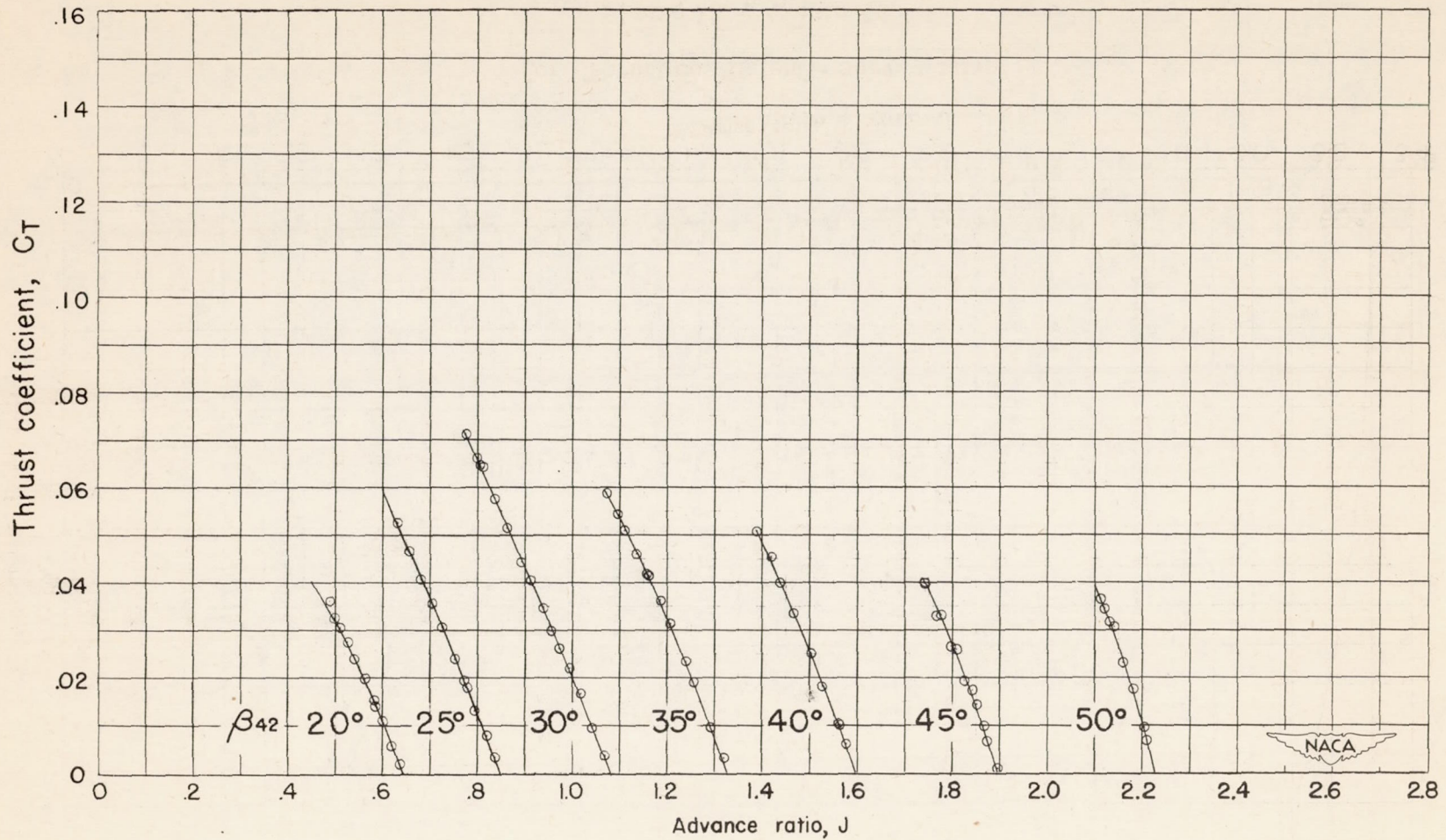
(b) Power coefficient.

Figure 11.- Continued.



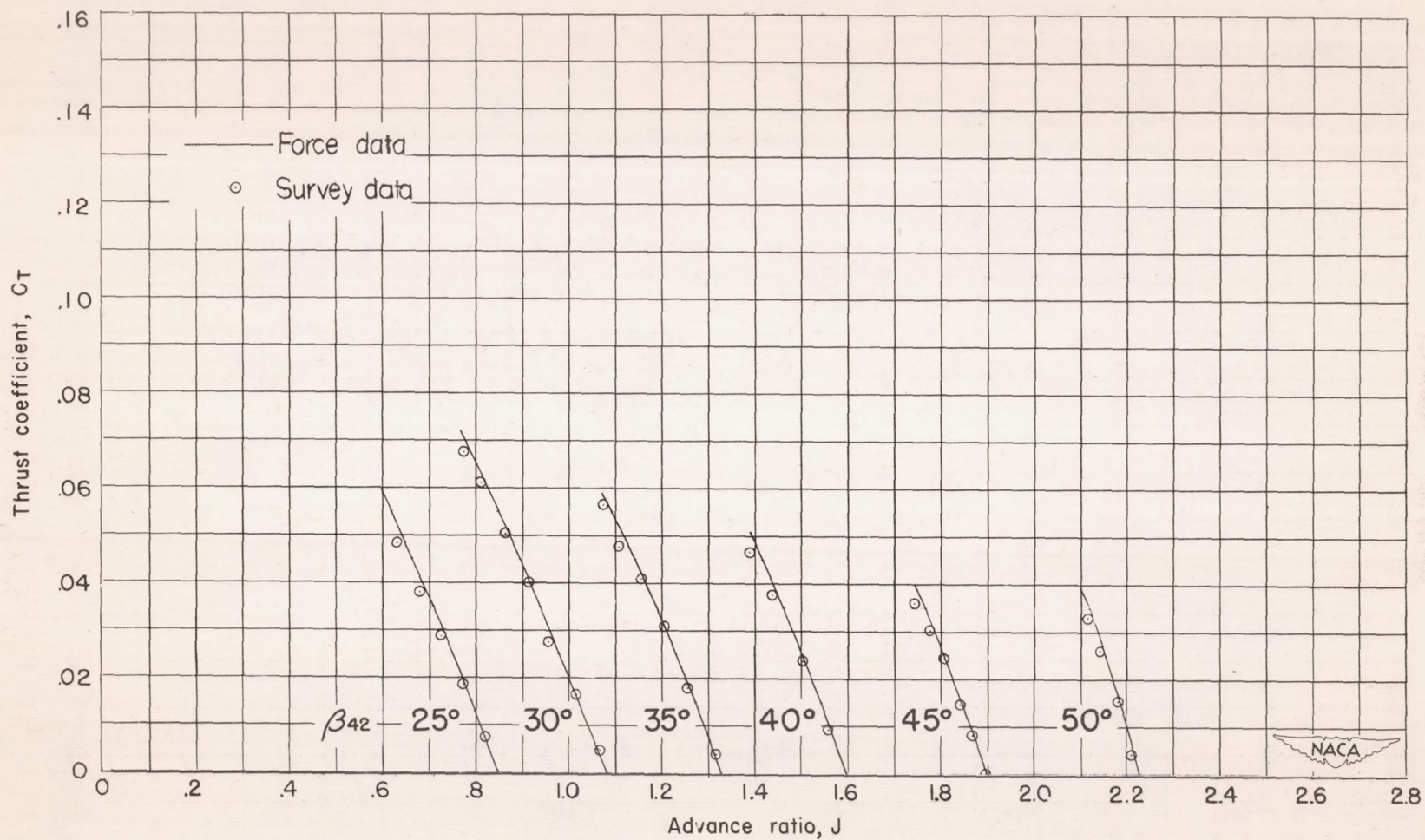
(c) Efficiency.

Figure 11.- .Concluded.



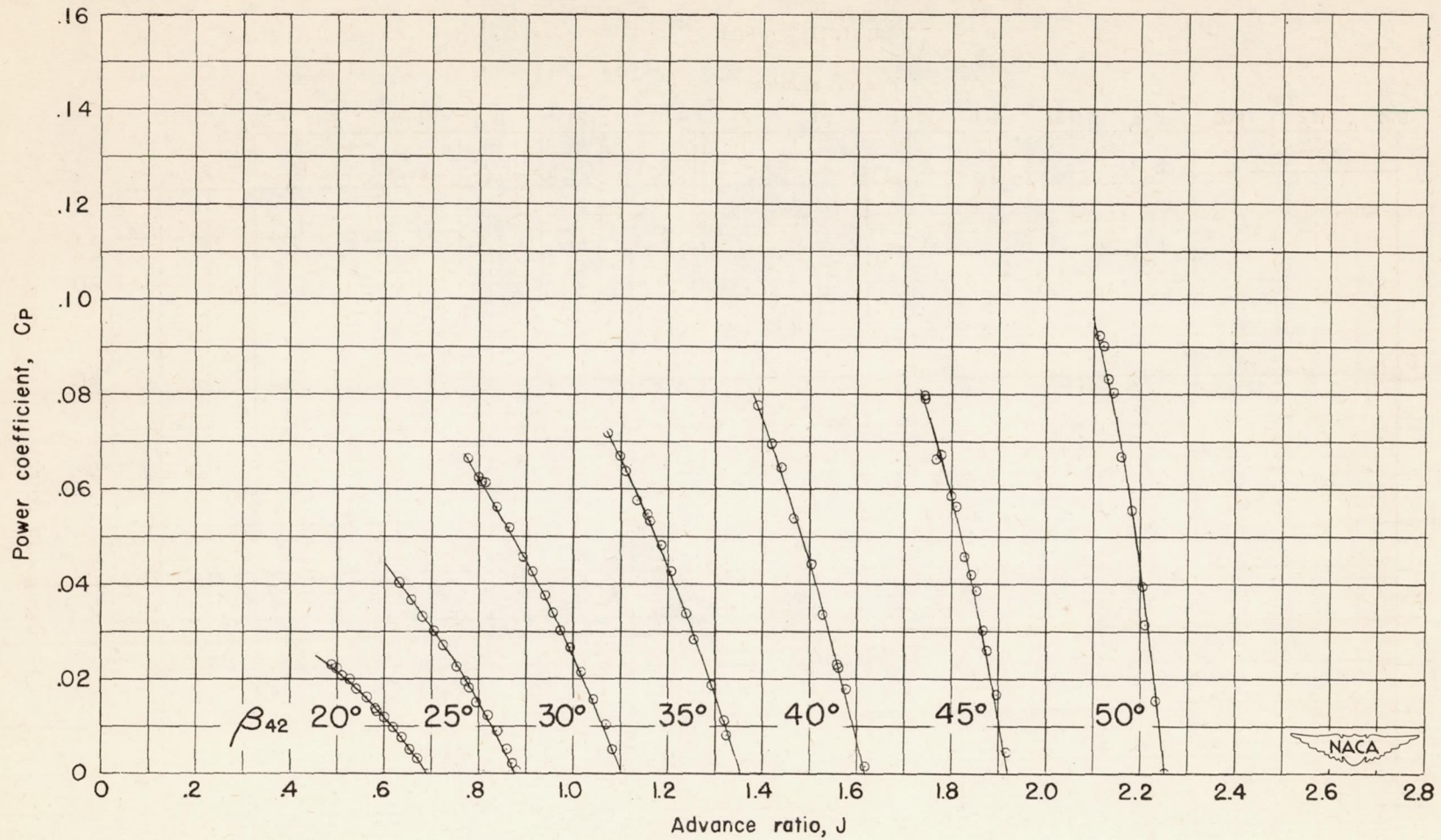
(a) Thrust coefficient - force data.

Figure 12.- Characteristics of set III at 1350 rpm.



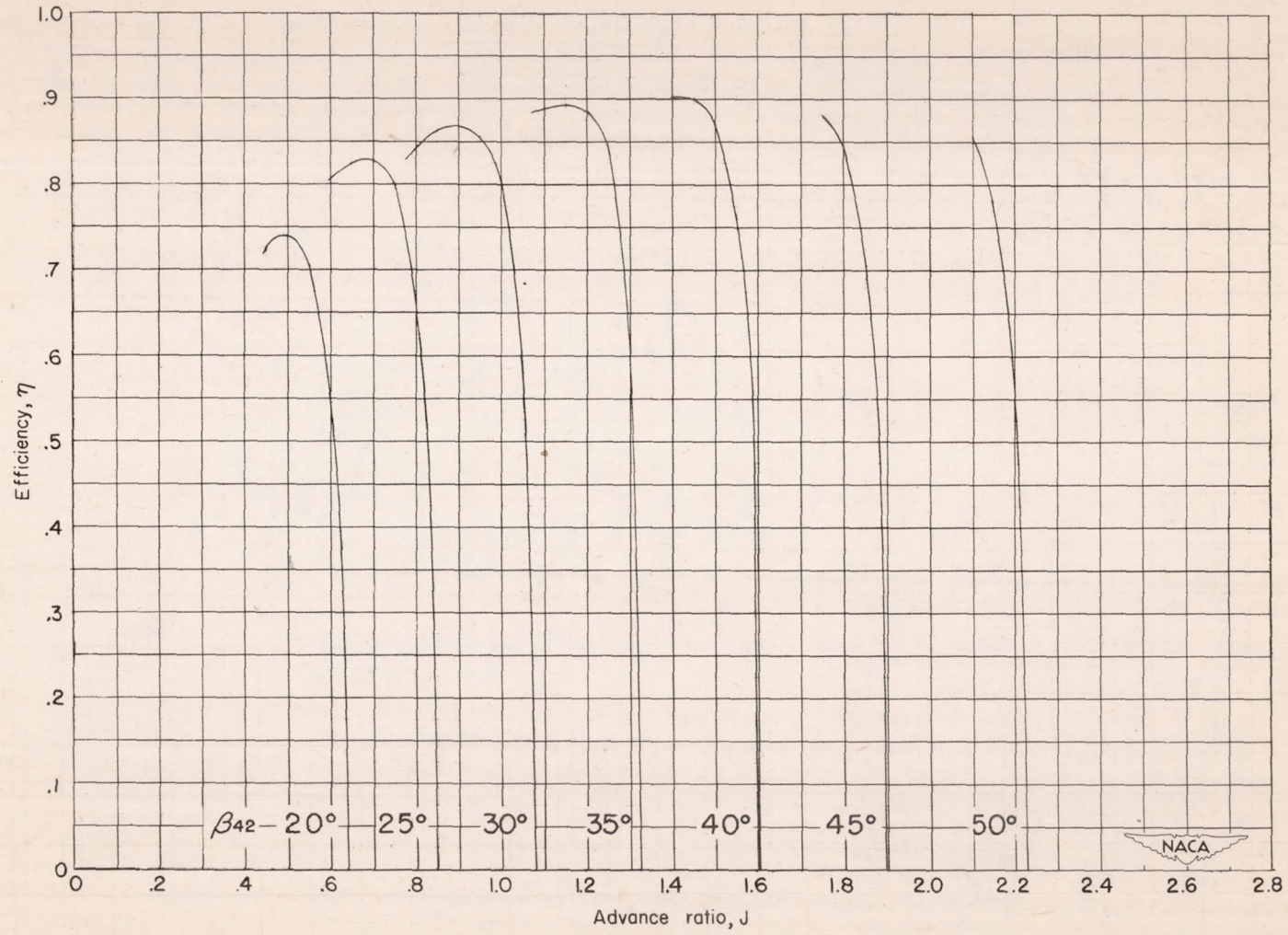
(b) Thrust coefficient - survey data.

Figure 12.-. Continued.



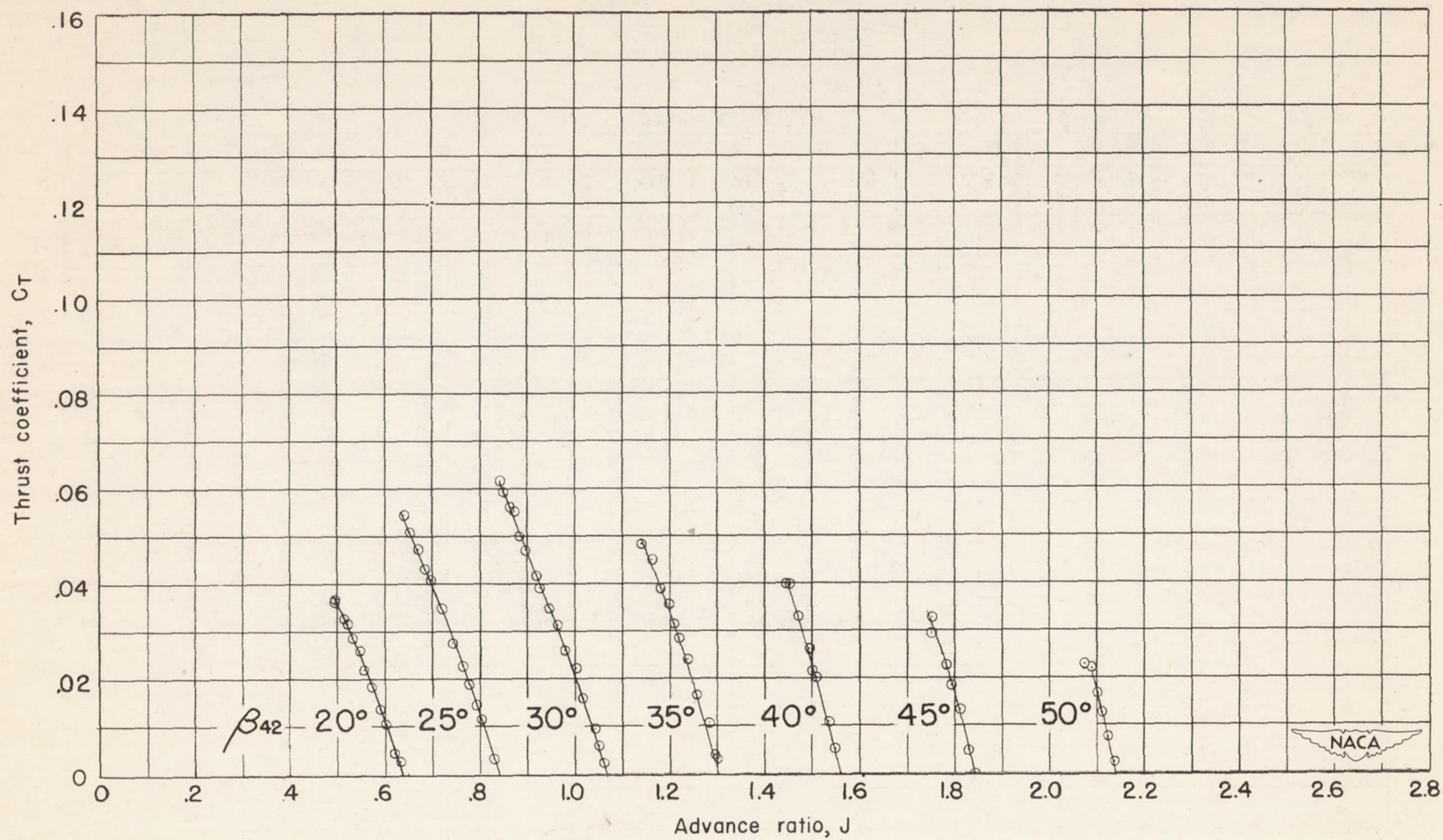
(c) Power coefficient.

Figure 12.- Continued.



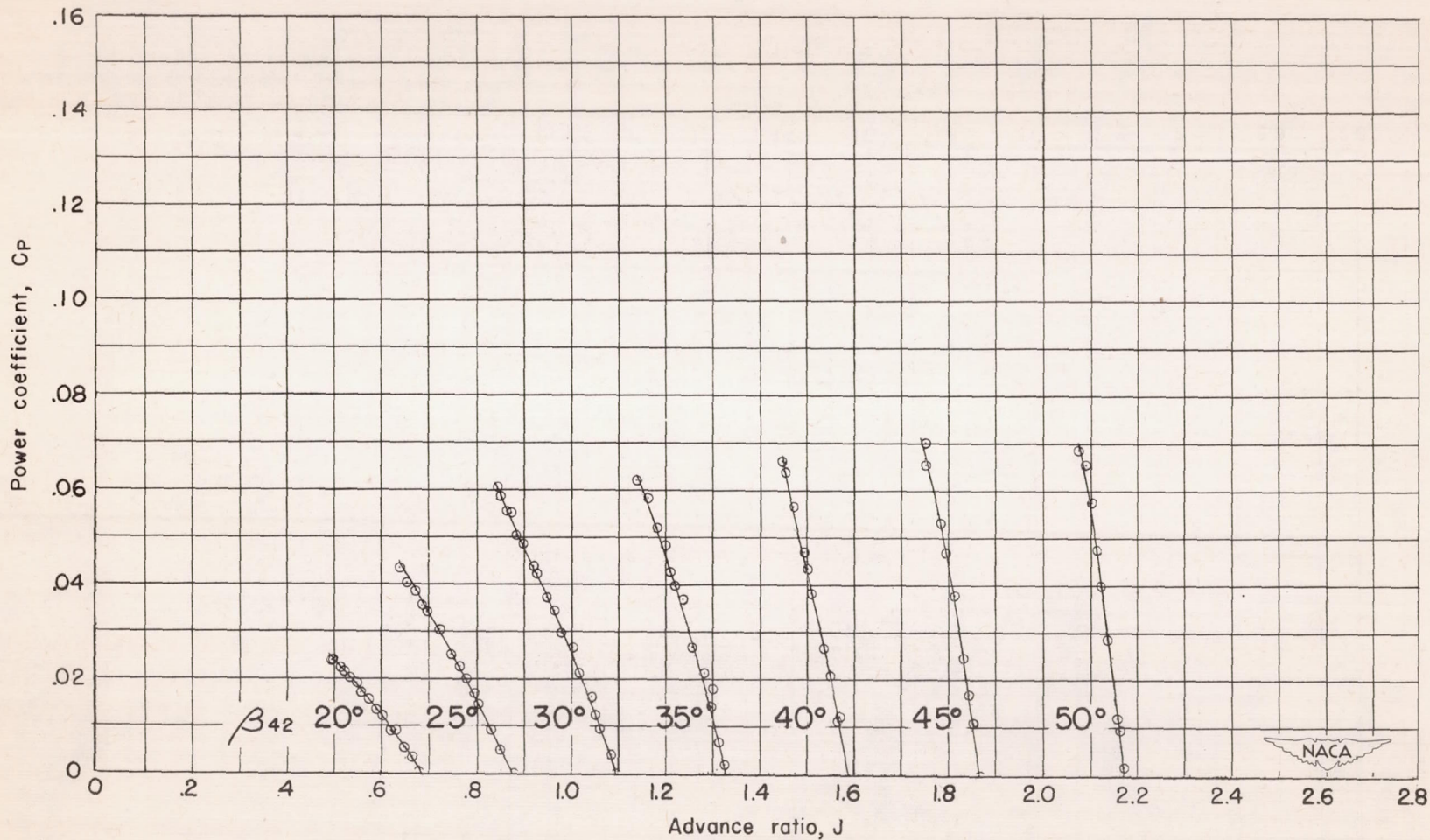
(d) Efficiency.

Figure 12.- Concluded.



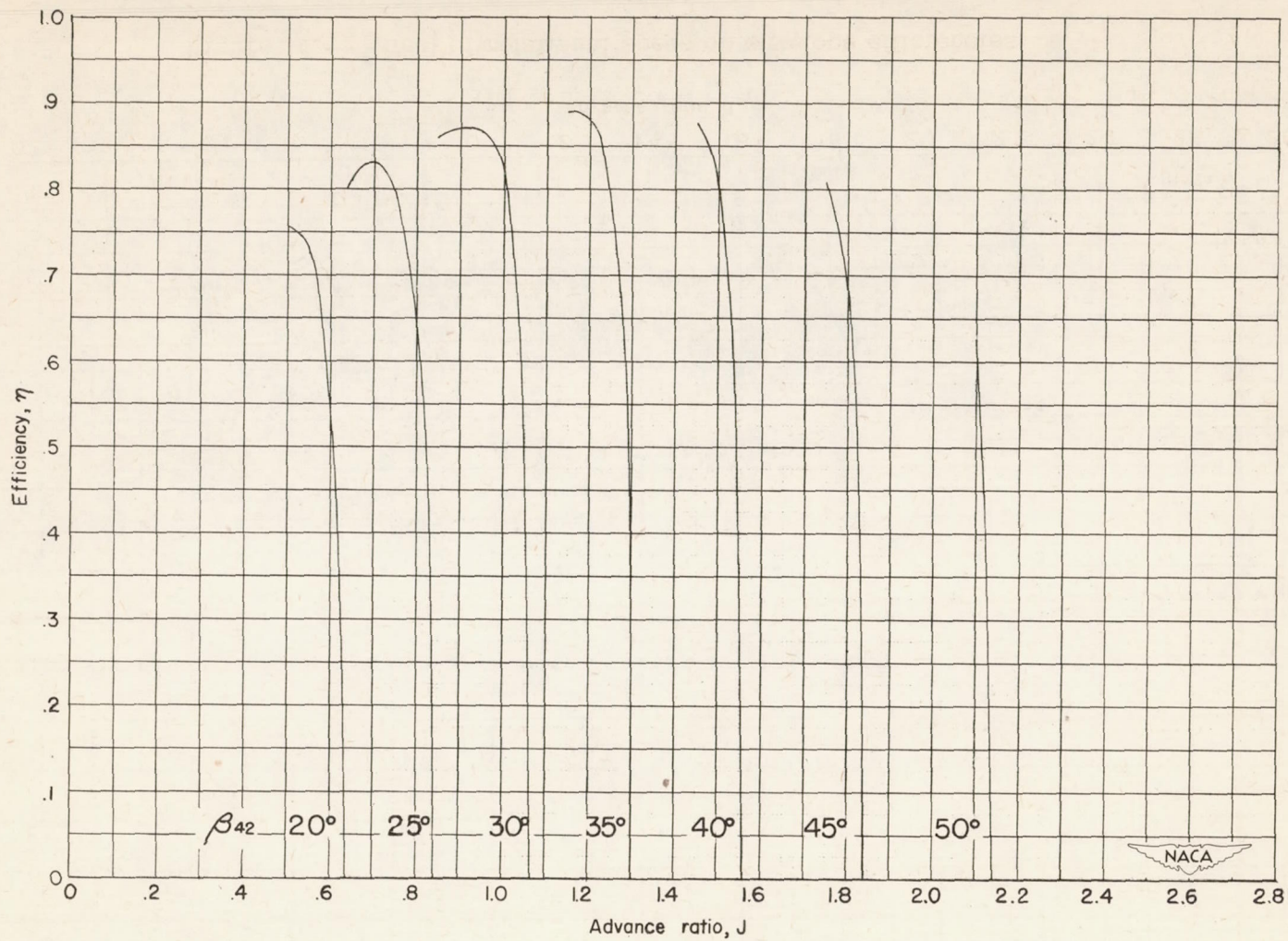
(a) Thrust coefficient.

Figure 13.- Characteristics of set III at 1500 rpm.



(b) Power coefficient.

Figure 13.- Continued.



(c) Efficiency.

Figure 13.- Concluded.

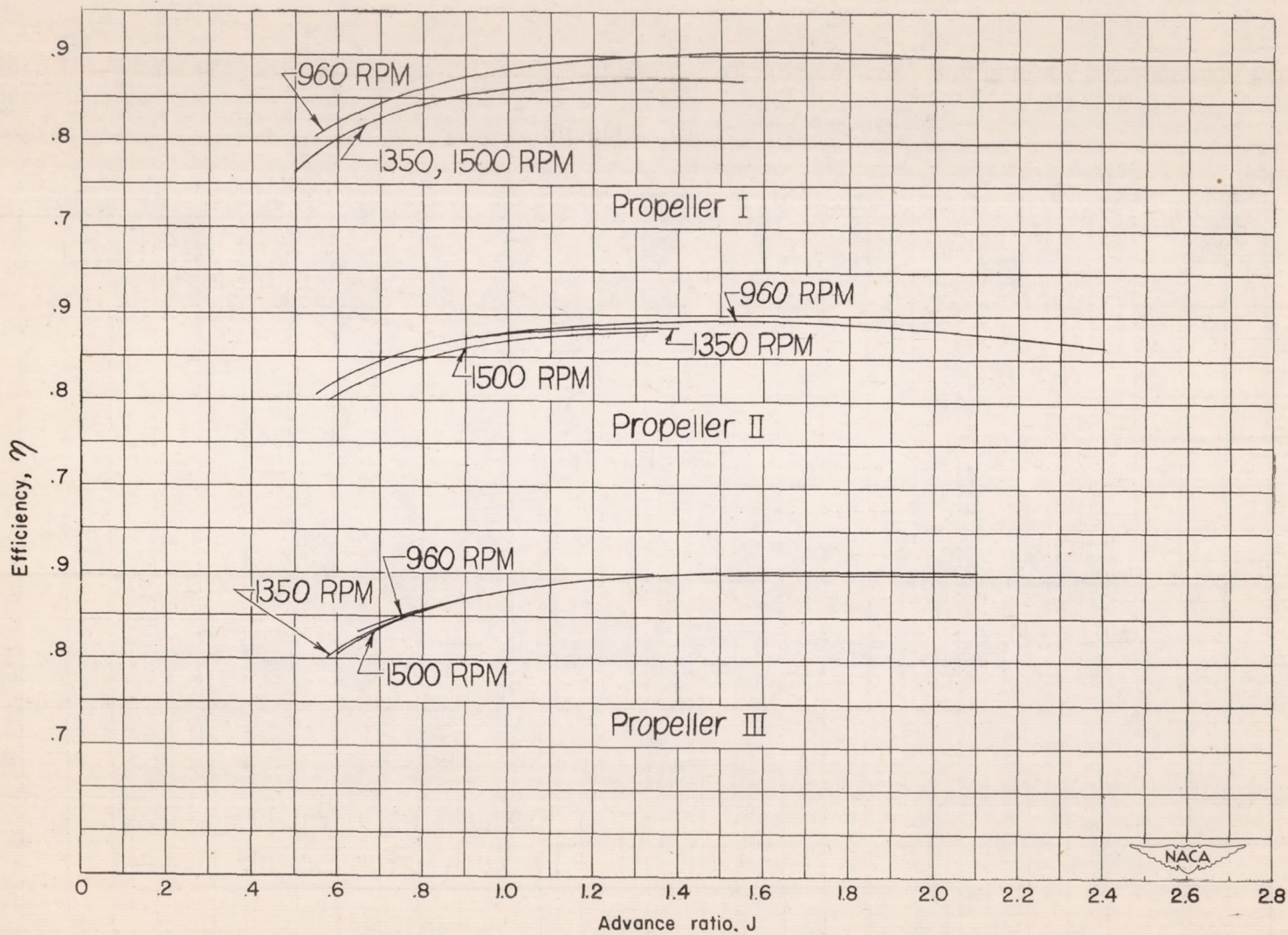


Figure 14.- Effect of rotational speed on envelope efficiencies.

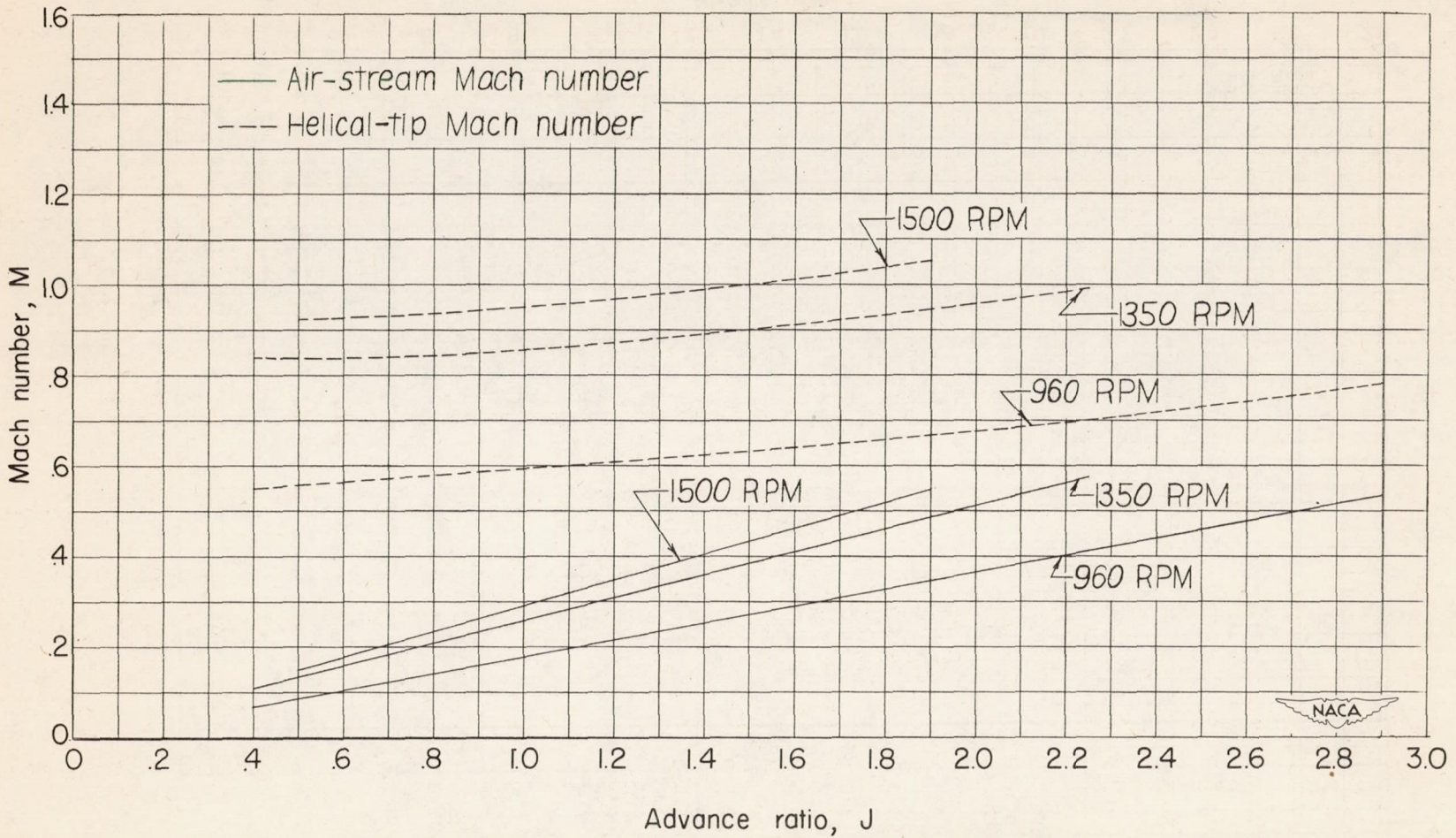


Figure 15.- Average variation of air-stream Mach number and helical-tip Mach number with advance ratio.

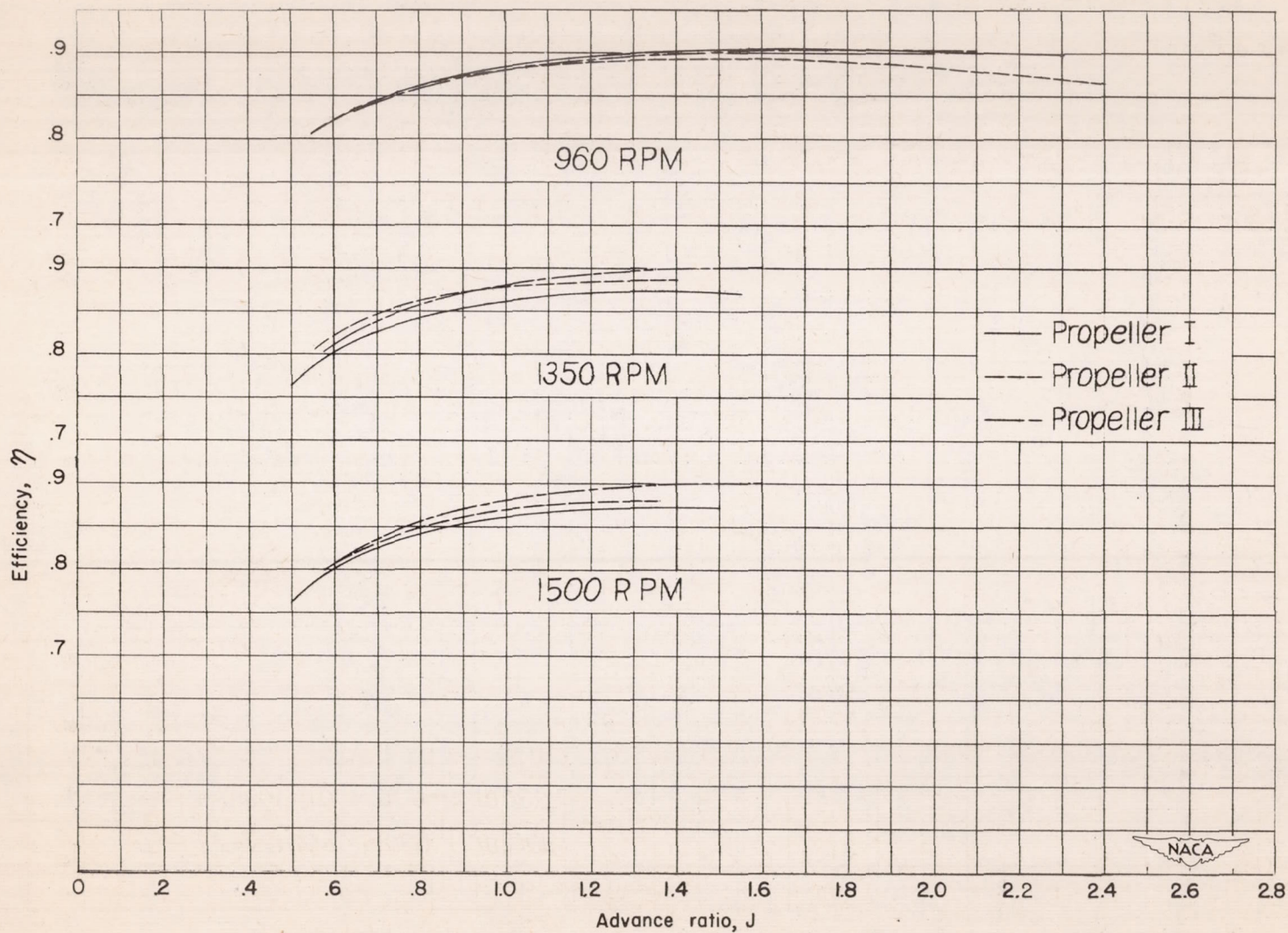


Figure 16.- Effect of blade design on envelope efficiencies.

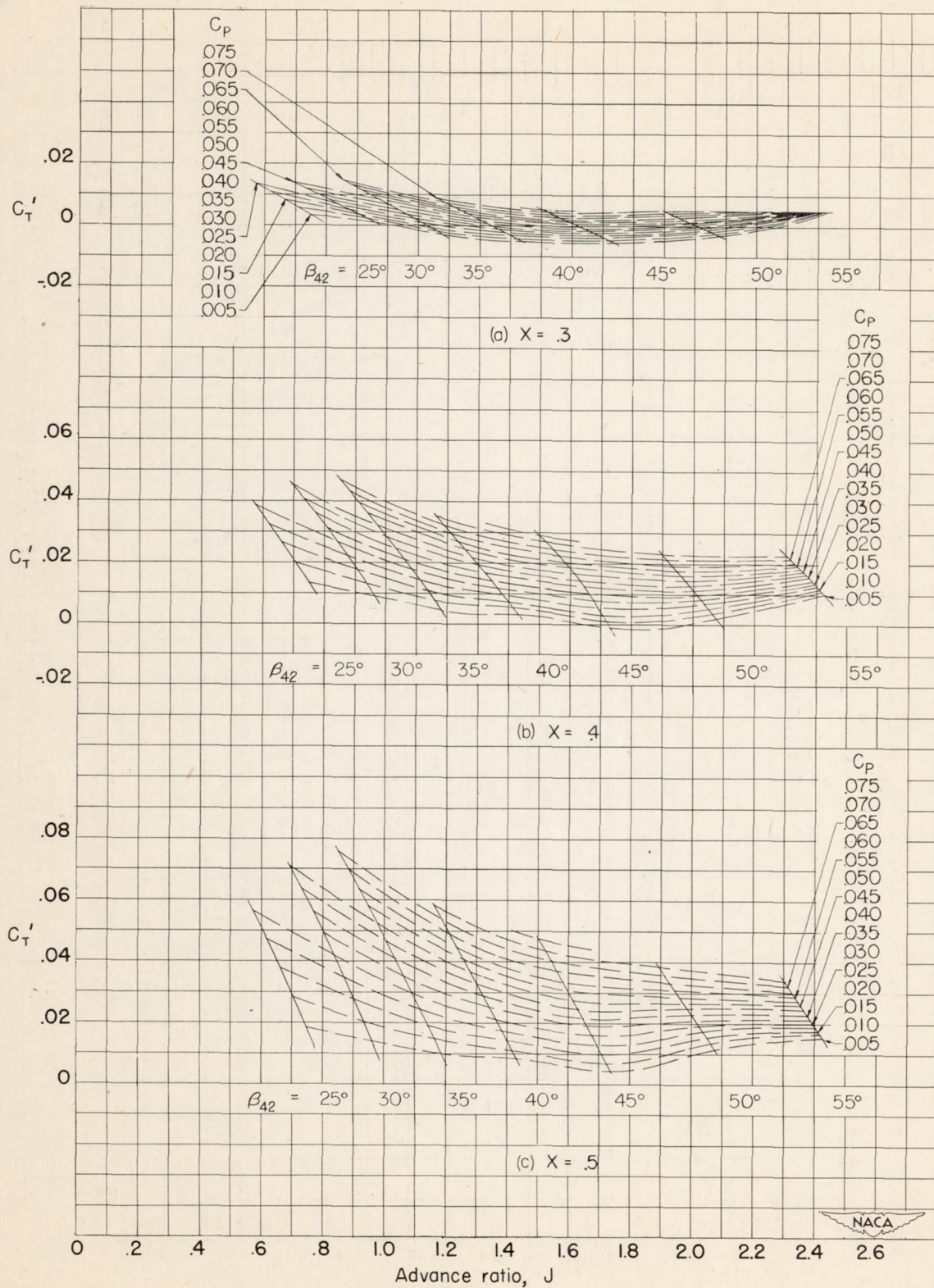


Figure 17.- Section thrust of set I from propeller surveys. 1350 rpm.

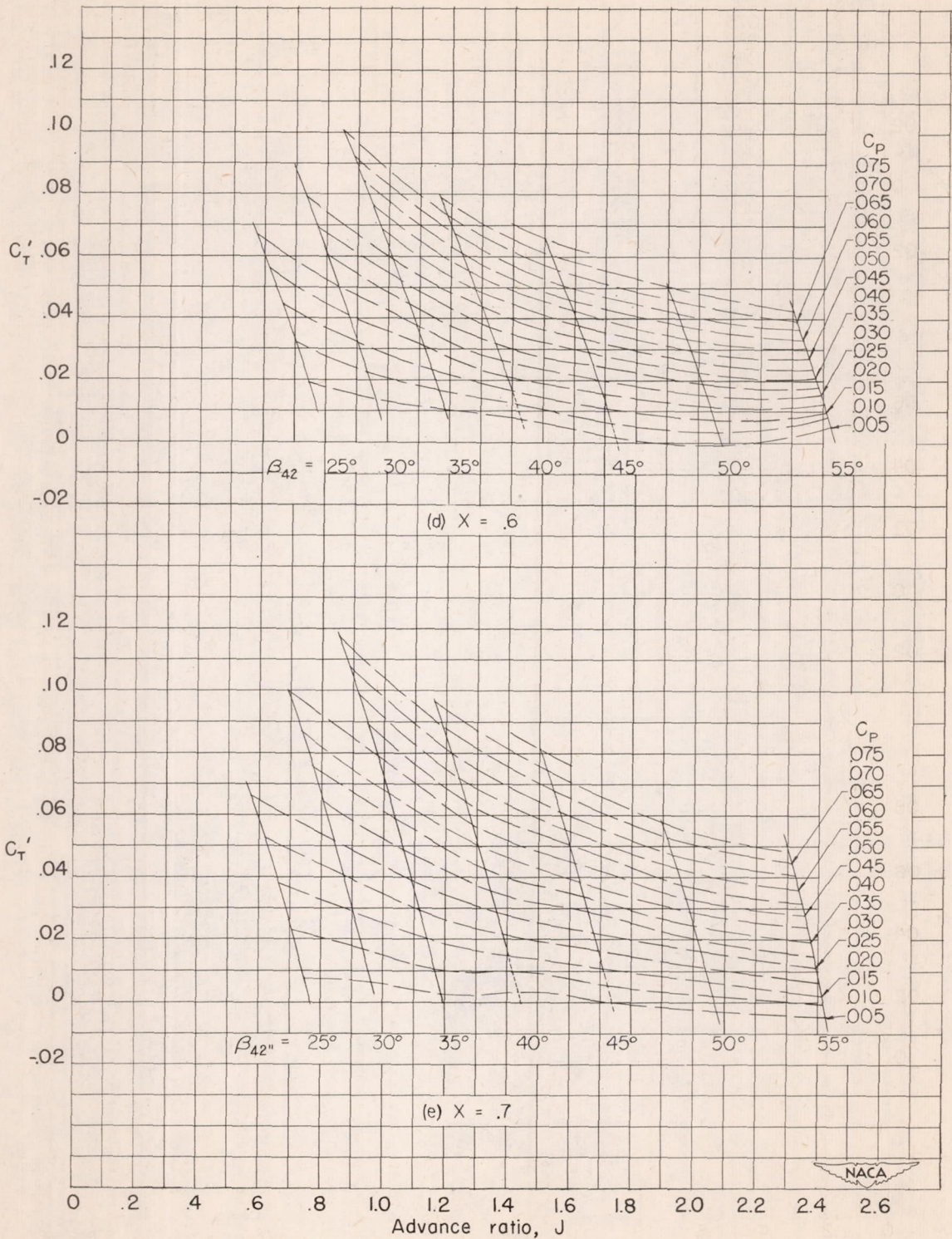


Figure 17.- Continued.

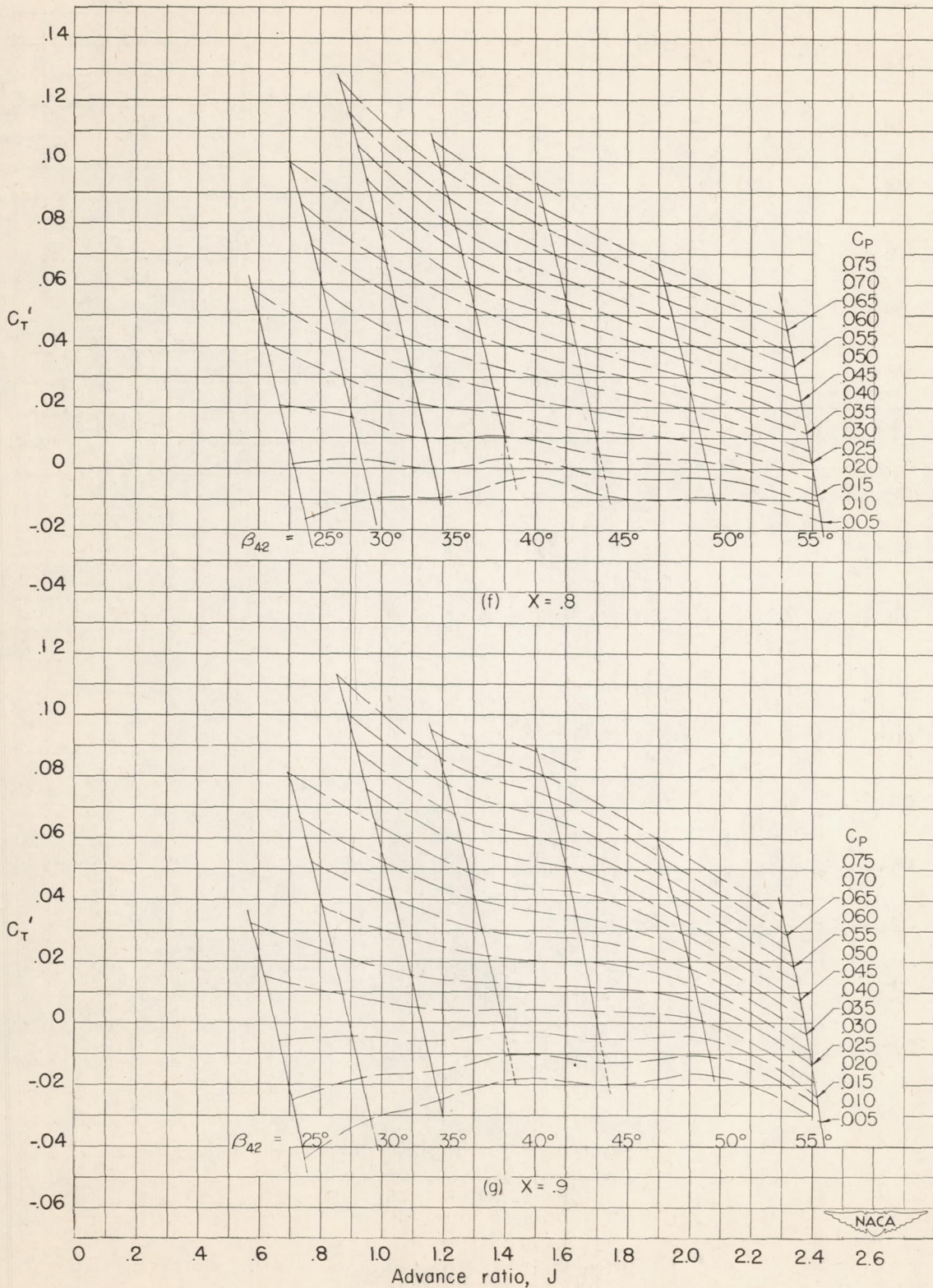


Figure 17.- Continued.

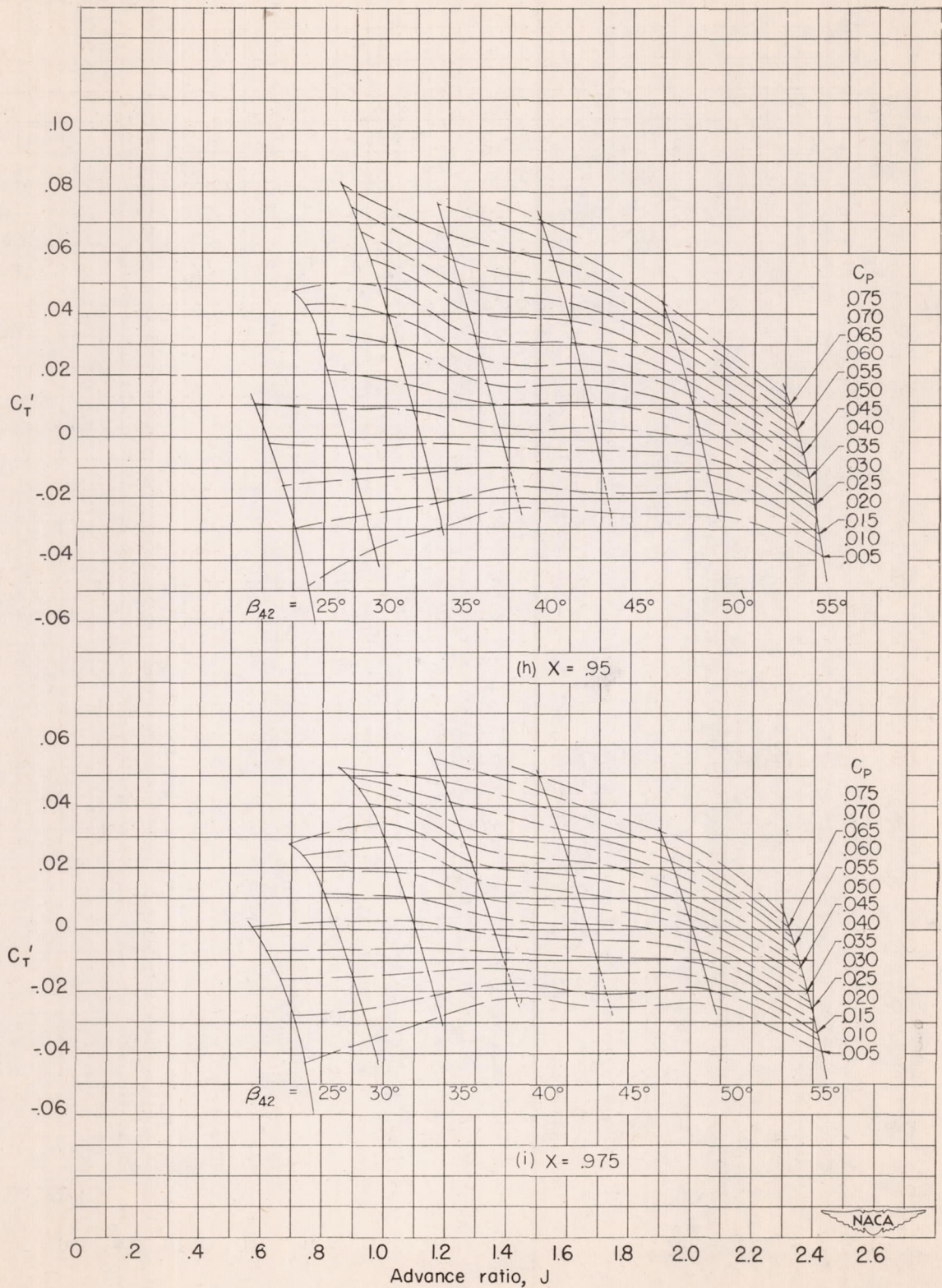


Figure 17.- Concluded.

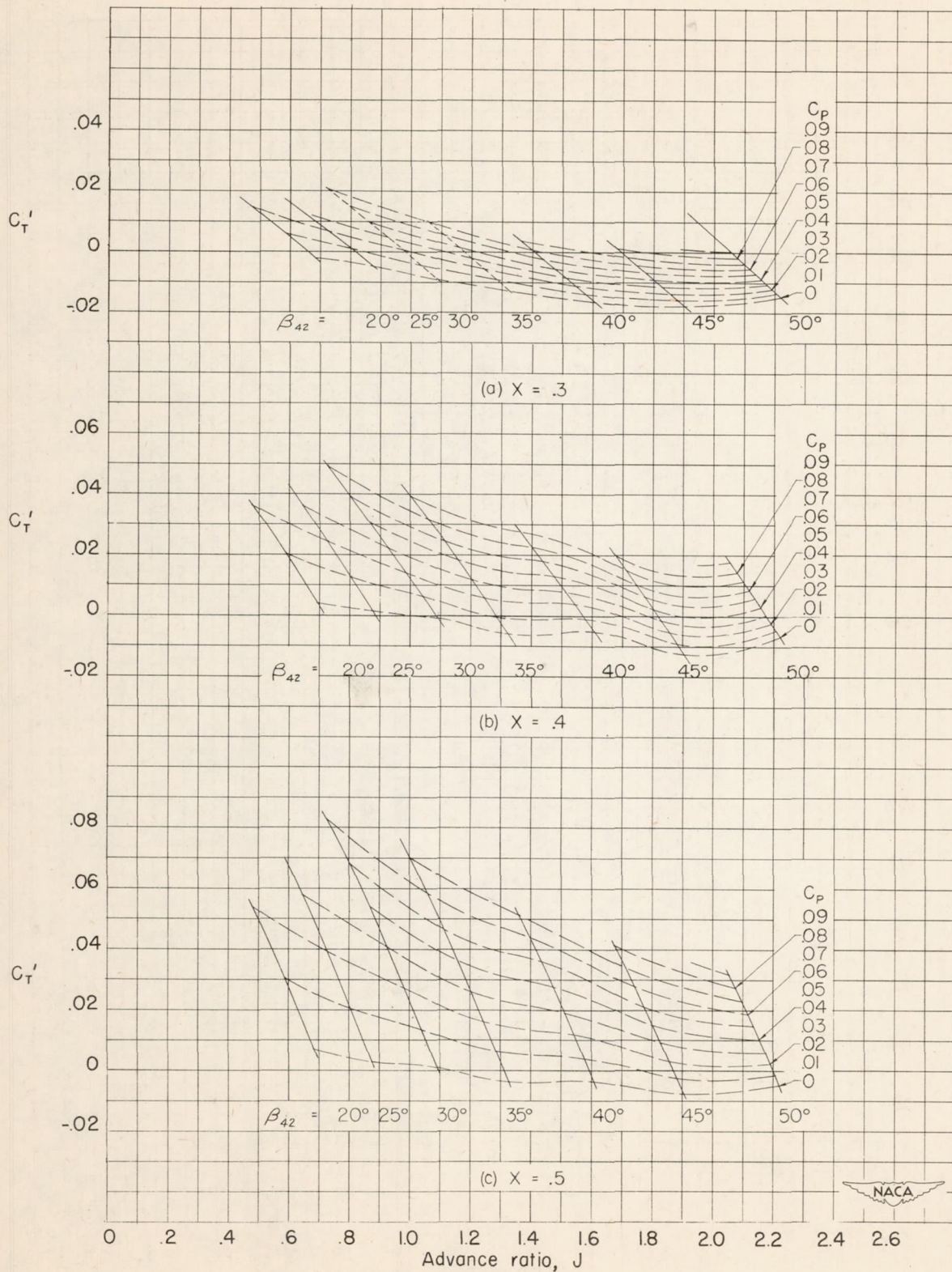


Figure 18.- Section thrust of set II from propeller surveys. 1350 rpm.

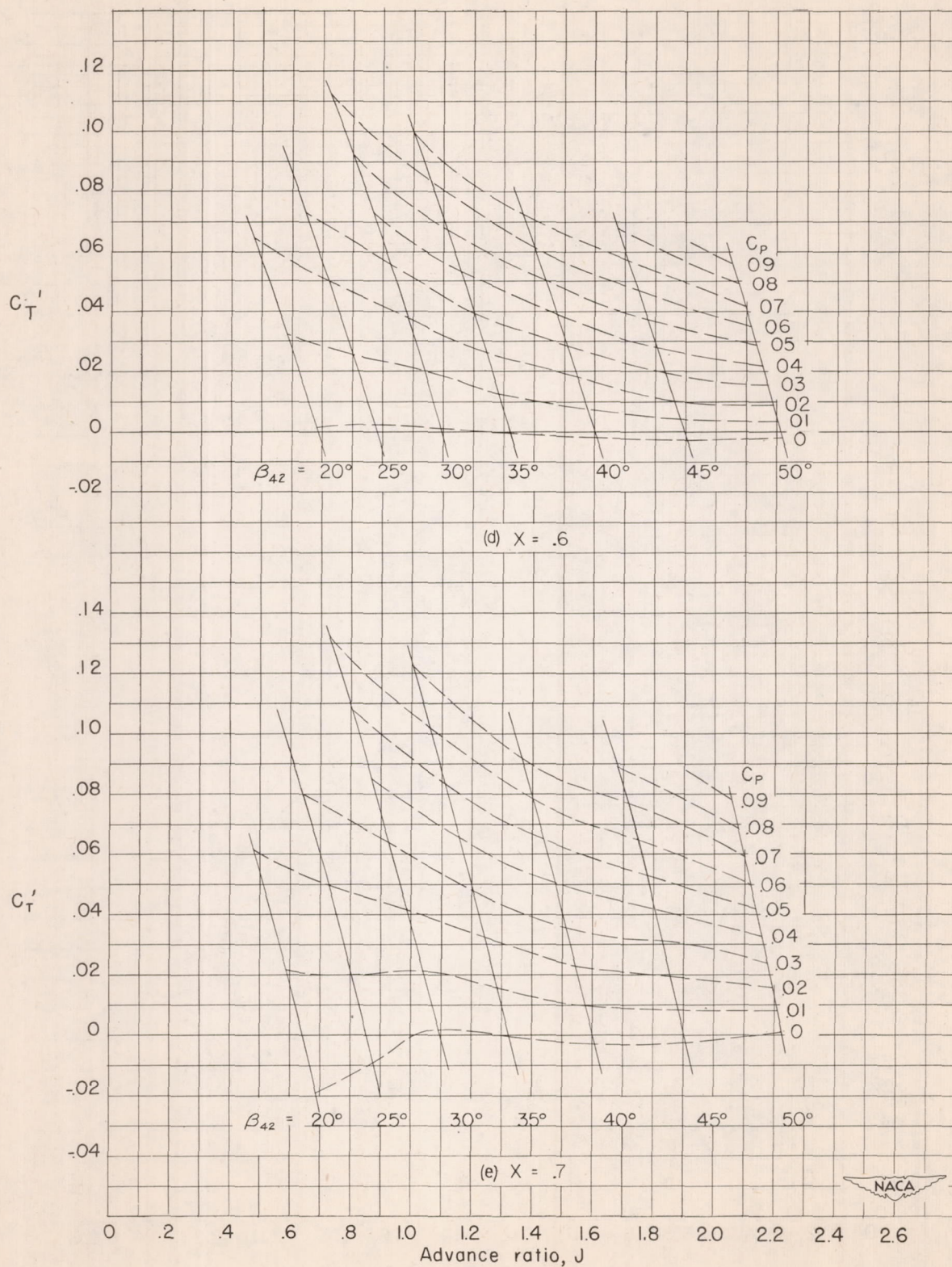


Figure 18.- Continued.

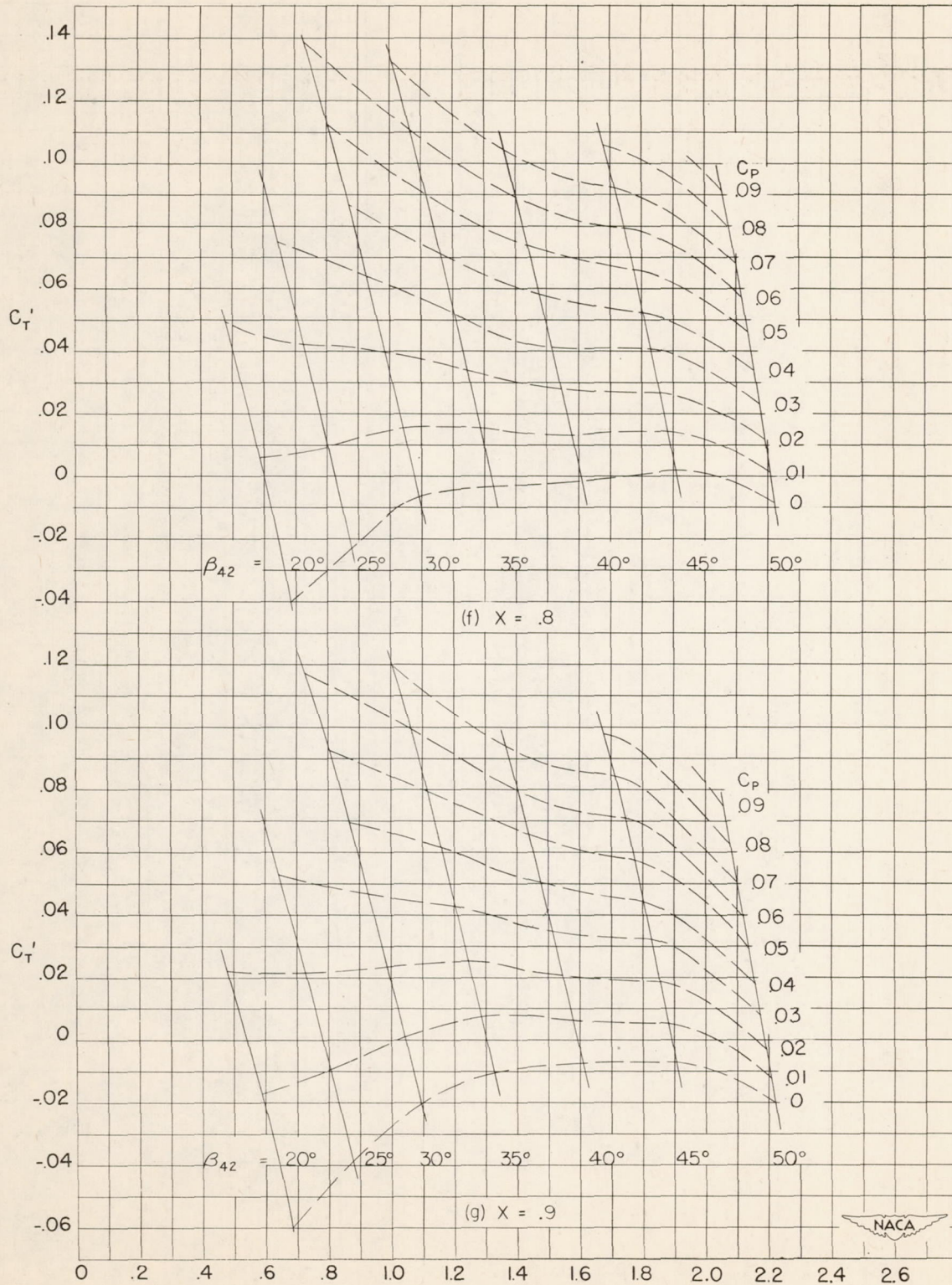


Figure 18.- Continued.

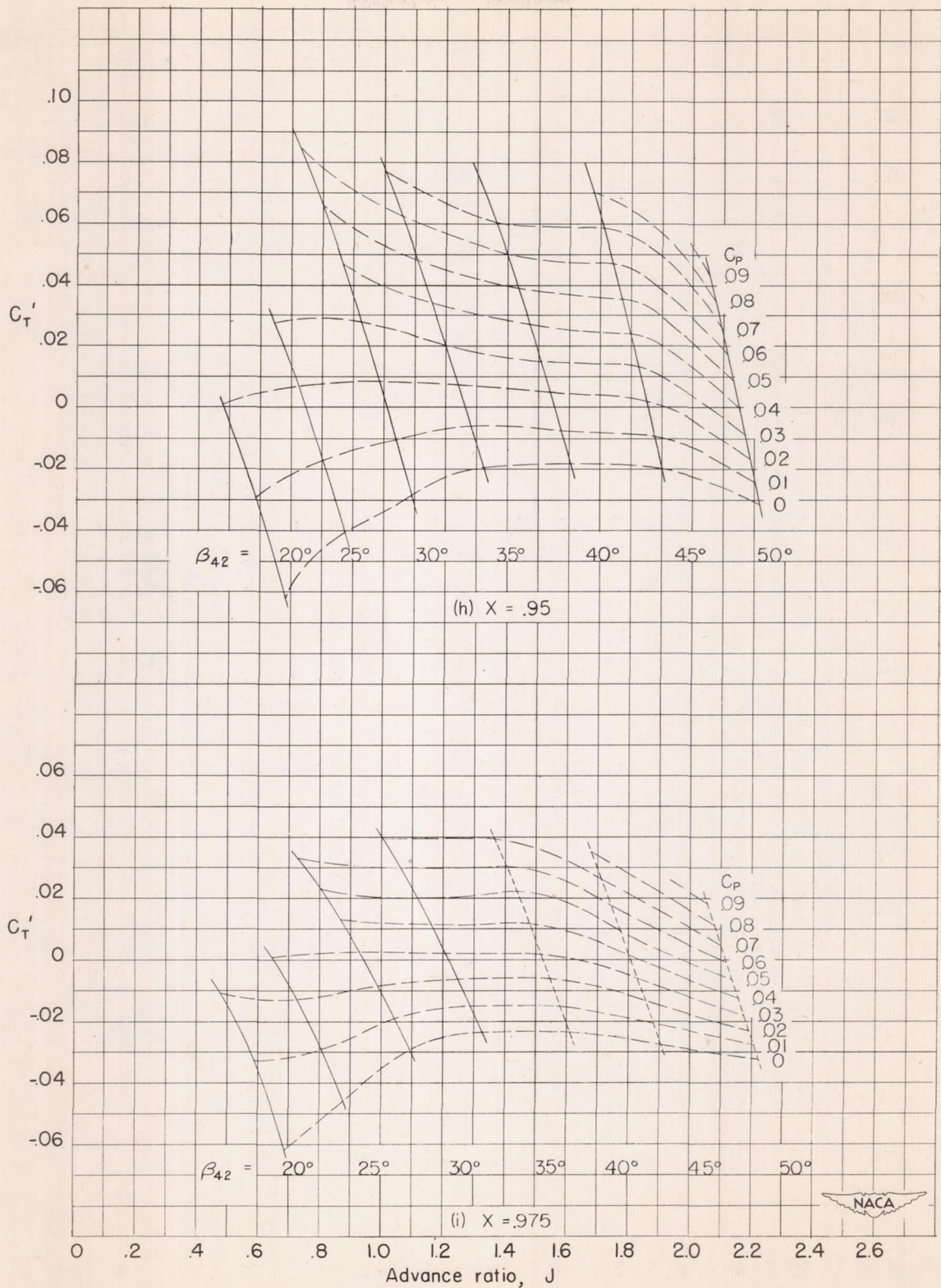


Figure 18.- Concluded.

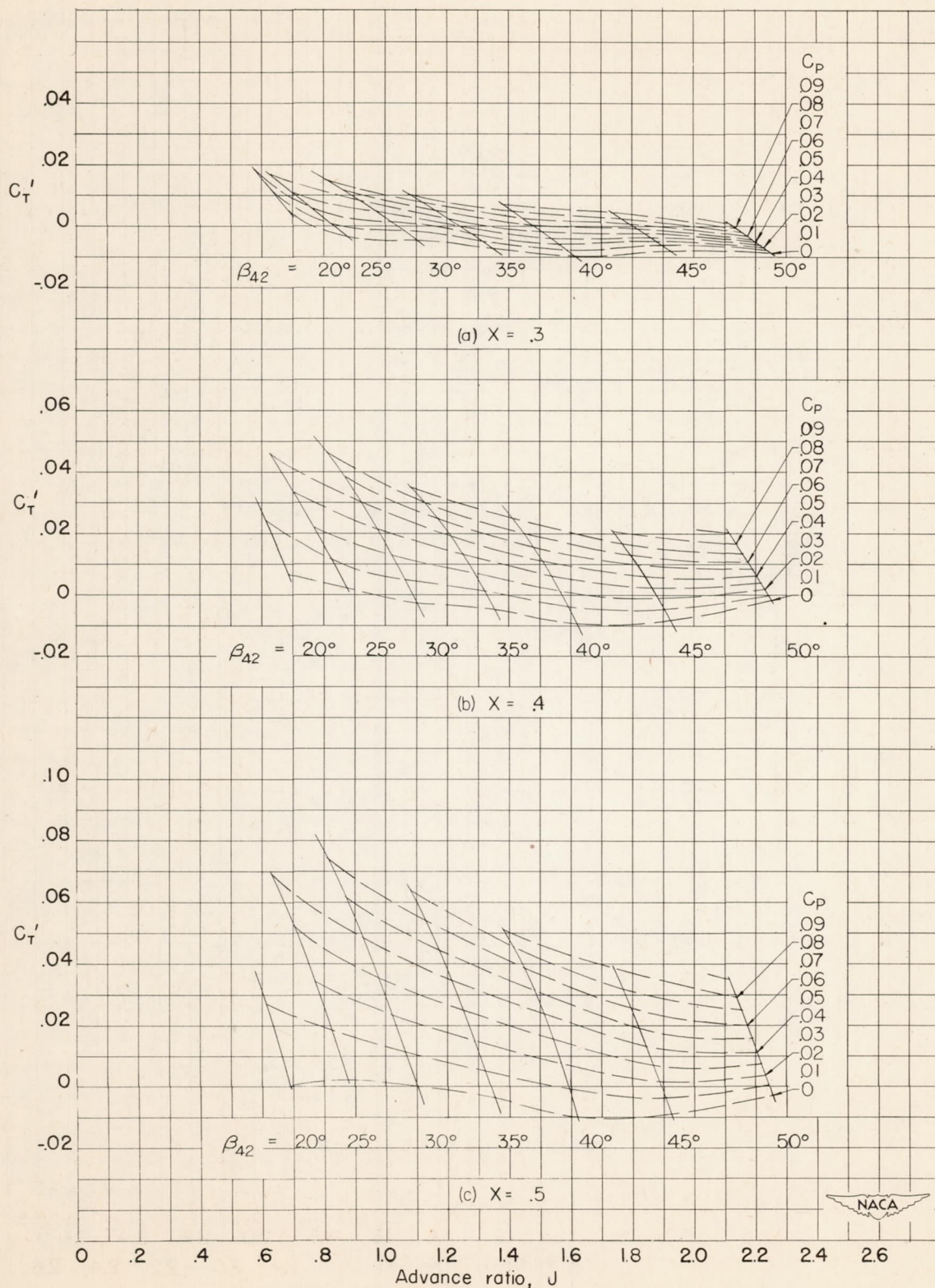


Figure 19.- Section thrust of set III from propeller surveys. 1350 rpm.

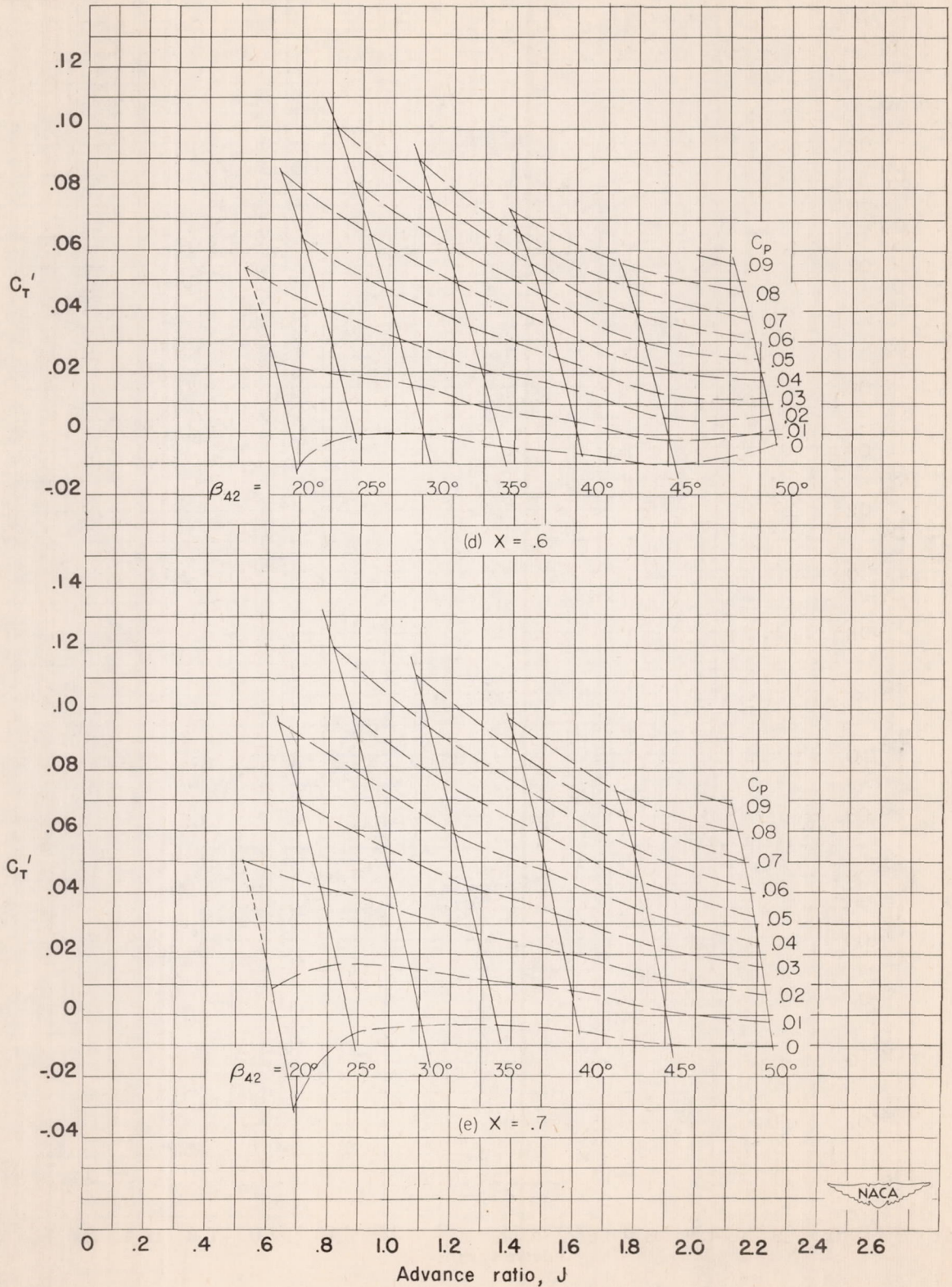


Figure 19.- Continued.

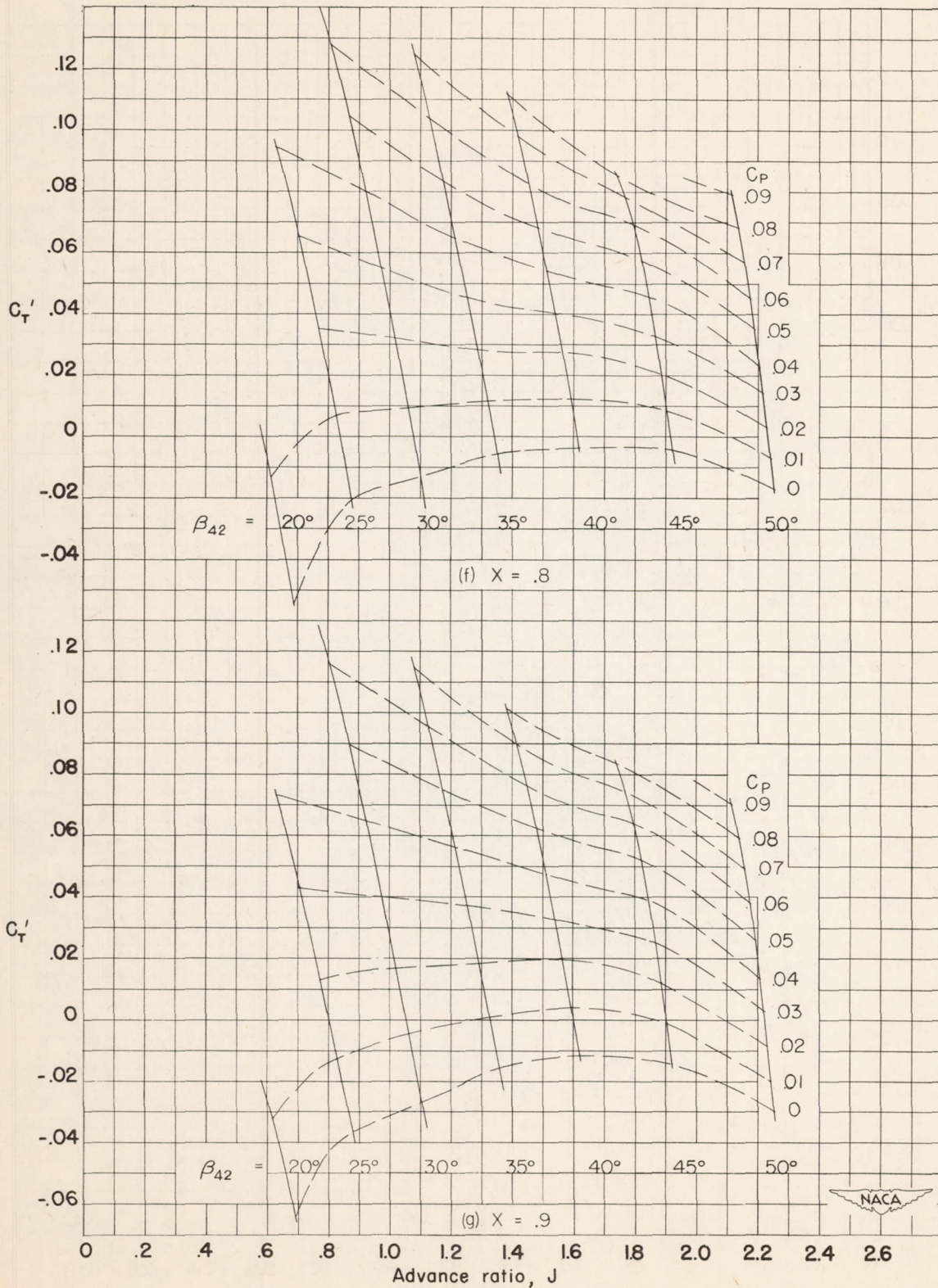


Figure 19.- Continued.

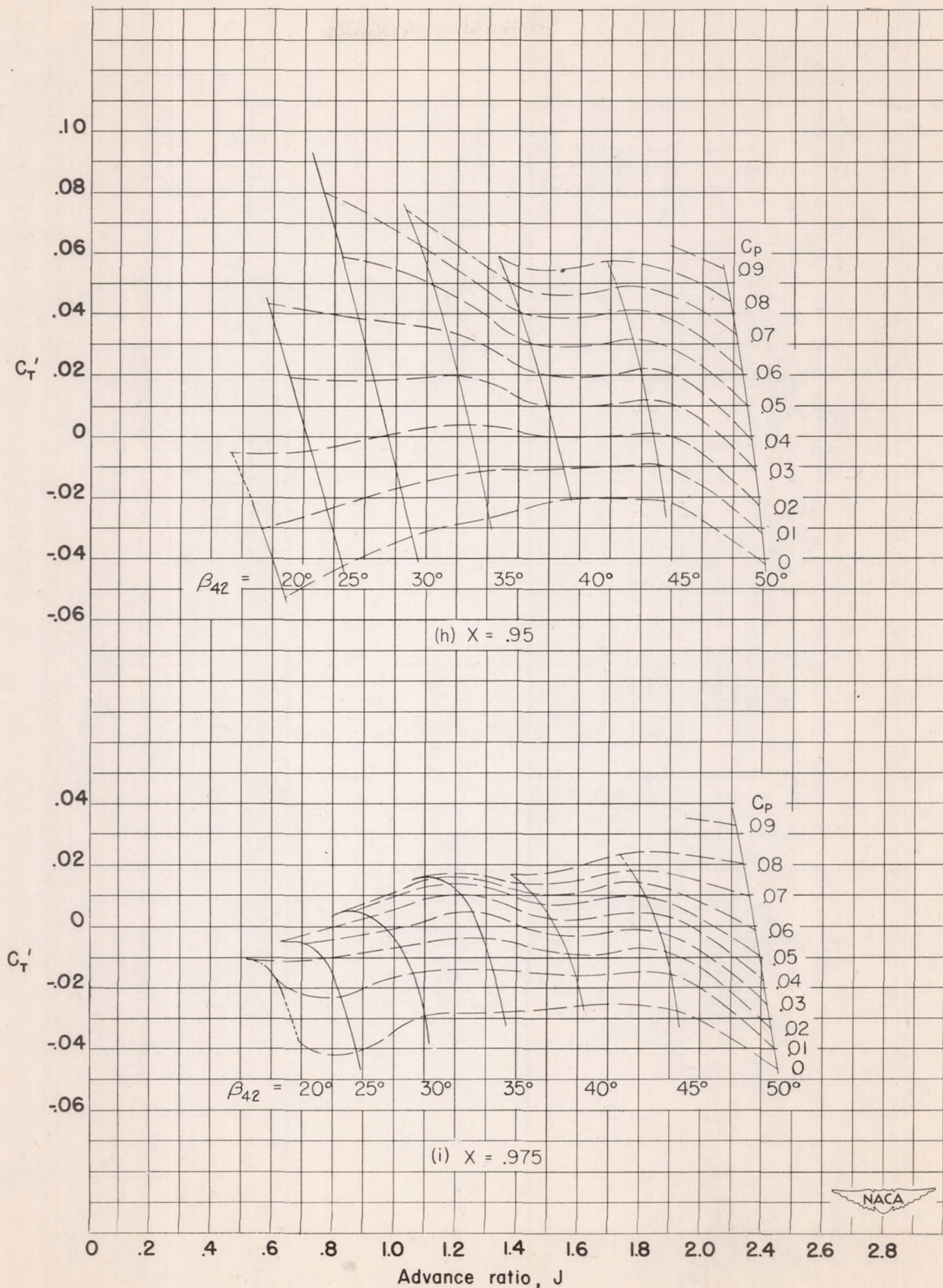
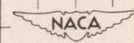


Figure 19.- Concluded.



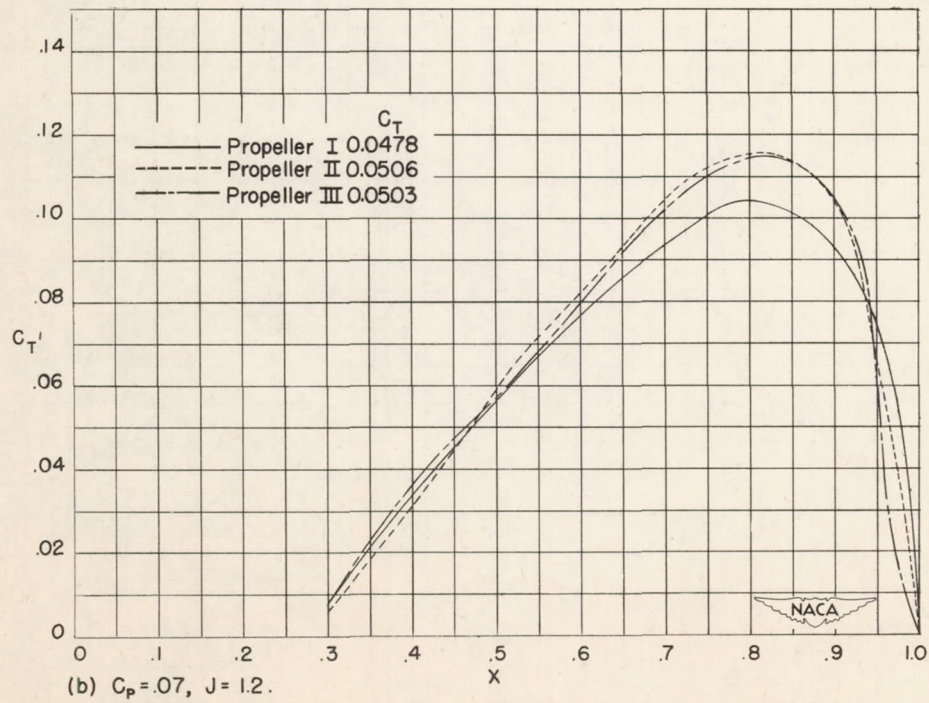
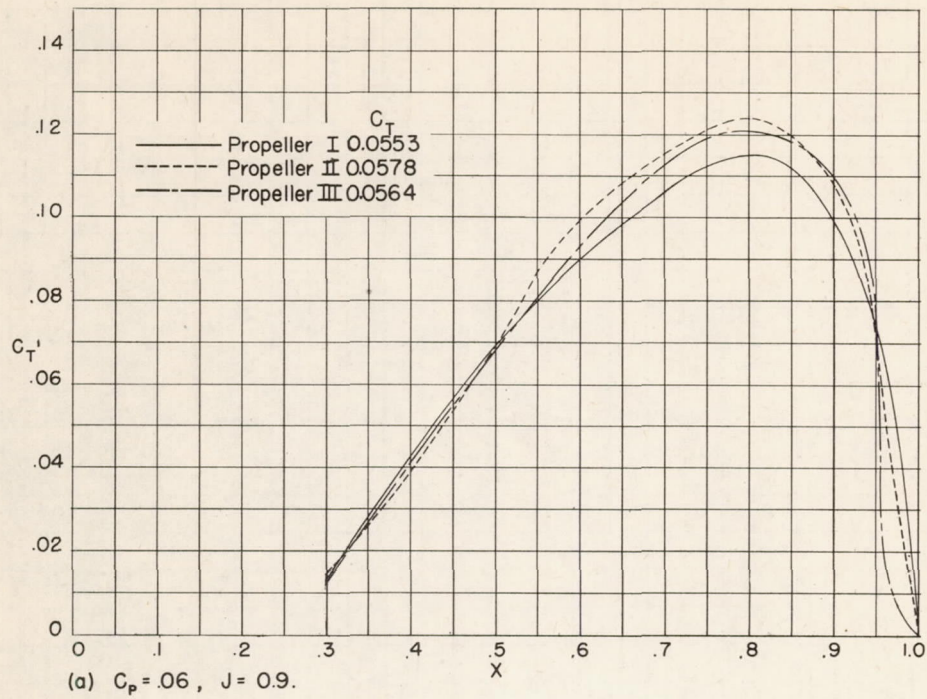


Figure 20.- Thrust-loading curves. 1350 rpm.

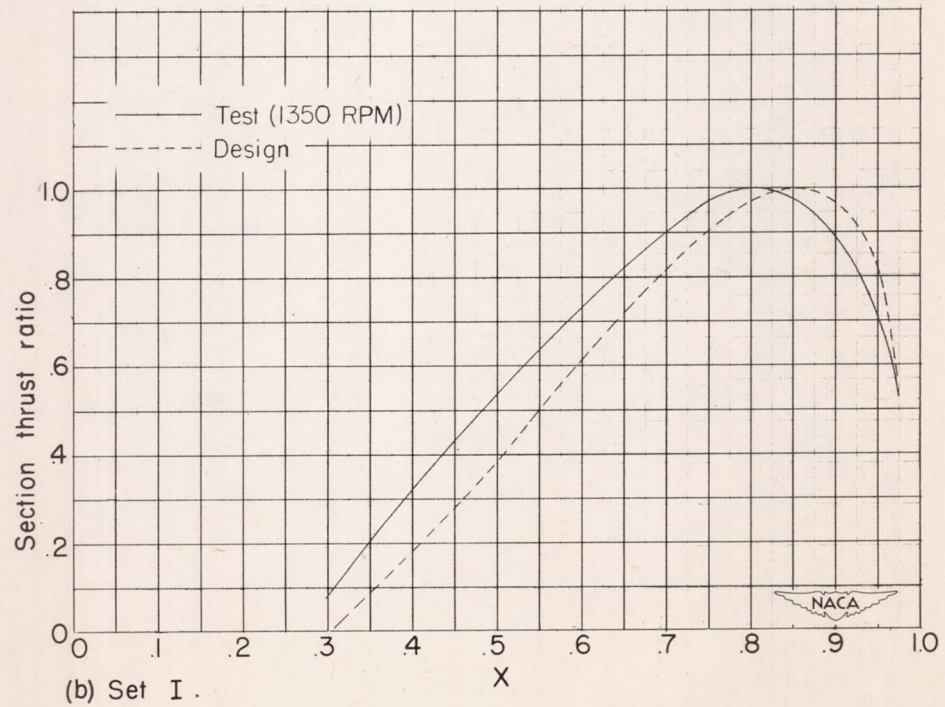
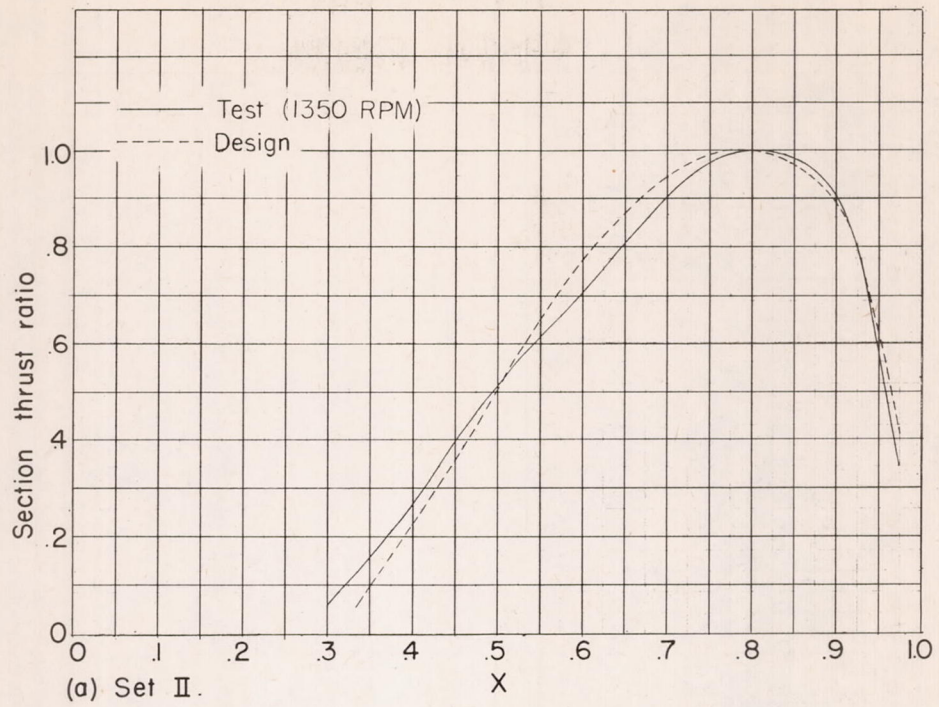


Figure 21.- Comparison of actual with design thrust-loading curves.

RECYCLED

LIBRARY OF THE
MAYOR OF NEW YORK

1954

THE LIBRARY OF THE MAYOR OF NEW YORK
IS A PART OF THE NEW YORK PUBLIC LIBRARY
ASTOR LENOX AND TILDEN FOUNDATIONS
100 N. 4th St. New York, N.Y. 10003

1954

RECYCLED

LIBRARY OF THE MAYOR OF NEW YORK

1954